

2009-05-01

The Manufacture and Testing of Perforated Composite Acoustic Panels

Blackburn, Robert

<http://hdl.handle.net/10026.1/4531>

All content in PEARL is protected by copyright law. Author manuscripts are made available in accordance with publisher policies. Please cite only the published version using the details provided on the item record or document. In the absence of an open licence (e.g. Creative Commons), permissions for further reuse of content should be sought from the publisher or author.

**The Manufacture and Testing of Perforated Composite
Acoustic Panels**

by

Robert Blackburn

A thesis submitted to the University of Plymouth

in partial fulfilment for the degree of

Master of Philosophy

Department of Mechanical and Marine Engineering

Faculty of Technology

In collaboration with GKN Aerospace Limited

May 2009

This copy of the thesis has been supplied on condition that anyone who consults it is understood to recognise that its copyright rests with its author and that no quotation from the thesis and no information derived from it may be published without the author's prior written consent.

The Manufacture and Testing of Perforated Composite Acoustic Panels

Abstract

The recent expansion of civil aviation has been accompanied by significant growth in the use of advanced composite structures with carbon fibre reinforced epoxy often the material of choice in many structures. Composite structures have a long history in engine nacelles, where an optimised design can both fulfil structural requirements and simultaneously provide an acoustic liner for sound attenuation. The "traditional process" involves the drilling of high-density multiple holes with the twin consequences of extended production times and machining waste. Elimination of this perforation process is an attractive target in a commercial environment. Structural performance could be improved by retaining fibre continuity whilst controlling fibre paths around the perforations through a moulding approach.

This thesis reports an investigation to evaluate novel approaches to moulding multiple perforations in composite structures and the application of those approaches in both traditional pre-preg and resin infusion processing technologies. Two approaches were explored: castable soluble pins and an adaptation of z-pinning technology. The composites produced using one of these techniques were subjected to mechanical testing (tension, compression and interlaminar shear) both dry and after exposure to hot/wet conditions. The laminates were also characterised for thickness variation, fibre volume fraction, degree-of-cure, glass transition temperature and acoustic impedance. These validations demonstrated that while significant improvements to property retention can be achieved for tensile loading conditions, certain compression conditions fail to achieve the same benefits. It was also found that a key aspect to implementing any perforation moulding technique lies in consistently achieving high quality hole definition to retain acoustic impedance performance.

From the concept characterisation, a preliminary weight and detailed cost analysis were developed to assess the industrial feasibility for the method developed. This analysis showed that, with further investigation and the right application selection, the benefits of the novel approach could be realised.

CONTENTS

Abstract	iii
List of Figures	vii
List of Tables	xvi
Acknowledgements	xviii
Author's Declaration	xix
Chapter 1: Project Introduction	1
1.1 <i>A Short History of Composites in the Commercial Aerospace Industry</i>	1
1.2 <i>Manufacturing Aerospace Composites</i>	11
1.3 <i>Project Introduction</i>	17
1.4 <i>Project Objectives</i>	22
1.5 <i>Project Approach</i>	23
Chapter 2: Literature Review	25
2.1 <i>Industrial Review</i>	25
2.2 <i>Biomimetic Design Considerations</i>	31
2.3 <i>Preforming</i>	34
Chapter 3: Manufacturing Trials	36
3.1 <i>The Acoustic Liner Panels (ALPs) of the AS-907 Outer Fan Duct (OFD)</i>	36
3.2 <i>Selecting Alternative Materials</i>	38
3.3 <i>Alternative RFI Processing Methodologies</i>	45

3.4	<i>Viable Pin Materials</i>	49
3.5	<i>Water Soluble Tooling</i>	54
3.5.1	Aquacore™/Aquapour™	54
3.5.2	Ceramcor	57
3.6	<i>Reusable Tooling</i>	66
3.6.1	FlexPerf.....	67
3.7	<i>Pin Material Development Conclusions</i>	76
3.8	<i>Thin Laminate Testing Trials</i>	76
3.8.1	Background.....	76
3.8.2	Approach	77
3.8.3	Compression Test Trials.....	79
3.8.4	ILSS Trials	82
3.8.5	Test Trial Conclusion.....	84

Chapter 4: Mechanical and Physical Material Characterisation..... 85

4.1	<i>Introduction</i>	85
4.2	<i>Hole Pattern Design</i>	88
4.3	<i>Predictive Methods</i>	93
4.4	<i>Test Results</i>	96
4.4.1	Comparing the Baseline Materials	97
4.4.2	Assessing Pre-Preg Performance.....	99
4.4.3	Assessing RFI Performance.....	100
4.4.4	Perforation Effects on Tensile Properties.....	101
4.4.5	Perforation Effects on Compression Properties.....	106
4.4.6	Effects of Perforation on ILSS	112
4.4.7	Comparisons to Predicted Performance	114
4.5	<i>Physical Data</i>	118
4.5	<i>Moisture Uptake</i>	122

4.6	<i>Acoustic Validation</i>	126
Chapter 5: Microstructure Characterisation		130
Chapter 6 - Industrial Application		142
6.1	<i>Weight Impact</i>	143
6.2	<i>Cost Analysis</i>	145
Chapter 7 - Conclusions		149
Appendix A: Publications		153
Appendix B: Open Area Calculation Method		214
Appendix C: Predictive Methods		216
Appendix D: Normalisation Methodology		218
Appendix E: Effective Areal Weight Increases		219
Appendix F: Performance Derived Weight Calculations		221
Appendix G: Calculations for Compression Capability		222
References		226
Bibliography		241

List of Figures

Fig. 1.1: Specific strength and relative weight per unit volume of typical aerospace materials	4
Fig. 1.2: A comparison of the specific modulus and strength between various composites, metals and polymers.....	5
Fig. 1.3: Comparing metal fuselage baseline to dedicated composite design.....	7
Fig. 1.4: Trend of composite structural applications in commercial aircraft.....	7
Fig. 1.5: Use of composite materials on the Boeing 777 as 10% of the structural weight	8
Fig. 1.6: Application of composites to the Airbus A340 at 15% of structural mass	8
Fig. 1.7: Application of composites to A380 aircraft at 20% of structural mass	9
Fig. 1.8: Application of composites to the Boeing 787 as 50% of structural mass	9
Fig. 1.9: Anticipated application of composites to the Airbus A350 XWB as 52% of structural mass.....	10

Fig. 1.10: Anticipated application of advanced composites to the Bombardier C-Series CS100 and CS300 as 46% of structural mass...	10
Fig. 1.11: Typical vacuum bag configuration.....	12
Fig. 1.12: Typical hot-melt pre-pregging schematic	14
Fig. 1.13: Typical solvented pre-pregging schematic.....	14
Fig. 1.14: Liquid resin infusion schematic (RIFT).....	15
Fig. 1.15: Liquid resin infusion schematic (RTM)	16
Fig. 1.16: Resin film infusion schematic.....	17
Fig. 1.17: Typical composite components found on a generic aircraft nacelle	19
Fig. 1.18: Bombardier Challenger 300 Aircraft.....	20
Fig. 1.19: Typical composite acoustic lining configuration.....	21
Fig. 3.1: Perforation pattern for development plaques	37
Fig 3.2: Comparing matrix properties	40
Fig 3.3: Common 2D weave styles	41
Fig. 3.3: Example construction of multi-axial NCF	43
Fig 3.4: Comparing fibre properties	45
Fig. 3.5: Configuration of GKN's current RFI process	46

Fig. 3.6: Proposed configuration of resin film positioned on fibre stack	46
Fig. 3.7: Proposed configuration of resin film stack under fibre stack	47
Fig. 3.8: Proposed configuration of fibre stack sandwiched between resin film	47
Fig. 3.9: M36 RFI Process Profile	47
Fig. 3.10: 100% Pin fracture of Aquacore cast detailing poor pin surface definition	56
Fig. 3.11: Ceramcor moulding trial showing zero pin formation due to trapped air	59
Fig. 3.12: Ceramcor moulding trial showing >95% pin formation due to vacuum	60
Fig. 3.13: Reinforced Ceramcor moulding showing flow issues caused by change in permeability	61
Fig. 3.14: 100% Ceramcor pin formation	61
Fig. 3.15: 1st Ceramcor lamination trial	63
Fig. 3.16: Honeycomb laminate consolidation	64
Fig. 3.17: Foam laminate consolidation	64
Fig. 3.18: Foam only consolidation	65

Fig. 3.19: Single layer pressure strip consolidation	65
Fig. 3.20: Double layer pressure strip consolidation	65
Fig. 3.21: Triple layer pressure strip consolidation.....	65
Fig. 3.22: FlexPerf insertion process	67
Fig. 3.23: Lay-up configuration for insertion process	69
Fig. 3.24: Ultrasonic horn equipment for pin insertion - Branson FS-90	69
Fig. 3.25: Photograph of FlexPerf moulded hole quality in RFI laminate.....	74
Fig. 3.26: Drilled RFI hole micrograph	74
Fig. 3.27: Moulded RFI hole micrograph	74
Fig. 3.28: Drilled PP hole micrograph	75
Fig. 3.29: Moulded PP hole micrograph	75
Fig. 3.30: Trial compression specimens with 1mm thickness	79
Fig. 3.31: ASTM D 695 compression test specimen.....	80
Fig. 3.32: Anti-buckling compression jig as specified for thin laminates in ASTM D 695 (shown with PTFE anti-buckling plates)	80
Fig. 4.1: Triangular area of hole pattern used for pitch calculations ..	89

Fig. 4.2: Hole pattern for test pieces.....	89
Fig. 4.3: Tensile specimen BS EN ISO 527 (250 x 30mm)	90
Fig. 4.4: Compression specimen ASTM D 695 (80 x 16mm)	90
Fig. 4.5: ILSS specimen BS EN 2563 (25 x 11mm)	90
Fig. 4.6: Final design for FlexPerf tooling and 5-Axis machining pattern	92
Fig. 4.7: Post machining of test plaque 0003	93
Fig. 4.8: Graphical comparison of the normalised properties for the two material systems (un-perforated)	97
Fig. 4.9: Perforation effects on the pre-preg material system	99
Fig. 4.10: Perforation effects on the RFI material system	100
Fig. 4.11: Pre-preg tensile modulus results.....	101
Fig. 4.12: RFI tensile modulus results	102
Fig. 4.13: Pre-preg tensile strength results	103
Fig. 4.14: RFI tensile strength results	104
Fig. 4.15: Non-perforated PP UTS failure	106
Fig. 4.16: Non-perforated RFI UTS failure.....	106
Fig. 4.17: Drilled PP UTS failure.....	106

Fig. 4.18: Drilled RFI UTS failure.....	106
Fig. 4.19: Moulded hole PP UTS failure	106
Fig. 4.20: Moulded hole RFI UTS failure	106
Fig. 4.21: Pre-preg and RFI compressive modulus results	108
Fig. 4.22: Pre-preg compressive strength results	109
Fig. 4.23: RFI compressive strength results	110
Fig. 4.24: RT non-perforated PP UCS failure.....	111
Fig. 4.25: RT moulded hole PP UCS failure.....	111
Fig. 4.26: RT drilled PP UCS failure.....	111
Fig. 4.27: RT non-perforated RFI UCS failure.....	111
Fig. 4.28: RT moulded hole RFI UCS failure.....	111
Fig. 4.29: RT drilled RFI UCS failure.....	111
Fig. 4.30: H/W non-perforated PP UCS failure	112
Fig. 4.31: H/W moulded hole PP UCS failure	112
Fig. 4.32: H/W drilled PP UCS failure.....	112
Fig. 4.33: H/W non-perforated RFI UCS failure	112
Fig. 4.34: H/W moulded hole RFI UCS failure	112

Fig. 4.35: H/W drilled RFI UCS failure.....	112
Fig. 4.36: Pre-preg ILSS results.....	113
Fig. 4.37: RFI ILSS results.....	113
Fig. 4.38: Comparisons of pre-preg tensile strength predictions to actual test data.....	114
Fig. 4.39: Comparisons of pre-preg tensile modulus predictions to actual test data.....	114
Fig. 4.40: Comparisons of pre-preg compression strength predictions to actual test data	116
Fig. 4.41: Comparisons of pre-preg compression strength predictions to actual test data	116
Fig. 4.42: Pre-preg laminate moisture absorption	123
Fig.4.43: RFI laminate moisture absorption	124
Fig. 4.44: Acoustic test plaque configuration	128
Fig.5.1: Section location in relation to hole position.....	130
Fig. 5.2: Moulded pre-preg hole at A-A.....	131
Fig. 5.3: Moulded pre-preg hole at B-B	131
Fig. 5.4: Moulded pre-preg hole at C-C.....	132

Fig. 5.5: Moulded pre-preg hole at D-D..... 132

Fig. 5.6: Moulded RFI hole at A-A 133

Fig. 5.7: Moulded RFI hole at B-B 133

Fig. 5.8: Moulded RFI hole at C-C 134

Fig. 5.9: Moulded RFI hole at D-D 134

Fig. 5.10: Standard RFI drilled hole 135

Fig. 5.11: Standard pre-preg drilled hole 135

Fig. 5.12: Drilled pre-preg planar view..... 136

Fig. 5.13: Moulded hole pre-preg planar view 136

Fig. 5.14: Drilled RFI planar view..... 137

Fig. 5.15: Moulded hole RFI planar view 137

Fig. 5.16: Hole-to-hole fibre distortion from RFI mouldings 137

**Fig. 5.17: Graphical approximation of fibre distortion from RFI
mouldings 138**

**Fig. 5.18: Graphical approximation of fibre distortion throughout
single ply from RFI mouldings 138**

Fig. 5.19: Pre-preg moulded hole to hole thickness variation..... 140

Fig. 6.1: Relative cost structure of acoustic liner panels from OFD .. 146

Fig. 6.2: Relative cost structure of OFD component	147
Fig. B.1: Triangular area of hole pattern used for pitch calculations	214
Fig. C1: Row type identification	216

List of Tables

Table 3.1: Theoretical lay-up options for equivalent NCF panel.....	43
Table 3.2: Analysis results from through thickness non-perforated infusion trials	48
Table 3.3: Categorized options for mandrel material selection.....	50
Table 3.4: Decision matrix for mandrel material down-selection.....	53
Table 3.5: Summary of FlexPerf trial results.....	72
Table 3.6: Results and failure modes of thin specimen compression trials	81
Table 3.7: ILSS specimen dimensions and trial results.....	83
Table 4.1: Test matrix.....	88
Table 4.2: Area reduction tensile predictions	95
Table 4.3: Area reduction compression predictions.....	95
Table 4.4: Laminate mechanical dataset	96
Table 4.5: Moulded hole perimeter physical analysis	119
Table 4.6: DSC results for degree-of-cure	121
Table 4.7: DMA results for glass transition temperature	121
Table 4.8: Acoustic test results.....	128

Table C1: Calculation table for reduction factors for application to non-perforate data	217
--	------------

Acknowledgements

Firstly I would like to thank Hannah for all her support and encouragement in completing this work and to Jacob for his welcome distractions and inspiring smiles.

The author is grateful to GKN Aerospace for their funding of the work through the Teaching Company Scheme (TCS) initiative and for the position of Development Engineer throughout the initial research period. Specifically, thanks go to Phil Healey for his mentoring and guidance on the project, Tom Ainsworth for his advice on the test methodology and all the members of the Materials Test Laboratory for their support and assistance in the material evaluation. Further thanks go to Iosif Progoulakis for the technical and philosophical discussions while at GKN and for helping make my time there a fun and memorable experience.

Gratitude and thanks are given to Dr Stephen Grove, Dr John Summerscales and Dr Tim Searle at the University of Plymouth for their advice, support and patience being key to this work. Further, I would like to thank the members of the TCS group and FoT Support Staff at Plymouth for all their support and assistance during my time as an associate.

While undoubtedly there are people omitted from this list who were influential in the work being completed their absence is not intentional and gratitude is extended.

Lastly I would like to offer thanks to my parents and family for all of their support and encouragement in conducting and concluding this work.

Author's Declaration

At no time during the registration for the degree of Master of Philosophy has the author been registered for any other University award.

This study has been part financed by the DTI through the Teaching Company Scheme and GKN Aerospace Limited in collaboration with the Department of Mechanical and Marine Engineering.

Relevant scientific seminars and conferences were attended. Papers were presented at some of these meetings. The details are on the following pages.

The word count of this thesis, excluding introductory pages and appendices, is 22, 973.

Signed.....

Date.....

Training attended:

Introduction to Composites Manufacturing: APMC
Plymouth, 22-26 October 2001.

TCS Module 1 – Communication Skills: Pi Management
Bath, 14-18 January 2002.

TCS Module 2 – Management Skills: Pi Management
Bath, 24-28 February 2002

23rd International SAMPE Europe Conference
Paris, 09-11 April 2002

Vacuum Infusion Technologies Seminar: APMC
Plymouth, 12 June 2002

Design with Composite Materials: APMC
Plymouth, 17-18 July 2002

Composite Manufacturing for Transport Applications: COMPOSIT
Thematic Network
Aachen, 5 November 2002

Aircraft Structural Design & Stress Analysis: University of Bristol
Bristol, 6-10 January 2003

TCS Module 3 – Business management Skills: Pi Management
Bath, 20-23 January 2003

24th International SAMPE Europe Conference
Paris, 1-2 April 2003

Composite Material Structures: Cranfield University
Cranfield, 28 April – 2 May 2003

TCS Module 4 – Globalisation: Pi Management
Bath, 2-5 June 2003

Resin Infusion: APMC
Plymouth, 30 September – 2 October 2003

Green Belt Six Sigma: CEM
Wrexham, May 2004

27th International SAMPE Europe Conference
Paris, 27-29 March 2006

Advanced Aircraft Composites: AMTAS
Seattle, 18-22 September 2006

8th International Conference on Textile Composites
Nottingham, 16-18 October, 2006

28th International SAMPE Europe Conference
Paris, 3-6 April 2007

Polymer Science & Technology: Polymer IRC
Sheffield, 29 October – 8 November 2007

29th International SAMPE Europe Conference
Paris, 31 March – 2 April 2008

3rd SAMPE Europe Technical Conference
Augsburg, 18-19 October 2008

Conference papers (see Appendix A):

C LoFaro, M Doyle, R Blackburn and R Maskell
Low Cost Manufacturing Using Novel Preforming and Resin Infusion
Technologies
26th SAMPE Europe International Conference
PARIS, 5-7 April 2005

R Blackburn, M Doyle C LoFaro and R Maskell
Recent Developments in Preform and Resin Infusion Technologies for
Primary Structural Aerospace Applications
37th SAMPE Technical Conference
SEATTLE, 31 October – 3 November 2005

A Abusafieh, R Blackburn, M Doyle, C LoFaro, R Maskell, and R Price
Process and Performance Enhancements in Resin Infusion Using an Epoxy-
Soluble Nonwoven Veil
27th SAMPE Europe International Conference
PARIS, 27-29 March 2006

R Blackburn, M Doyle, C LoFaro, R Maskell and D Ponsolle
Recent Advancements in Materials for Liquid Resin Infusion Processes
3rd SETEC Technical Conference
AUGSBURG, 18-19 September 2008

Chapter 1: Project Introduction

1.1 A Short History of Composites in the Commercial Aerospace Industry

In the hundred years since the Wright brothers' first flight at Kitty Hawk the aerospace industry has become one of the most technically advanced and challenging areas of the engineering world. The developments that followed this act of innovation brought a new opportunity for travel, allowing people to reach distant and exotic destinations within a timescale of hours as opposed to days or weeks. This fundamentally changed the way that people viewed the world and also how they conducted their business. The aeroplane became a key facilitator of economic growth, world trade, tourism and military influence, establishing it as a symbol of economic power in the process.

In the last 15-20 years, the civil aviation industry has seen a boom in the use of and dependence on air travel by both businesses and tourists. Air travel grew by approximately 7% a year in the 1990's (SBAC, 2003). By 2000 scheduled airlines were carrying 1.5 billion passengers annually, with these numbers forecast to double by 2010 (SBAC, 2003). This growth in passengers has been made possible by developments in civil aircraft with large long haul aircraft such as the Boeing 747 enabling the tourist industry to expand further to include new and exotic destinations. Within the UK the aerospace industry comprises around 15,000 companies creating direct employment for some 120,000 people and a further 250,000 through

indirect links (SBAC, 2006). In 2005 the aerospace industry in the UK generated a turnover of £22 billion and has been forecast to be worth over £1000 billion by 2022, providing it retains its 12% share of the global market. Naturally there are uncertainties that the industry must face and overcome. To achieve this, the three most prominent factors are:

1. A need to reduce the cost margins of civil airlines caused by multi-national regulation and a global financial downturn;
2. The risk of growth constraint caused by emissions and air traffic management regulations which are expected to be implemented in the next 20 years; and
3. Proposals for high-speed intra-continental rail links with centre-centre travel eliminating travel to airports and extended (counter terrorism) check-in times.

The major way that many aerospace companies tackle these issues is to develop their products to have lower operating costs for the airlines by reducing the fuel consumption per passenger. In modern commercial airliners each 0.5kg of fuel saved is equivalent to a 1.5kg reduction in CO₂

emissions through lighter structural mass (Yu, 2007). These operating costs may be reduced by the increased use of advanced materials such as fibre reinforced plastics that offer lower weight for the equivalent Young's modulus and strength of conventional aerospace alloys.

These materials are not in principle a new technology. The significant improvements to their properties and processing over the last 30 years have given them the title of 'advanced materials'. These developments and improvements have mainly seen the toughness and temperature performance of the materials increase as well as their commercial viability through reductions in manufacturing costs. As with most technologies these changes came about through a better understanding of the behaviour and processing of the materials, resulting in a fuller appreciation of their potential by engineers and designers within the industry. This now allows the use of composites in novel applications previously dominated by metals and accelerates the progress of composites as the material of choice for the future.

Until recently, composites were of comparable cost to titanium due to the high price of the constituent ingredients and the initial capital expenditure required for their processing. This is now changing as the primary objective for composite suppliers in the 21st century is to make them an affordable technology applied in aeronautical engineering processes that will use their full potential. The benefits that composites provide over metals such as aluminium, steel and titanium are their

stiffness-to-weight and strength-to-weight ratios combined with their anisotropic properties, in that their strength in each direction can be varied to suit the application and hence mechanical properties can be optimised with respect to overall structure weight. This high strength-to-weight ratio makes composites such as carbon reinforced epoxy attractive to aerospace applications where weight is a sensitive and expensive element in all structures. The performance of carbon fibre reinforced epoxy composites is illustrated in Figs. 1.1 and 1.2 in comparison to other common engineering materials.

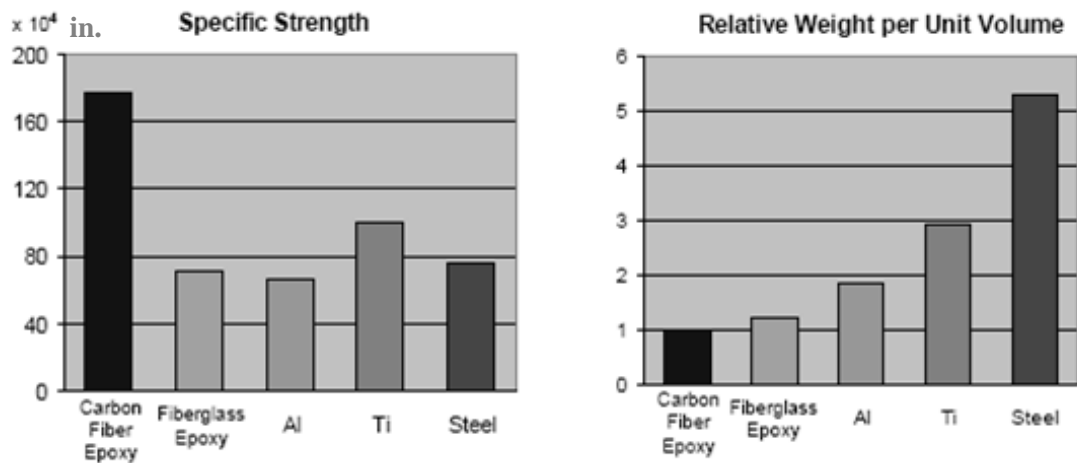


Fig. 1.1: Specific strength and relative weight per unit volume of typical aerospace materials (Polland et al., 2006)

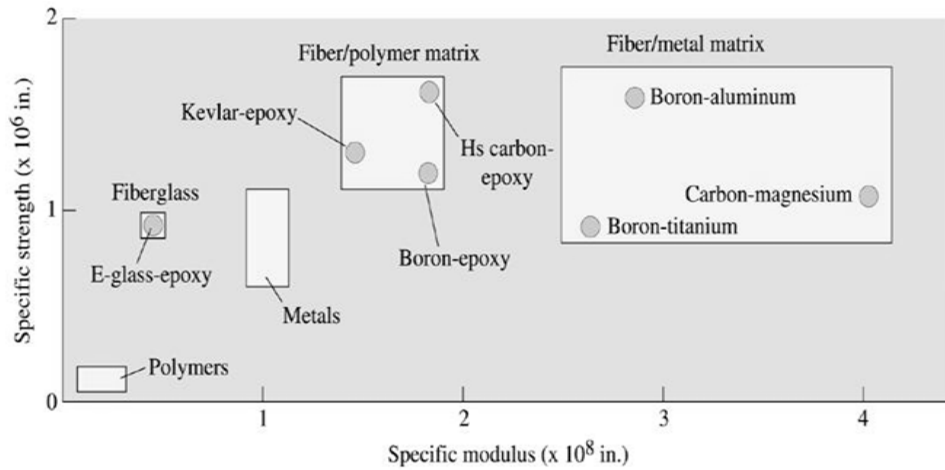


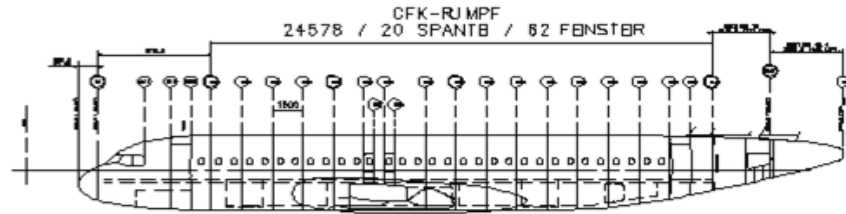
Fig. 1.2: A comparison of the specific modulus and strength between various composites, metals and polymers

(http://www.ccm.udel.edu/Personnel/homepage/class_web/Lecture%20Notes/2004/54)

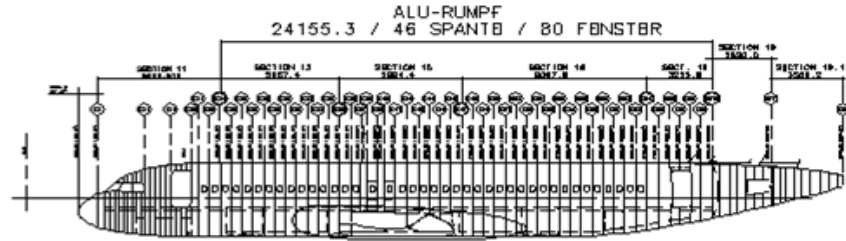
Traditionally the aerospace industry has been slow to incorporate the use of composites into their structures due to reservations over the long term performance of these materials while they are still considered ‘new technology’. With the recognition of the need to reduce operating costs for airline companies and the emergence of lower cost manufacturing methods where the expensive autoclave is eliminated, there is now an increase in the use of composites on new civil aircraft as the large manufacturers start to fully appreciate the benefits these materials can bring. A particular manufacturing benefit seen by the industry is the ability to integrate structures with composite materials and reap the rewards of quicker manufacturing times through the elimination of mechanical fasteners and secondary assembly. This is evident through the discussions of Polland et al. (2006) on how;

‘...composite structures offer new possibilities for design and manufacture – much larger integral structures are possible than can typically be achieved with metallic structure. This provides improved structural efficiencies as there are fewer joints and splices necessary. Having fewer bigger, more integrated parts also makes for more efficient manufacture – faster factory flow times; less infrastructure and fewer tools.’(p.2)

Fig. 1.3 shows a theoretical design approach for the Airbus A320 where a composites-focussed design philosophy enables larger sections with fewer components compared to the metallic baseline. It is claimed that such a change in design approach could present fuselage weight savings of the order of 15% but would require significant changes to design approaches in composite materials to fully utilise the flexibility that tailoring the fibre position can provide. This increased use of composite materials in the commercial airframe industry is illustrated in Fig. 1.4 where the timeframe these increases have occurred over is shown as a function of composite structural weight in new aircraft programmes. The applications that composites have found to offer benefits in are further illustrated in Figs. 1.5-1.10 where their structural use on the most recent commercial aircraft is highlighted.



Example:
Generic Airbus Standard Body



Example:
For comparison only => A320 metal fuselage

Fig. 1.3: Comparing metal fuselage baseline to dedicated composite design

(Rueckert et al., 2003)

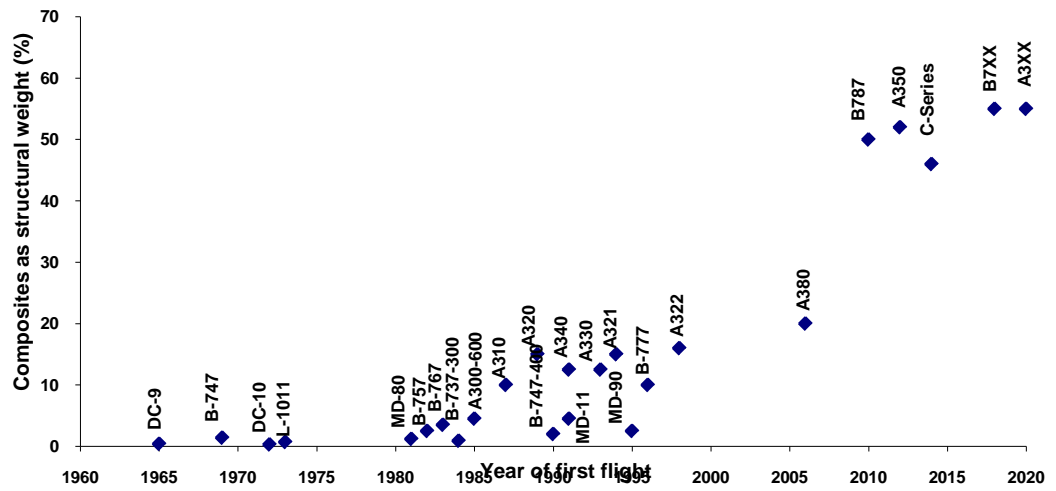


Fig. 1.4: Trend of composite structural applications in commercial aircraft

(Harris et al., 2001) (NOTE: Updated by author to include A380, B787, A350, C-Series and expected levels for next generation single aisle aircraft)

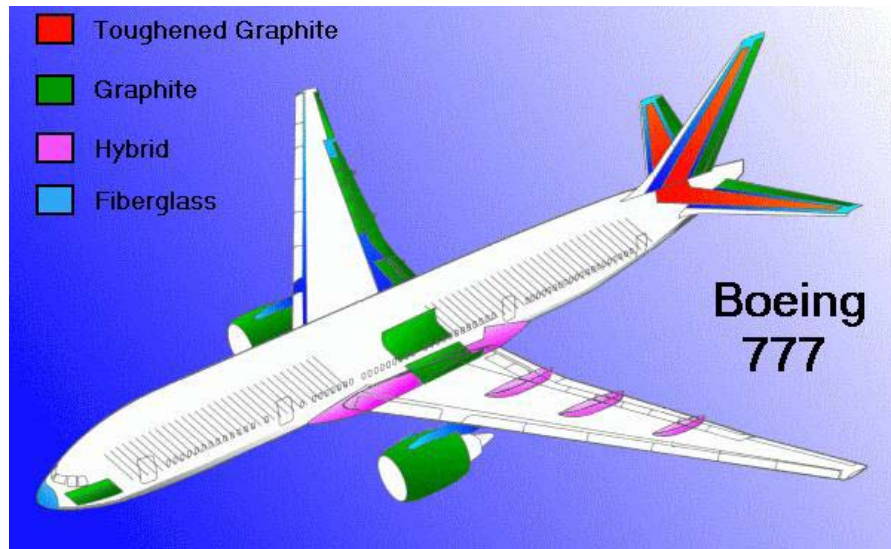


Fig. 1.5: Use of composite materials on the Boeing 777 as 10% of the structural weight

(The Aviation History On-line Museum, <http://www.aviation-history.com/theory/composite.htm>, 1999)

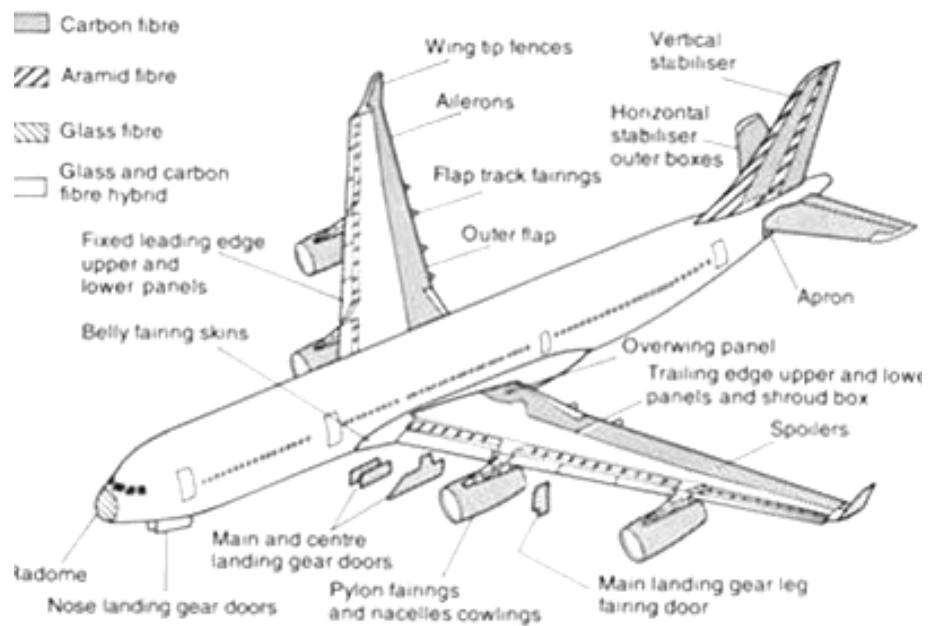


Fig. 1.6: Application of composites to the Airbus A340 at 15% of structural mass
(Cutler, 1999)

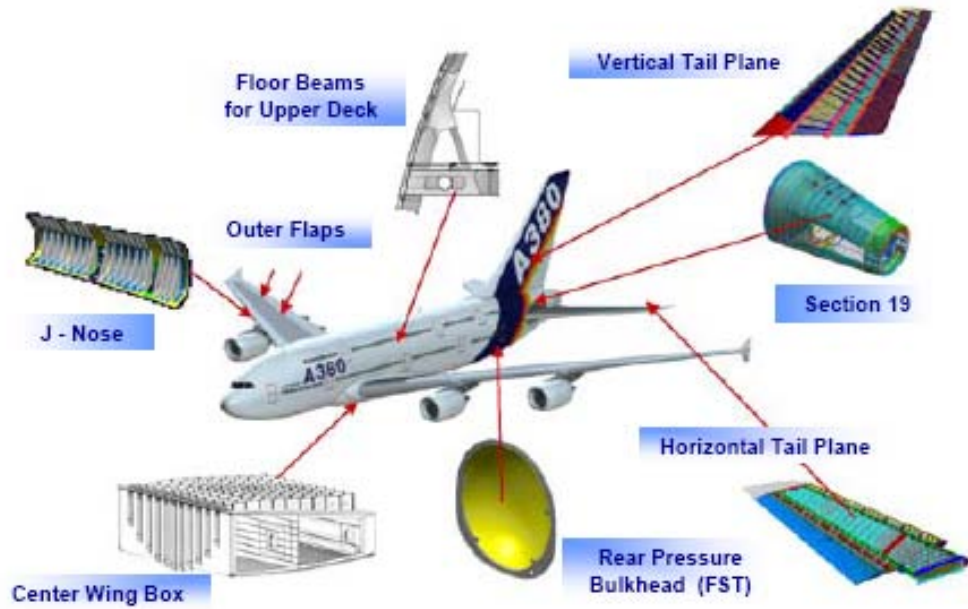


Fig. 1.7: Application of composites to A380 aircraft at 20% of structural mass
 (Pora & Hinrichsen, 2001)

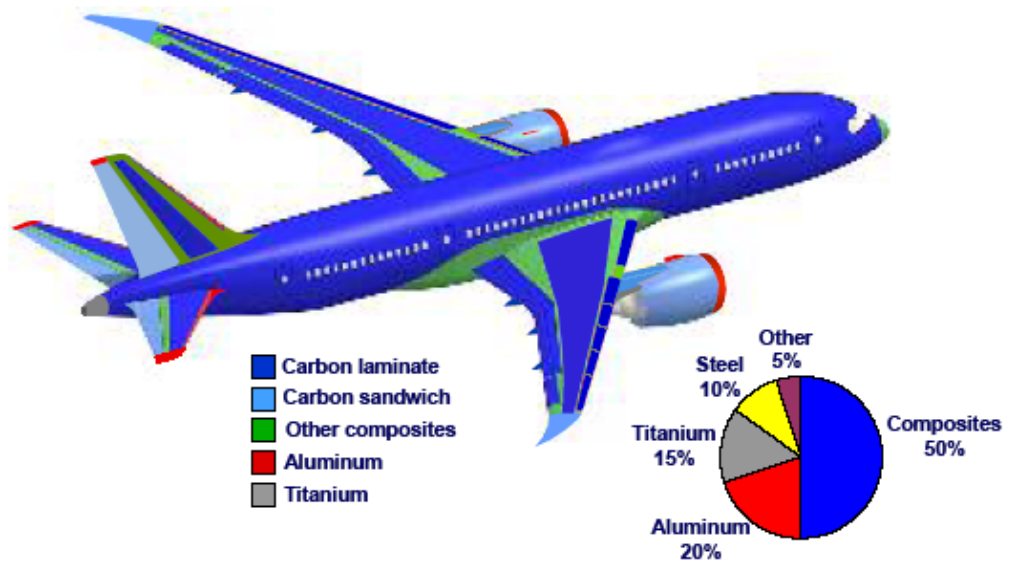


Fig. 1.8: Application of composites to the Boeing 787 as 50% of structural mass
 (Polland et al. 2006)

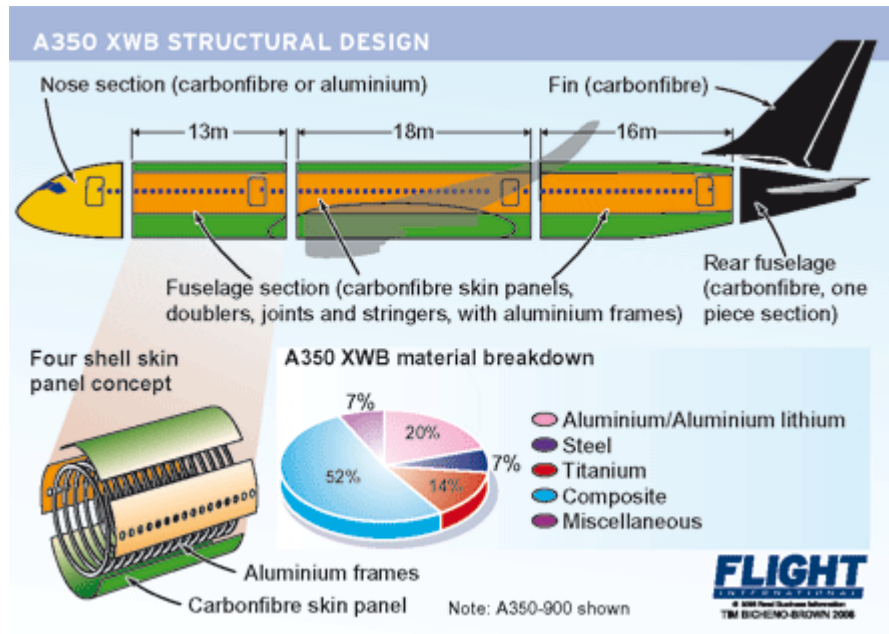


Fig. 1.9: Anticipated application of composites to the Airbus A350 XWB as 52% of structural mass (Kingsley-Jones, 2006)

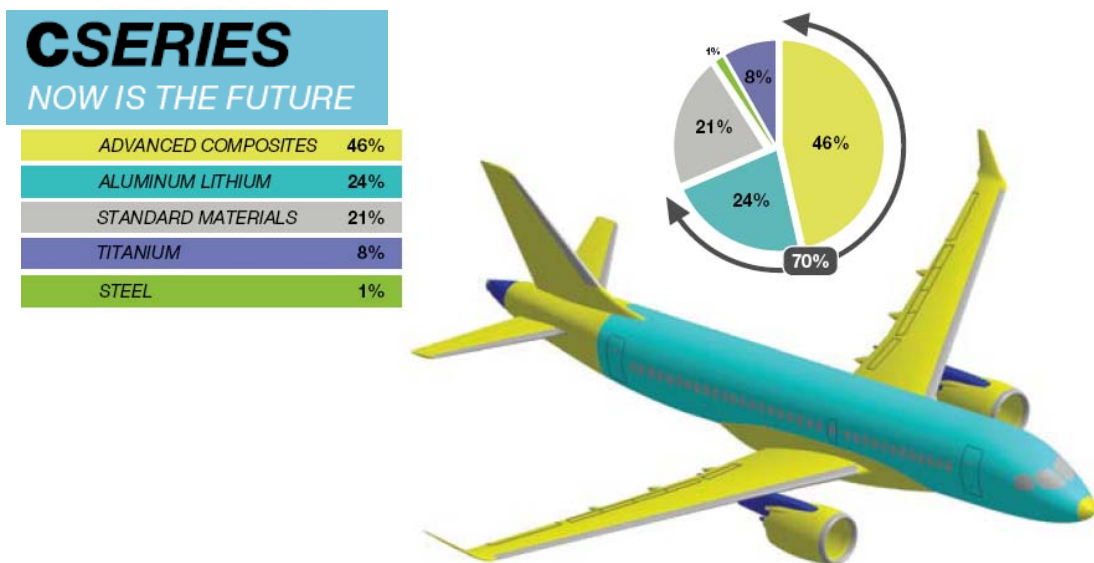


Fig. 1.10: Anticipated application of advanced composites to the Bombardier C-Series CS100 and CS300 as 46% of structural mass (Bombardier, 2008)

1.2 Manufacturing Aerospace Composites

As with most, if not all engineering materials, there are numerous methods by which composites can be processed from their constituent ingredients into technological products. Traditional composite manufacturing techniques in the aerospace industry utilising planar 2D reinforcements have focussed on the need to add positive pressure to the laminate during cure. This is utilised to attain the high fibre volume fractions (55-60%) and low level of voids (<2%) that provide the material properties required for aircraft structures.

This study is focussed on two specific processing techniques. One of these is considered to be the traditional manufacturing technique for aerospace composites and the other, although not new, is not widely used in the commercial aerospace industry. Both methods fall under the generic term 'Vacuum Bag Processing' with one significant difference between them in that the Vacuum Bag and Autoclave (VB+A) approach uses high levels of positive pressure (up to 10 bar) in combination with vacuum, while a Vacuum Bag Only (VBO) approach relies only on the creation of a sealed vacuum environment and atmospheric pressure. Vacuum Bag Processing utilises an airtight membrane sealed to the tool over the uncured part, a vacuum is then drawn through a valve in the membrane while heat and external positive pressure is applied to cure the composite (see Fig. 1.11).

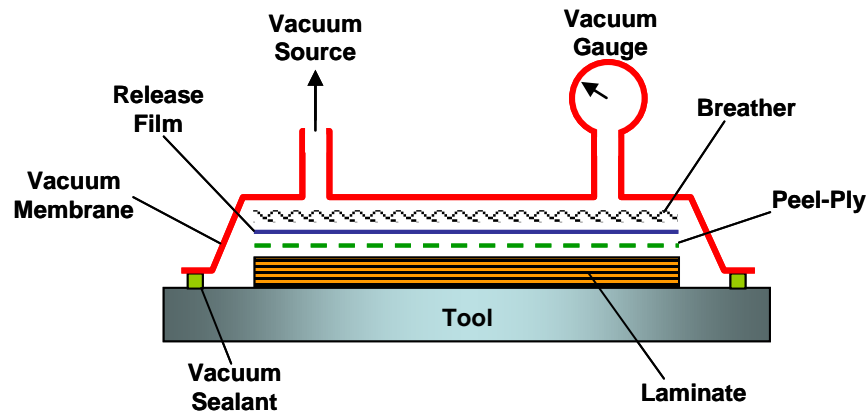


Fig. 1.11: Typical vacuum bag configuration

The purpose of applying this vacuum is to compress the reinforcement to increase fibre volume fraction while simultaneously reducing the volatile release temperature of the composites matrix and helping remove any volatiles from the resin as it reaches minimum viscosity. As discussed the main difference between these two methods is that with the first and more traditional method an autoclave is used to apply a positive pressure (up to 10bar) to the composite during cure while the second uses only a sealed vacuum and atmospheric pressure for consolidation and void removal with a conventional oven or heated tooling to achieve cure. The latter method here is far more energy efficient as it is not necessary to heat ‘parasitic’ air and the whole mass of the tool to achieve a cured composite. There is a further consideration in so far as the reinforcement fabric normally has a power-law compressibility. It is inevitable that vacuum only pressures will never achieve fibre volume fractions attained with autoclave processes. From previous experience for a

woven reinforcement, V_f may be ~35% (no consolidation), ~55% (1 bar) or ~60% (7 bar). Traditional VB+A materials typically provide a higher performance level than those suitable for VBO. This is due to two key factors in VB+A materials where:

- particulate toughening modifiers can be positioned within the ply construction during manufacturing,
- thermoplastic toughening modifiers can be used as the consequent increase in viscosity can be overcome with the high autoclave cure pressure.

Material for VB+A is usually in the form of 'pre-preg' where the fibre is pre-impregnated with resin which is then B-staged by the material supplier. This is usually done by either a hot melt method (where blocks of resin are melted onto the fibre as it is passed through a series of rollers and nips) as shown in Fig. 1.12 or by the fabric passing through a solvent bath (where the resin is pre-dissolved and the solvent then evaporated off with heat after impregnation) as shown in Fig. 1.13. It is usual for pre-preg materials made through the solvent process to require higher autoclave pressures as a consequence of the higher resin viscosity and increased level of volatiles trapped in the product owing to the nature of the process.

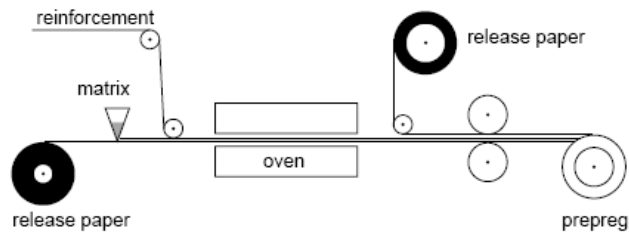


Fig. 1.12: Typical hot-melt pre-pregging schematic (Hexcel Corporation, 2005 a)

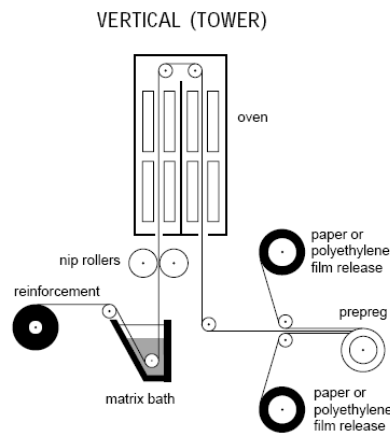


Fig. 1.13: Typical solvented pre-pregging schematic (Hexcel Corporation, 2005 a)

The main barrier to the use of composites on civil aircraft has historically been the high cost associated with the materials and their processing. Consequently this stimulated resin formulators to adapt their systems for use with methods that carry a lower processing cost. This ultimately led to the development of a wide selection of vacuum processing techniques based around the same general principles and known collectively as RIFT (Resin Infusion under Flexible Tooling) processing

(Summerscales and Searle, 2005). As the name implies these methods rely on the use of vacuum (and heat) to form the composite during processing and generally incorporate a similar part lay-up to the autoclave method. The majority of these processing techniques rely on relatively long resin flow distances for the liquid resin being drawn through a dry fibre stack via a pressure gradient limited to one atmosphere drop. This process is shown in Fig. 1.14 and the alternative closed mould approach known as Resin Transfer Moulding (RTM) is depicted in Fig. 1.15. RTM will usually be used instead of RIFT where tighter thickness tolerances, increased geometrical complexity or higher resin pressures are required. Whilst RIFT relies solely on atmospheric pressure to drive the resin due to the limiting consolidation forces available on the vacuum membrane, RTM can utilise additional pressure on the resin due to the use of rigid matched moulding.

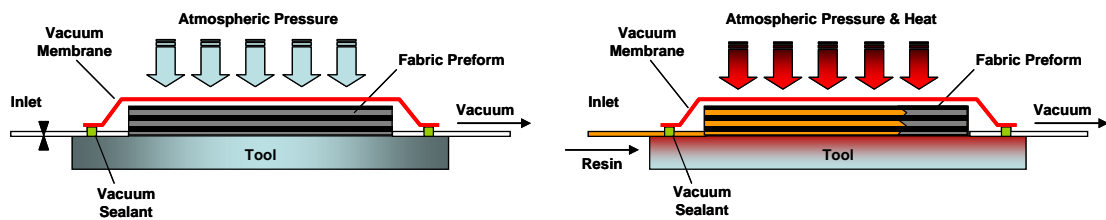


Fig. 1.14: Liquid resin infusion schematic (RIFT)

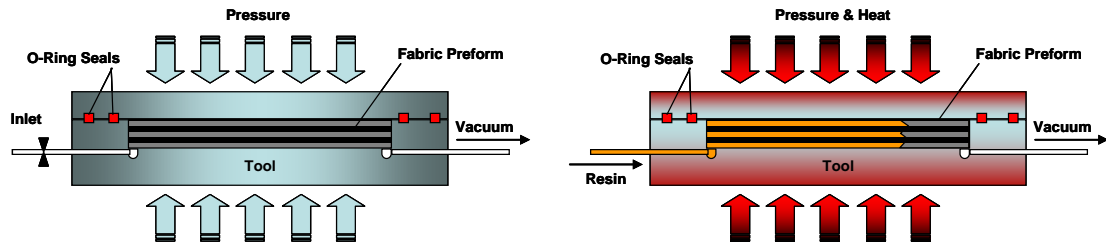


Fig. 1.15: Liquid resin infusion schematic (RTM)

A further method within the RIFT group of processes is known as Resin Film Infusion (RFI) which utilises the resin in the form of a film. The materials used in RFI processing are very similar to the traditional pre-preg materials in that the resin and fibre are both laid into the mould simultaneously, with the difference that the B-staged resin contains no fibre and is applied to the reinforcement in the form of a film to create a semi-preg (i.e. one side dry fibre, one side resin coated), this approach is illustrated in Fig. 1.16. In this process, pressure is applied so that as temperature increases and the resin changes to a liquid state it is drawn into the dry fibre. The dry fibre provides an efficient route for the extraction of any residual air or volatile components, which is a distinct benefit if compared to traditional pre-preg.

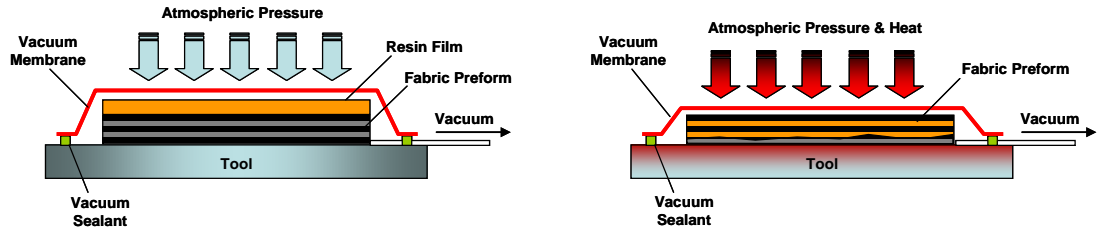


Fig. 1.16: Resin film infusion schematic

Although not a new process in composites processing, RFI is new to civil aviation, and is included in the resin infusion category as offering cheaper and lighter products to new aircraft without sacrificing performance. GKN Aerospace Services are one of the current leaders in this field and as the industrial partners to this study released a significant amount of background knowledge to implement it in this context. The resin for this method is manufactured in a similar manner to the hot melt prepreg production but with the absence of fabric as a carrier. Both the prepreg and RFI material systems used in this study consisted of an epoxy resin/carbon fibre combination. For the majority of aerospace composites, the combination of high temperature capability, solvent resistance and ease of processing make epoxy resin the polymer of choice.

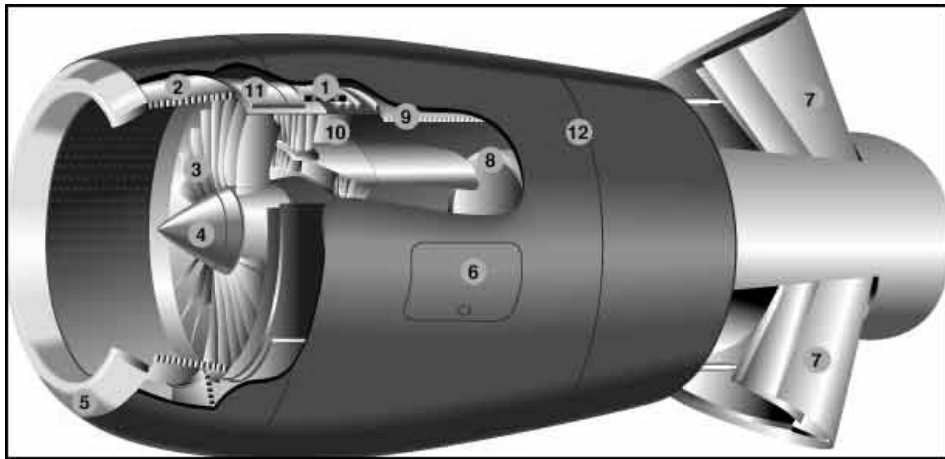
1.3 Project Introduction

The work reported here is based on an industrial study of a proposed manufacturing set of principles for an existing composite

aerospace component. The study aimed to evaluate the potential to balance three important design elements:

- Mechanical properties
- Weight
- Cost

The component of interest was an Acoustic Lining Panel (ALP) found on the inside surface of aircraft engine nacelles (Item 2 in Fig.1.17) and specifically the ALP in the Outer Fan Duct (OFD) of the AS-907 Nacelle. The AS-907 engine is the power-plant of the Bombardier BD-100 Challenger 300 Aircraft, shown in Fig. 1.18.



1.	Electronic Control Unit Casing: Epoxy carbon pre-pregs
2.	Acoustic Lining Panels: Carbon/glass pre-pregs, high temperature adhesives, aluminium honeycomb
3.	Fan Blades: Epoxy carbon pre-pregs or Resin Transfer Moulding (RTM) construction
4.	Nose Cone: Epoxy glass pre-preg, or RTM
5.	Nose Cowl: Epoxy glass pre-preg or RTM construction
6.	Engine Access Doors: Woven and UD carbon/glass pre-pregs, honeycomb and adhesives
7.	Thrust Reverser Buckets: Epoxy woven carbon pre-pregs or RTM materials, and adhesives
8.	Compressor Fairing: BMI/epoxy carbon pre-preg. Honeycomb and adhesives
9.	Bypass Duct: Epoxy carbon pre-preg, non-metallic honeycomb and adhesives
10.	Guide Vanes: Epoxy carbon RFI/RTM construction
11.	Fan Containment Ring: Woven aramid fabric
12.	Nacelle Cowling: Carbon/glass pre-pregs and honeycomb

**Fig. 1.17: Typical composite components found on a generic aircraft nacelle
(Hexcel Corporation, 2002)**



Fig. 1.18: Bombardier Challenger 300 Aircraft

(http://en.wikipedia.org/wiki/Bombardier_Challenger_300, 2008)

The primary purpose of these acoustic linings is to attenuate engine noise and reduce its environmental impact thus assisting airlines to comply with stringent noise pollution regulations. The typical configuration of these parts is a barrelled sandwich structure using an aluminium honeycomb core sandwiched between two fibre-reinforced composite skins. The inner of these two skins is a perforated face sheet that when combined with the cells of the honeycomb and the solid backing face dampens the noise of the engine over a given frequency range in the mode of a conventional Helmholtz resonator, this configuration is illustrated in Fig. 1.19.

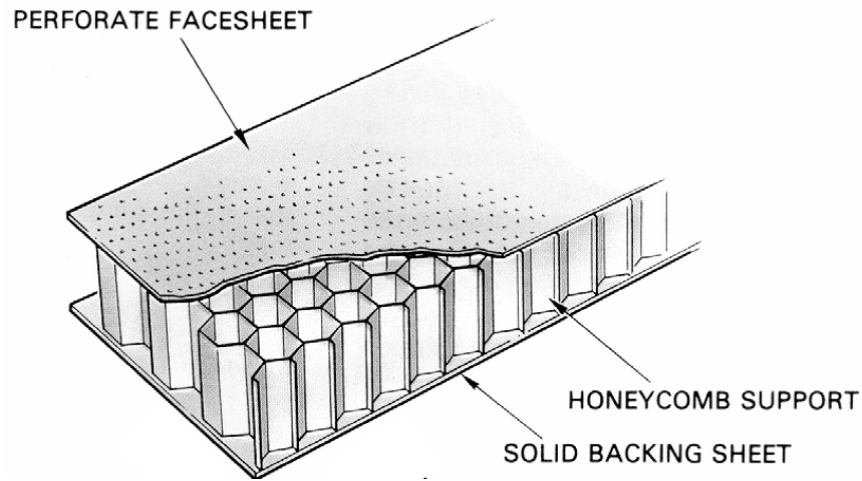


Fig. 1.19: Typical composite acoustic lining configuration (Elnady et al, 2004)

The solid backing face also provides the main structural support to the panel. The perforations of the face-sheet are typically 1-2mm in diameter and can be found at a density of 10,000–40,000 per square metre.

With current acoustic panel technology the perforated acoustic sheet is typically manufactured using an abrasion method to cut the holes. On modern aircraft, composites in nacelle structures account for approximately 50% of the structural component volume yet only 10% of the overall component weight.

With composite versions of these panels, aggressive machining reduces the load bearing capabilities due to fibre damage, and all mechanical properties of the face sheet are usually proportionally reduced during component structural design based on the reduced cross-sectional area. The proposed method for increasing those mechanical properties is to ensure fibre continuity is retained by producing the holes during the

laminate fabrication phase so that fibre follows a deviated path, with no damage, in the laminate. This then introduces the potential for weight saving via the use of thinner laminates and/or lighter cores and cost savings from reduced machining times.

In this approach to the manufacture of acoustic panels, stitched fabrics are preferred over woven configurations due to the reduced constraint from interleaving and their inherent drape properties. RFI is the chosen process because the un-impregnated fibres would have less resistance to in-plane distortion than the pre-impregnated alternative.

1.4 Project Objectives

The objectives of this study were to develop a method for moulding perforated laminates and to investigate differences in their mechanical properties compared to the existing abrasion method. In comparing the mechanical performance of the two methods, there is an additional target of evaluating any changes brought on due to environmental exposure of such a structure. With the microstructures of the laminates expected to vary considerably it must be considered that the presence of higher resin contents around the moulded holes will induce greater environmental susceptibility. Whilst it is beyond the scope of this thesis, it is possible that this may be no worse than susceptibility to machining damage.

The potential benefits from this approach would allow GKN to gain a distinct commercial advantage over its competitors when tendering for future nacelle contracts.

1.5 Project Approach

This study was implemented on an existing flying design so as to incorporate the known performance of an established acoustic pattern and a validated composite configuration for evaluating the differences of both manufacturing approaches. A further opportunity brought by this approach was to evaluate the suitability of an RFI process for the manufacture of acoustic lining panels.

The study followed a structured path from initial process development, through mechanical evaluation to final analysis. The initial stages were a series of development trials to establish a suitable method of moulding the acoustic perforations. Factors such as hole quality, fibre damage/distortion, processing capability and cost were used to evaluate the suitability of each approach. With the process established, each of the material systems were then mechanically evaluated as standard laminates, as drilled perforates and as moulded perforates under both dry/ambient and hot/wet conditions. Each process was then analysed in terms of performance, microstructure and cost to establish the viability of such an approach for part manufacture. To evaluate the structural integrity of a

perforated plate and to provide a direct comparison between each manufacturing approach it was anticipated that data would be generated in both the base-line material system and an alternative. With the initial stress analysis of the component leveraging an area reduction approximation a cross check was included in this study for comparative purposes.

Chapter 2: Literature Review

2.1 Industrial Review

The techniques for the manufacture of continuous fibre reinforced polymer–matrix composites have been reviewed elsewhere (Åström, 1997, Dave et al., 1999, Gutowski, 1997, Campbell Jr, 2003). Certain processes have been considered in greater detail:

- Vacuum bagging, including autoclave cure (Ciriscioli, 1990, Seferis, 2000, Noakes, 1992, McBeath et al., 2000);

- Liquid moulding technologies (LMT) or liquid composite moulding (LCM), including resin transfer moulding (RTM) (van Harten, 1993, Potter, 1997, Rudd et al., 1999, Beckwith et al., 1998, Kruckenburg et al., 2001, Parnas, 2000, Advani, 2000);

- Resin infusion under flexible tooling (RIFT) (Williams et al., 1996, Abraham et al., 1996, Cripps et al., 2000, Summerscales et al., 2005, Beckwith, 2007a, Beckwith, 2007b, Beckwith, 2007c);

- Resin film infusion (RFI) (Black, 2003, Han et al., 2003, Qi et al., 1999);

- Filament winding (Peters et al., 1991);

- Pultrusion (Meyer, 1985 , Starr, 2000);

However, as the focus of this thesis is high-fibre volume fraction continuous high-modulus fibre composites for shell type structures in the aerospace industry, only two of the above are appropriate, namely vacuum bagging with autoclave cure (which is the “traditional” aerospace technique) and the resin infusion family of techniques. As discussed previously the latter has the potential for significant cost reduction in aerospace manufacturing. This potential has been known for some time (Shuart et al., 1998, Potter, 1999, Marsh, 2002), and the specific study of Rudd et al. (1999) found that the application of infusion moulding over traditional pre-preg use could potentially offer relevant savings in excess of 50% per kg composite price. These potential savings are further shown in the extensive study of Bader (2002) where performance equivalence for a variety of material and process options allows a direct weight and cost analysis to be made.

Despite this potential there have been limitations in material performance and process robustness (Smith, 1999, Hubert et al., 2005, Rueckert et al., 2002, Stenzenberger, 1993) that until recently have restricted the wider acceptance of infusion moulding for advanced aerospace serial production. Improvements to process robustness have been demonstrated and studied widely (Hinrichsen et al., 2001, Abaris Training, 2004, Celle et al., 2008, Stadtfeld et al., 2005, Kruckenburg et al., 2001, Heider et al., 2001, Simacek et al., 2002, Koorevaar, 2002) where advances in the understanding of the process fundamentals combined with developments in the field of material technology have given end users the confidence to implement these novel approaches into more demanding aircraft structures. This is specifically evident in the work of Braniff (2002) where the introduction of infusion technology into volume flight surface components has been demonstrated to provide a 20% cost saving for finished component compared with a metallic equivalent. The recent advances in material technology for infusion processing (LoFaro et al., 2003, LoFaro et al., 2005, Mortimer et al., 2005, Abe et al., 2005, Blackburn et al., 2005, Abusafieh et al., 2006, Hexcel Corporation, 2005 b, Beier et al., 2008, Blackburn et al., 2008) have provided a new variety of advanced materials that are starting to open up the wider acceptance for infusion processing. The resulting composite performance is increasingly close to that of new generation toughened pre-pregs without any adverse effects on the processing aspects, offering potential production cost

savings. Of these new materials it has been Hexcel's M36 Epoxy Film (Hexcel Corporation, 2007) that has been of particular interest to this study for its combination of improved properties within the vacuum only RFI process preferred in this study. This preference arose due to the expected higher cost of implementing a liquid moulding tool design and equipment for moulded perforation fabrication. The M36 product is discussed and evaluated later.

Evaluating the implementation of new developments for aerospace applications, Tenney et al. (2001) have reviewed the state of the art at the turn of the 21st Century and concluded that through the combination of (a) new material advancements, (b) the generation of reliability based design methodologies and (c) improving the robustness of manufacturing technology, composites will play a significant part in future aerospace technological advancements. The relevance of this conclusion to the present study is the way in which new product developments may be included in the manufacturing process at the conceptual stage. Interestingly the views on composite product design of Potter (1992) emphasised the necessity to encapsulate all the cross-functional activities through the design cycle stage in order to establish all the potential issues during the development phase of a product.

Reviewing previous work in moulding acoustic perforations it was apparent that Morgan (1989) had demonstrated the suitability of an RTM approach for use on P&W 4000 engine blocker doors of the Boeing 747

and 767 aircraft. Here the approach replaced an existing aluminium configuration and provided an approximate 25% weight saving through the use of integrated design. A concern with this approach for the components in this study were the significant differences in curvature of the components and hence the likely difficulties that could be found with a rigid closed mould approach. In addition an important aspect of the current study was to evaluate moulding methods that were applicable to the existing pre-preg material and to larger structures.

The introduction of holes to continuous fibre composites is known to cause performance reductions due to the stress concentrations and fibre discontinuity. However, it is a necessary feature of composite use for assembly and attachment. An extreme example of this requirement is with the Saab Gripen multi-role combat fighter aircraft, where the carbon fibre reinforced epoxy main wings contain approximately 8000 drilled holes for mechanical fastening (Morgan op. cit.). A further requirement for the introduction of holes in composite structures is (as with the component in question here) where profusion is required (e.g. the attenuation of sound). In these cases the hole sizes and frequency are of an order of magnitude different to those of the previous example. In ALP the scale can be classed as perforations. The typical manufacturing techniques employed for achieving these perforations (as with the component of this study) is mechanical removal of material through drilling. The machining and drilling of composites is an extensive subject in its own right. Many studies

have been conducted to evaluate the effects of machining and drilling on the material and also into design of the optimal tooling to conduct the operations in terms of tool life cycle and machining cycle time (Åström, 1997, Abrate et al., 1992 a, Abrate et al., 1992 b, Gordon and Hillery, 2003). The potential for component damage from these operations is high unless great care is taken in tool and parameter level selection. Fibre break-out at the laminate back face, delamination at the hole edge or the induction of matrix cracking or micro-cracking from the abrasion forces are the usual defect types that can be induced. In addition the heat generation during machining can initiate accumulated thermal degradation of the matrix around the holes.

The effects of perforations on the performance of continuous fibre laminates have been studied previously in the context of a drilling mechanism to bore the holes after laminate production (Abrao et al., 2007, Pahr, 2003). However there is little publicly available analysis of the performance effects of moulding such perforations. Morgan (1989) discusses the implementation of such an approach through liquid composite moulding but data is not presented nor are comparisons made between drilling and moulding effects of the perforations. Pahr (op. cit.) has presented a modelling approach for analysing the influence on laminate performance from acoustic level perforations ($<2\text{mm}$ hole diameter, proportion of affected surface area $>5\%$) on first ply failures. The two-scale modelling analysis developed therein showed good agreement between

experimental and numerical results for first ply failure and stiffness. In a similar, yet less analytical fashion, Godage (2002) has evaluated the drilled perforation effects in composite laminates for GKN Aerospace and specifically those around acoustic liner panels in the fan ducts of the AS-907 and AS-977 engine nacelles. This work established a link between the reduction in laminate cross-sectional area and the static stress concentration of the perforations combining to cause the performance reductions witnessed. The study further observed that through changing the perforation pattern the stress concentrations could be minimised. This led to the idea of tailoring hole pattern for optimal acoustic and mechanical performance in the future.

2.2 Biomimetic Design Considerations

An interesting associated topic for this study is that of Biomimetics. This developing area is an enabling discipline which looks towards biology and other aspects of nature for ideas that may be adapted and adopted for solving engineering problems (Benyus, 1997, Forbes, 2005, Hawken et al., 1999, Smith, 2002, Vogel, 2003). Tenney et al. (ibid.) regard the area as an important source of ideas for future step changes in aero technology. Chen et al. (2002, 2004), used scanning electron microscopy to study the cuticle of an insect: the Hydrophilidae beetle. Insect procuticle is a composite of chitin fibres (bundles of high molecular weight polysaccharide microfibrils)

in a proteinaceous matrix which is protected by an outer epicuticle (wax, lipid and protein without the fibres) layer. The layers are thus similar to structural laminate (procuticle is typically 10-100 μm thick and provides shape and mechanical stability) and gelcoat (epicuticle is 0.1-0.5 μm thick and acts as an environmental barrier). The fibres in the procuticle are arranged in a series of thin lamina with various orientations for which several models exist. Chen et al (ibid.) found evidence to support several of these models dependent on the position within the cuticle. At holes in the cuticle (pore canals), the fibres were found to “round these holes continuously”. This configuration was implemented in $0^\circ/90^\circ$ woven glass fibre composite with holes preformed around circular pins and compared to drilled holes in the same laminate. The preformed holes consistently gave higher tensile strengths than the drilled holes with the percentage relative gain increasing with the hole size (from 37% for a 4 mm hole to 52% for a 14 mm hole). Unfortunately, the paper gives neither the specimen width (a width of ~25 mm is implied by one of the Figures) nor the strength of the laminate without a hole.

Gunderson and Hall (1993) studied a preformed-hole design that allows for fibre continuity in the region surrounding the hole. Preforming redistributes the stresses with respect to a conventional drilled-hole composite. The design significantly improved open-hole tensile and compressive strength but reduced bearing strength for the preformed-hole specimens in comparison to the drilled-hole specimens. The improved

properties corresponded to failure mechanisms being distributed through a greater volume of material in the preformed-hole specimens relative to the drilled-hole specimens, thus demonstrating improved damage tolerance.

Skordos et al. (2002) studied the functional design of a campaniform sensillum in *Calliphora vicina* (commonly known as the blowfly or bluebottle). The sensillum transfers environmental information to the insect's nervous system by mechanical coupling, transduction and encoding mechanisms. It is generally an oval opening in the cuticle (6-24 μm long by 2-5 μm wide) covered by membrane layers. The chitin microfibrils in the cuticle extend around the hole so that it is equivalent to a formed hole in a sheet of fibrous composite. A 2-D finite element analysis was undertaken for circular and elliptical (with the major axis equivalent to the circle diameter) holes. For circular holes in a tension field, the maximum strain energy density (MSED) relative to a specimen with no opening was increased by 4.6 times (formed hole: FH) or 11 times (drilled hole: DH). For an ellipse with the major axis parallel to the tensile axis the increases were 2.6 times (FH) and 4.6 times (DH). For an ellipse with the major axis normal to the tensile axis the increases were 9.7 times (FH) and 22.0 times (DH). The formed hole had an MSED value about half that of a drilled hole in all three cases: the ratio DH/FH was 1.82 (parallel ellipse), 2.29 (normal ellipse) and 2.36 (circle).

These biological occurrences of reinforced or 'moulded' holes suggest how hole moulding might be implemented into a composite

laminate. This is particularly pertinent to infusion processing of dry textile reinforcement prior to cure.

2.3 Preforming

Weimer et al. (2000) considered the approach of net shaped preforming where the holes were made prior to the introduction of the resin matrix and without breaking the reinforcing fibres. Although this work was specifically targeted at low frequency large holes for the purpose of fastening and joining, it did conclude that the approach offered cost-effective post process integration, despite the strength reduction seen in moulded holes over drilled counterparts with some reinforcement styles under tensile loading. It was found that the cases with reductions present were attributed to the damaging effect punching the holes had on the dry fibres. This was supported further through the improved performances found in textiles with lower fibre coverage than those with the reductions (e.g. open structure 3D weave showing improvements over highly nested structure NCF's). Further to this Warrier et al. (1999) demonstrated that in multi-directional laminates the effects of through thickness (embroidered) reinforcements around a hole can significantly improve the load levels before damage onset.

Several studies analysing the potential benefits of moulded singular holes have been conducted (Warnet et al., 2007, Chang et al., 1987, Lin et

al., 1995 a, Lin et al., 1995 b) with differing conclusions being drawn about the validity of the approach when considering a single hole. For example, Warnet et al. (2007) found that utilising an open moulded hole over a drilled hole in flat braided composites did not provide any strength increases, although the hole geometry of the work is not clearly presented. In the works of Chang et al. (op. cit.) and Lin et al. (op. cit.) the presence of moulded holes over drilled holes in some cases did show strength improvements with Lin concluding that the benefits of moulded holes is more prevalent when edge distances are smaller. Further to these studies Ng et al. (2001) found that the failure sequence of a singular moulded hole can be well predicted by a progressive failure analysis establishing that initiation of tensile failure occurs in the matrix first at the hole edge and then rapidly progresses across the laminate cross-section. The load directed yarns then receive the load prior to tensile failure.

This foregoing review supports the investigative and experimental exercise carried out in the present study and provides useful reference data for the prediction and analysis of the experimental approaches. It also highlights the criticality of maintaining fibre integrity when considering moulded hole configurations in composite material.

Chapter 3: Manufacturing Trials

3.1 The Acoustic Liner Panels (ALPs) of the AS-907 Outer Fan Duct (OFD)

There are two important aspects in the design of ALP components: the pattern of the acoustic perforations and the mechanical properties of the virgin face sheet.

The hole pattern specified for optimum performance of the AS-907 OFD ALPs, from the initial programme design, requires a hole diameter of 1.58mm (± 0.08 mm), linear pitch of 8mm (± 0.64 mm) and an inter-row off-set pitch of 4mm (± 0.64 mm). This combination gives a face-centred square/hexagonal array design as illustrated in Fig. 3.1. Normally these panels are moulded to a specific curvature to match the barrelled nature of engine nacelles. However for this study, all laminates produced were flat for ease of manufacture, testing and analysis. The curvature requirement was kept in mind for manufacturing suitability. For the initial development of a moulding process a plaque size of 100x100mm was selected incorporating 200 perforations in the AS-907 pattern, as illustrated in Fig. 3.1.

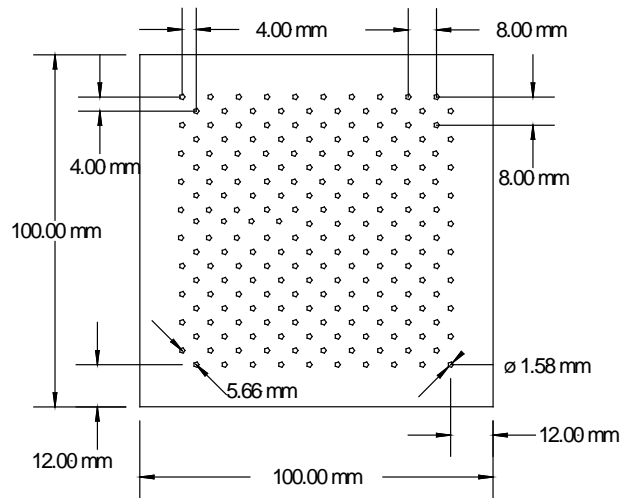


Fig. 3.1: Perforation pattern for development plaques

The materials used in the original component design are carbon-epoxy laminate incorporating a standard modulus AS4 fibre and toughened pre-preg 8552 epoxy system, both from Hexcel Composites Inc (Hexcel Corporation, 2003). The grade of this pre-preg material used was a 280g/m^2 five-harness satin weave of 3k AS4 fibres pre-impregnated with the 8552 epoxy. This was then configured in four plies of 0° and 90° fibre orientations balanced as $[(0/90)_2]_S$ given the orthogonal fibre orientation on different fabric faces. At the time of design this material offered GKN the state-of-the-art in terms of composite technology performance but through the use of a five-harness weave the designer will have required a 3k carbon tow for minimal fibre distortion at the cost of using a higher priced fibre. With most fibre types costs are similar for 3k and 6k tows, but increasing tow size to 12k typically halves this material cost (Rudd et al., 1999).

The use of aluminium honeycomb to create the sandwich structure requires that the design also incorporates an additional ply of glass pre-preg scrim between the skin and core for protection against galvanic corrosion.

With the project taking a fresh look at the manufacturing methodology for the selected component, it was also appropriate to evaluate improvements to composite materials technology made since the original design. Not only was the established pre-preg material evaluated with respect to moulding holes but also a different processing approach was analysed giving a direct comparison to the base-line production route and also the principles of moulding the acoustic perforations.

3.2 Selecting Alternative Materials

The alternative process evaluated alongside the base-line pre-preg was Resin Film Infusion (RFI). By utilising RFI, additional potential cost savings could be added to the investigation in the forms of:

Flexibility in fibre/reinforcement selection through a non-impregnated material;

Component weight savings through lower resin density specific to the M36 matrix (10% reduced resin density translates to 3% reduced composite density) and;

Increased productivity since an autoclave is not required for cure.

Utilising data collected from previous GKN programmes, it was known that an equivalent thickness design in RFI for the AS-907 configuration would require 900 g/m² of carbon and 500 g/m² of epoxy resin film. This film was another Hexcel product, M36, and was selected due to its previous qualification for production use by GKN. At the time of this work it was the only known resin film system of aerospace grade on the market that was suitable for vacuum-only manufacture. A film at a weight of 250g/m² was available for the study at GKN. The relative performance of the two resin systems is shown in Fig. 3.2. Both matrix systems are toughened through thermoplastic inclusions with the higher toughness of 8552 a result of a higher thermoplastic loading. The modulus and strength differences can be assigned to differences in the cross-link density achieved in each.

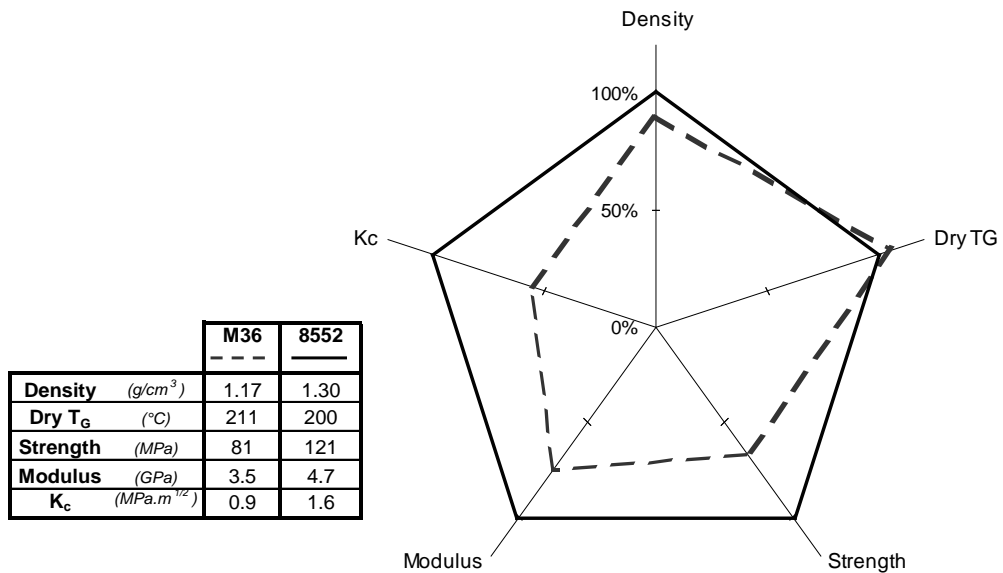


Fig 3.2: Comparing matrix properties

[Compiled by author from product datasheets]

The scope of reinforcement selection possible with RFI meant high deposition type reinforcement could be evaluated for the potential of reducing costs through the larger tows (~12k) and reduced lay-up times. In this instance non-crimp fabric (NCF) reinforcement was selected for evaluation due to a combination of attributes:

Tape like construction

Ability for in-plane fibre manipulation

Possible suitability for hole moulding

Availability in high areal weights ($>300g/m^2$)

NCF's are a reinforcement style used extensively in the marine and wind turbine composite industries and have long been thought to hold huge potential in the aerospace industry through providing tape like performance for out-of-autoclave processing. Improved fibre dependent properties are achieved through the reduced deformation (or crimp) of the fibres in the fabric architecture. Purely unidirectional fibres are difficult to use in resin infusion due to low permeability; woven fibres incorporate crimp (common styles illustrated in Fig. 3.3), and therefore yield reduced in-plane mechanical properties and also require an ancillary material to hold the fibres in place.

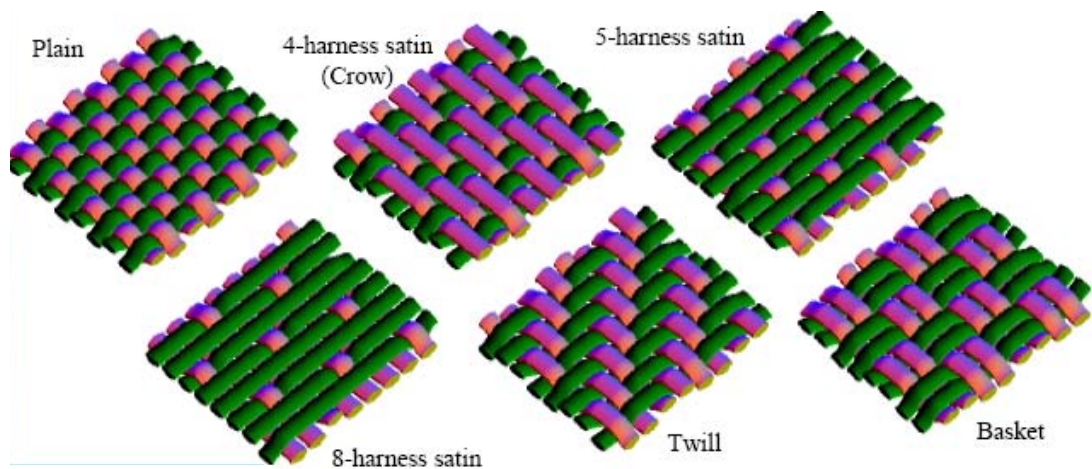


Fig 3.3: Common 2D weave styles (Bolick et al., 2006)

NCF's are layers of aligned uni-directional fibres held together by a stitching process. These materials can range from a simple two layer bi-axial construction to more complex and heavier architectures where each

ply of the NCF is equivalent to a single tape ply. The presence of the stitching does cause some small disruptions to the fibres causing the materials not to be true 'non-crimp' and which gives a small in-plane performance deterioration compared to unidirectional fibre performance.

Although a 5-harness satin was studied rather than NCF's, LoFaro et al. (2004) found that polyester stitching in preform assembly reduced the tensile and compression performance of the laminate by between 10-15%. As discussed by Bibo et al. (1999) initial developments in carbon NCF's demonstrated significant reductions in performance levels compared to unidirectional pre-preg. More recent advances in NCF technology as discussed by Blackburn et al. (2008) and a greater understanding of the effects of the stitching have led to improved properties and hence a wider acceptance of these textile forms within the aerospace industry. Here Blackburn demonstrates a 17% reduction in 0° Tensile Strength is observed in uni-directional NCF's compared to the pre-preg tape equivalent. Any remaining knock-down factor is compensated through the multi-axial characteristic of these materials that give the equivalent of multiple plies to be positioned in a single operation and the consequent manufacturing benefits. When this is combined with the fact NCF's use high filament count tows to achieve their coverage then it becomes easy to see why their performance and cost effectiveness are attractive to the aerospace industry.

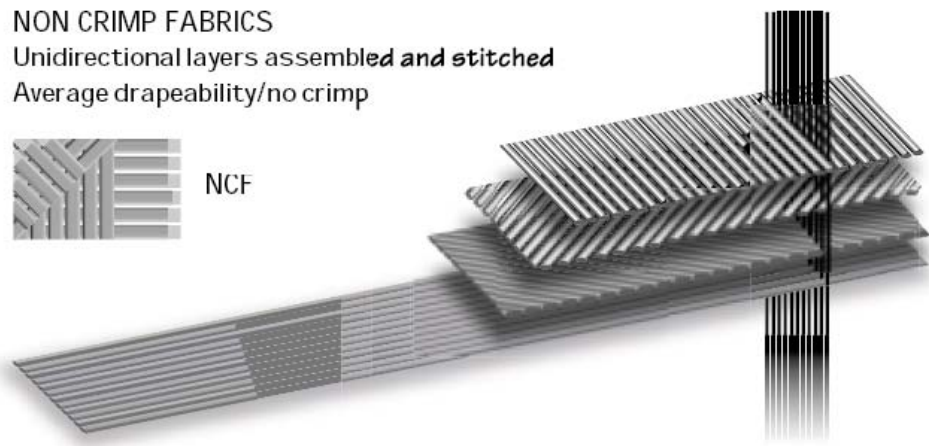


Fig. 3.3: Example construction of multi-axial NCF

(Hexcel Corporation, 2005)

The process of moulding acoustic perforations into a thin plate would be expected to cause gaps in a dry fabric, so it was decided to consider an NCF lay-up greater than two plies thick, since for each distorted tow there is a higher probability of a less distorted tow being in an adjacent ply to help bear any loading. With this in mind a suitable equivalent NCF lay-up would thus consist of two plies of resin film combined with one of the following lay-up choices wherein the resin placement approach would have to be considered (i.e. interleave vs. bulk layer):

Table 3.1: Theoretical lay-up options for equivalent NCF panel

No. of plies	4 x 300 g/m ²	4 x 225 g/m ²	6 x 150 g/m ²
Orientation sequence	[0/90, 90/0] _s	[0/90, 90/0] _s	[0/90, 90/0, 0/90] _s

The final selection for the project was dependent on the quality available in low areal weight NCFs ($<250\text{g/m}^2$ per layer) where tow spreading is required to minimise fibre gaps. The commercially available areal weights of suitable quality and cost fabrics eliminated the lighter configurations leaving a 300g/m^2 nominal target areal weight. Allowing $\pm 5\%$ on the nominal target gave a range of $315\text{-}285\text{g/m}^2$ bi-axial configuration ideally incorporating standard modulus carbon fibres. From sampling various manufacturers in the NCF market two products were found to meet these requirements. The first of these was a T700 310g/m^2 from Saertex. This utilised high filament count tows (24k) to retain fibre coverage at the low areal weight. The second material was a 12k HTA 285g/m^2 from Devold. This was specially manufactured for this investigation and demonstrated a lower amount of fibre spreading in the tows resulting in a very open textile. This was accepted for further evaluation at the early stage of the investigation as it was not known whether the increased fibre gaps would counter the distortion likely to be induced during the perforation moulding. A comparison of the baseline 3k AS4 fibre against the 24k T700 and 12k HTA is illustrated in Fig. 3.4.

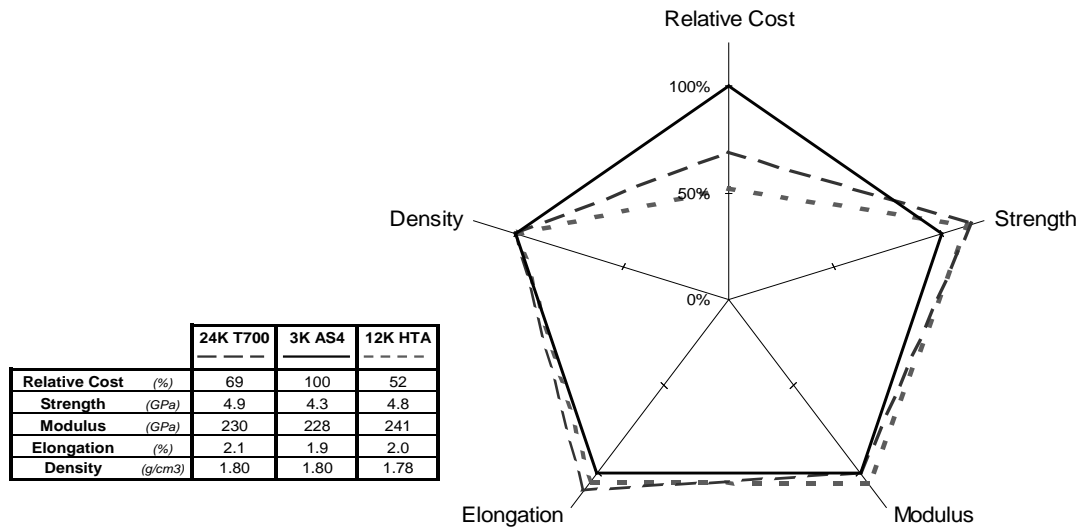


Fig 3.4: Comparing fibre properties

[Compiled by author from manufacturer's information]

3.3 Alternative RFI Processing Methodologies

Although GKN had established and qualified an RFI process with M36 resin it was deemed appropriate for this study to investigate alternative approaches for perforation moulding. The existing RFI process relied on an interleaving approach with a ply of resin film placed adjacent to each ply of fabric. With the process of moulding perforations requiring an array of micro-scale mandrels inserted through the thickness of an uncured laminate there are benefits in reducing fibre distortion if the interleaved resin could be confined to a surface stack and reduce any additional resistance on the fibres' movement. This approach has the potential to optimise the RFI process through allowing maximum fibre manipulation and lay-up flexibility. However, this still left a question over

the key change to the infusion approach. With the existing method, the interleaved resin was only required to infuse the thickness of one carbon ply of approximately 0.5mm (with 450g/m² carbon reinforcement). Whilst there may be benefits in using the fibre as a dry stack and infusing the resin film through the full thickness, the method was un-tested. To investigate this further a series of trials was conducted to evaluate variations on the existing RFI process using the two NCF products selected in four stacking sequences of:

Standard interleave as a base-line (Fig. 3.5)

Resin stacked on bag surface (Fig. 3.6)

Resin stacked on tool surface (Fig. 3.7)

Resin split between tool and bag surface (Figs.3.8)



Fig. 3.5: Configuration of GKN's current RFI process



Fig. 3.6: Proposed configuration of resin film positioned on fibre stack



Fig. 3.7: Proposed configuration of resin film stack under fibre stack



Fig. 3.8: Proposed configuration of fibre stack sandwiched between resin film

For each sequence the panels were laid up in a 12 ply quasi-isotropic configuration using the process control limits established from GKN's qualification of the M36 resin film system outlined in Fig. 3.9.

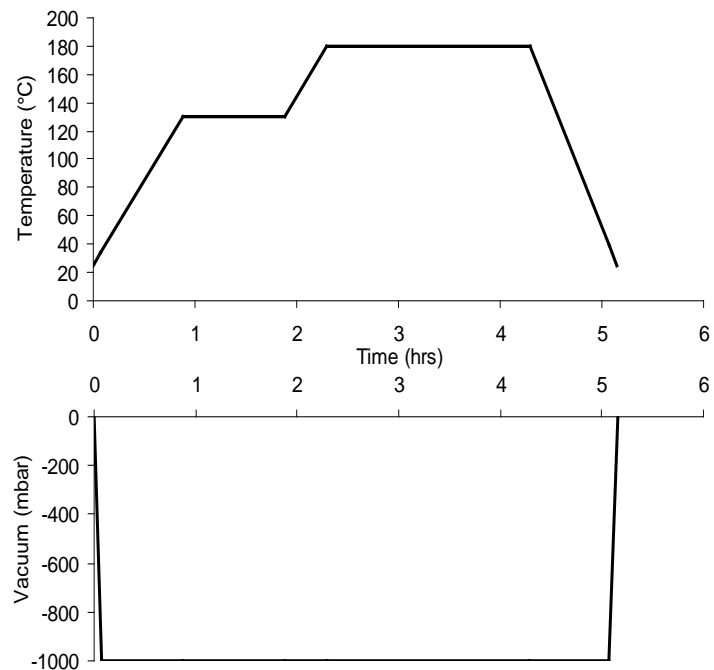


Fig. 3.9: M36 RFI Process Profile

(Typical process tolerances: $\pm 1^\circ\text{C}/\text{min}$ on ramps, $\pm 3^\circ\text{C}$ on holds and vacuum levels of within 20mbar absolute and a leak rate to reach no higher than 70mbar after 5 minutes)

Each panel was evaluated through visual inspection, cured ply thickness (CPT), fibre volume fraction and void content (both via acid digestion). The results of these are shown in Table 3.2 and are ranked in accordance with their visual evaluation for surface defects, here the ranking system was developed by the other around the detailed inspection of the laminate quality.

Table 3.2: Analysis results from through thickness non-perforated infusion trials

<i>NCF</i>	Configuration	<i>Visual</i>	CPT (mm)	V _f (%)	V _v (%)	Rank
24k T700	Interleaved	Surfaces showing no surface cavitations or dry spots. Resin infused uniformly. Carbon tows aligned with minimal gaps.	0.308	55.9	1.2	1
	Sandwiched	Slight resin richness on each surface. Carbon tows aligned with minimal gaps.	0.337	51.1	1.2	4
	Resin tool side	Surfaces showing no surface cavitations or dry spots. Resin infused uniformly. Carbon tows aligned with minimal gaps.	0.311	55.3	0.9	1
	Resin bag side	Surfaces showing no surface cavitations or dry spots. Resin infused uniformly. Carbon tows aligned with minimal gaps.	0.309	55.8	1.1	1
12k HTA	Interleaved	Surfaces showing no surface cavitations or dry spots but resin rich pockets at inter tow gaps.	0.291	52.2	1.0	5
	Sandwiched	Surfaces showing no surface cavitations or dry spots but resin rich pockets at inter tow gaps.	0.288	53.4	1.2	5
	Resin tool side	Surfaces showing no surface cavitations or dry spots but resin rich pockets at inter tow gaps.	0.293	53.3	1.2	5
	Resin bag side	Resin rich central spot on bag surface at 50% coverage with resin rich pockets at inter tow gaps.	0.287	54.5	1.2	8

NOTE: Ranking score based on 1 = Best, 8 = Worst

One of the main results of this work was an obvious difference in the fibre spreading in the two fabric types, with the smaller tow size of the lower weight 12k HTA material causing poorer fibre coverage and resulting in a poorer surface quality. The conclusions drawn from these trials were that the RFI approach is flexible enough to utilise a through-thickness infusion approach without detriment to laminate quality while the T700-based NCF was the better product for the project based on the reduced fibre deviation (resin rich tow gaps) and the slightly better compaction. For the remainder of the study a full through-thickness approach was maintained as opposed to the standard interleaf configuration.

3.4 Viable Pin Materials

In moulding perforations into a carbon fibre laminate the obvious approach is the use of a tooling mandrel for each hole, which requires a bed of pins. Such an approach offers a wide selection of potential materials. Evaluating the requirements of the materials highlights the properties of particular interest to be:

Dimensional stability at 1-2mm diameters

Thermal stability up to 200°C

Surface co-efficient of friction (for removal ease)

Inert to resin system

In addition there were standard considerations such as cost, life-cycle and complexity. As well as the variation in material type there were also different approaches to how the mandrel pins could be used, utilising one or more of the materials. These could be separated into three groups of non-reusable, semi-reusable and reusable pins. With the properties of interest established it was feasible to identify a list of potential materials under each pin type; these are categorised in Table 3.3.

Table 3.3: Categorised options for mandrel material selection

Mandrel Type	Non-reusable	Semi-reusable	Reusable
Material Type	Eutectic salt (water soluble ceramic)	Temporary powder coated aluminium pins	Small PTFE tubing with reinforced insert
	Sodium silicate bonded sand		
	Polyvinyl alcohol bonded micro-spheres		Expanding rubber coated metallic pins
	Gypsum plaster		
	Aquacore™/Aquapour™ (water soluble polymers)		Release coated metallic pins
	Macro carbon tubing		
Low melt temperature alloy (e.g. tin-lead-bismuth)			

Analysing each of these categories offers a method of selection for
a) mandrel use and then b) processing efficiency.

A non-reusable mandrel would offer the benefit of the pins being melted or washed from the cured laminate and hence eliminate the problems associated with the physical removal of a tool through the thickness of the laminate. However, such an approach brings a relatively higher processing cost per hole produced and a low recycling factor. In the case of a lead-tin alloy this represents an approximate processing cost of 10p per pin with 90% of the material non-reclaimable in each production cycle. In addition the low rigidity and toughness of materials in this category are potentially problematic for the insertion process; this is particularly apparent in the ceramic materials due to their brittle nature. Any of the low melting point alloys under this category are generally soft and malleable making these small diameter pins susceptible to damage and distortion.

Semi-reusable pins offer the potential to combine the advantages of non-reusable and reusable mandrels. A 'wash-away' coating would bring the removal benefits of non-reusable pins while a metallic or composite core would offer reduced tooling costs and improved dimensional stability over a non-reusable approach. One area likely to cause difficulty would be the achievable tolerance on coating thickness over an array of pinned mandrels.

Reusable pins would probably offer the lowest process cost per hole, provided a suitably robust material is utilised. This approach may also offer the most acceptable level of variability in hole quality ensuring

acoustic performance levels are maintained at their current level. This approach however will bring the problems of overcoming the frictional and bond forces for removal and the risk of parts having irremovable pins in serial production increasing the risk of component scrap.

After careful consideration and extensive research into availability, cost and practicability the selection of pin materials was narrowed down to a choice of three. These were two water-soluble non-reusable systems (discussed in Section 3.5) and one re-usable metallic system (discussed in Section 3.6). Each approach was then taken forward for further investigation through processing trials with through-thickness RFI.

Table 3.4: Decision matrix for mandrel material down-selection

Material	Mandrel Type	Availability	Manufacturing	Life Cycle	Cost	Total
Eutectic salt (water soluble ceramic)	Non-reusable	✓	✓	✓	✓	4
Sodium silicate bonded sand	Non-reusable	✗	✗	✗	✓	1
Polyvinyl alcohol bonded micro-spheres	Non-reusable	✗	✗	✗	✗	0
Gypsum plaster	Non-reusable	✓	✗	✗	✓	2
Aquacore™/Aquapour™ (water soluble polymers)	Non-reusable	✓	✓	✓	✓	4
Macro carbon tubing	Non-reusable	✗	✗	✓	✗	1
Low melt temperature alloy (e.g. tin-lead-bismuth)	Non-reusable	✗	✓	✓	✗	2
Temporary powder coated aluminium pins	Semi-reusable	✗	✗	✗	✗	0
Small PTFE tubing with reinforced insert	Reusable	✗	✗	✗	✓	1
Expanding rubber coated metallic pins	Reusable	✗	✗	✗	✗	0
Release coated metallic pins	Reusable	✓	✓	✓	✓	4

NOTE: Score based on 4 = Best, 0 = Worst

Using the decision matrix in Table 3.4 three tooling approaches were selected for research trials in the form of:

- Aquacore™/Aquapour™ - Advanced Ceramics Research Inc. (Water-soluble polymers, Section 3.5)
- Ceramcor - Ceramic Core Systems Ltd. (Water-soluble ceramic, Section 3.5)

- FlexPerf™ - Aztex Inc. (Release coated metallic mandrel system, Section 3.6)

3.5 Water Soluble Tooling

The use of a soluble tool removes the problem of overcoming frictional forces and bond strengths without causing laminate damage associated with removing re-usable tooling. An additional performance benefit may be attainable if the tool can be dissolved after secondary bonding to honeycomb has taken place. This will reduce the percentage of blocked holes associated with this stage of the production process and hence retain the designed acoustic performance. These grades of tooling materials rely on being dissolved to a solution state in water to enable their initial shaping and casting with the residual moisture then being evaporated to leave a solid tool on which further processes can be applied.

3.5.1 Aquacore™/Aquapour™

Background

These materials are a product of research and development company ACR, based in Tucson, Arizona, whose main activities are based around Fibrous Monolithic Composite Ceramics and Rapid Prototyping/Manufacturing. Their Aquacore™ and Aquapour™ products are marketed as water-soluble tooling materials for complex polymer

composite parts and honeycombs. The materials consist of ceramic microspheres blended into a thermally resistive polymer. In essence both materials are equivalent but in different forms. Aquacore™ is a ready-to-use pre-mixed paste and Aquapour™ is in powder form requiring the addition of water before use. Both products are marketed as being stable up to 190°C and soluble in cold water. To aid the investigation of these products a flexible master mould was manufactured utilising a silicone rubber cast around an array of metallic pins. Due to the time constraints of the investigation the master mould was created around an existing array of pins. Although not identical to that of the AS-907 design this was similar enough to be representative for manufacturing trials (i.e. dimension and frequency of pins) and its availability reduced the development time for these trials.

Aquacore

The pre-mixed variant of this tooling system has a texture similar to that of damp coarse sand giving it a degree of shape retention when unsupported, allowing room temperature moulding. Three trials were conducted with this product utilising the silicone master mould and atmospheric pressure. To produce the mandrels the mixture was transferred to the mould and consolidated under vacuum, this was done in stages in order to compact the material into the tight pin dimensions. The mould was then heated to 125°C for three hours under vacuum to set the material, a

slow cool down rate was then used to reduce the risk of damage through thermal shock. At room temperature the parts were removed from the mould for evaluation, as shown in Fig. 3.10. It was found that this material is not suitable for intricate mouldings of this scale due to the brittle nature of the fine detail structure.

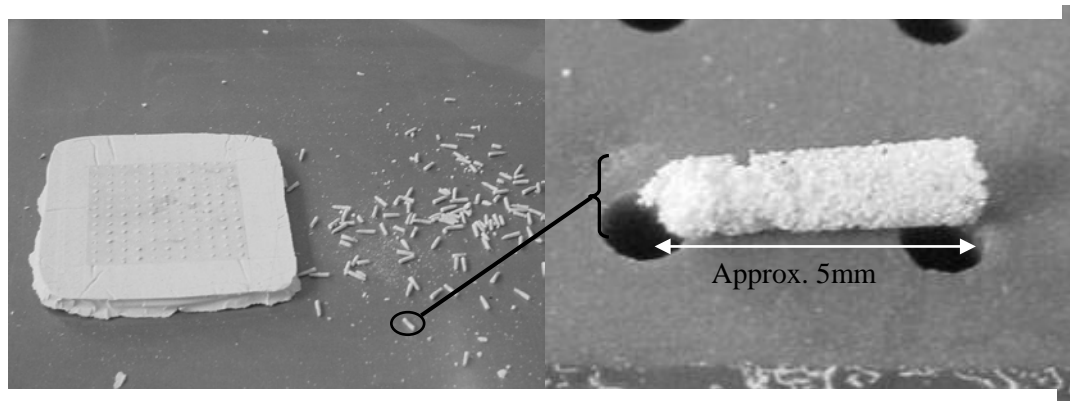


Fig. 3.10: 100% Pin fracture of Aquacore cast detailing poor pin surface definition

As shown, complete pin breakout was observed during de-moulding, on close inspection the surface of the fractured pins was found to suffer from poor definition with a highly porous structure.

Aquapour

The powdered grade of the material required pre-mixing with water at a recommended ratio of 8 parts powder to 3.5 parts water by volume (or 5:3 by weight). Once mixed to a liquid suspension the Aquapour was

poured into the mould based on the claim of effective use in taking up intricate shapes.

Following this procedure, three trials were conducted to investigate the possible benefits in pin definition that the water-based mixture appeared to offer. However the results upon de-moulding the tool were 100% pin fracture with poor pin definition.

Conclusion

The results of these trials adequately demonstrated that both forms of this particular material were unsuitable for this application due to the materials' low toughness and poor stability when used on an intricate micro-scale.

3.5.2 Ceramcor

Background

Ceramic Core Systems Ltd is a UK company with expertise in water soluble ceramic tooling. The product, marketed as Ceramcor, is a powdered eutectic salt that can be moulded into a fused solid. It is available in various grades, each of which has a different processing temperature and final toughness. Processing the material requires the powder to be heated to its molten state and then cooled to enable casting. One particular benefit is

that once set it can be melted back down and re-cast without any degradation in its properties.

Material

The grade investigated for this project was Ceramcor 145, due to its relatively low melting point of 160°C and casting temperature of 170-180°C. The solubility rate for Ceramcor is approximately 10min/kg at a water temperature of 60°C where the ‘wash-out’ characteristic is due to 70% of its constituents being water-soluble. Once dissolved Ceramcor cannot be reclaimed in the same form. The ability to re-melt the material required any laminate production to be done with a dual cure approach where the initial perforation moulding be done at <160°C followed by a free standing post cure of the laminate at 180°C to achieve the required thermal performance.

Tooling

An effective way of melting the material was found to be a conventional non-contact element deep fat fryer, where the high temperatures could be applied to the powder while it was hand-stirred to achieve a uniform temperature. The same mould as with the Aquacore™ products was used to provide a flexible yet resilient tool into which the hot fluid could be cast.

Moulding Trials

As shown in Fig. 3.11 the first moulding trial produced a poor quality casting due to trapped air in the mould coupled with a thermal shock lock-off caused by the temperature difference between the molten material and the cooler mould.

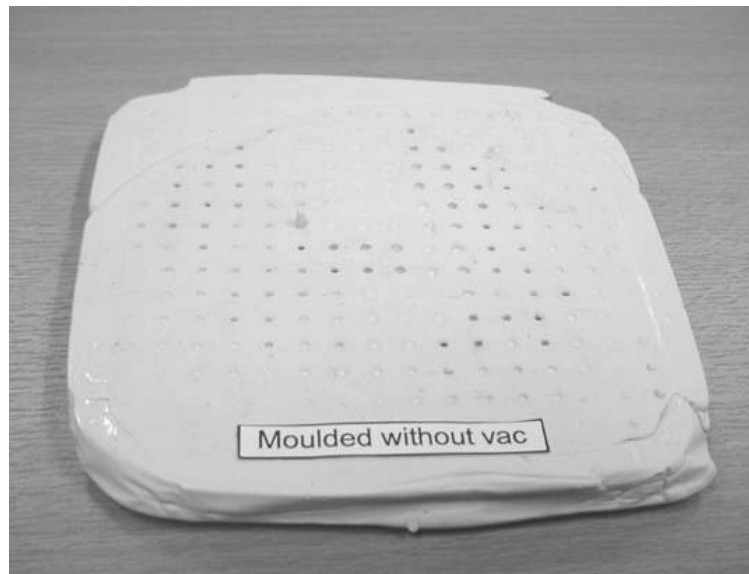


Fig. 3.11: Ceramcor moulding trial showing zero pin formation due to trapped air

To alleviate the problem of trapped air during casting, the base of the tool was pierced and subjected to vacuum to evacuate each cavity. Figure 3.12 shows the improvement achieved in material flow through this modification.

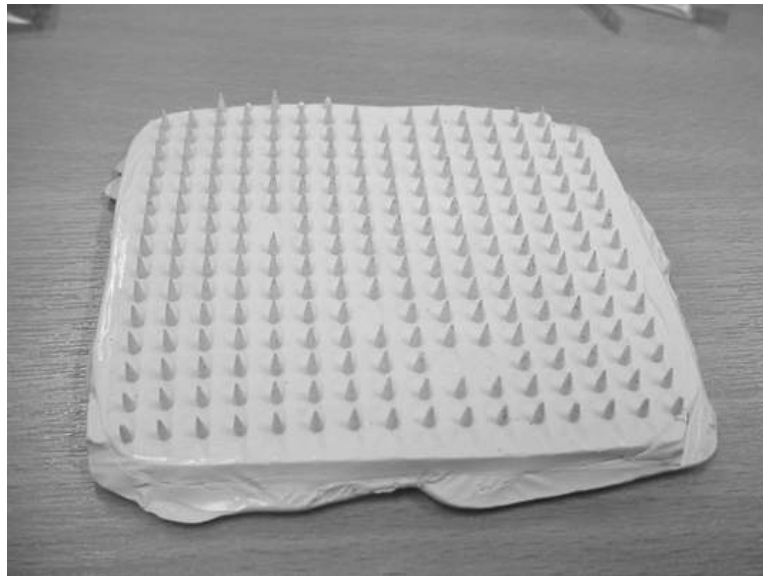


Fig. 3.12: Ceramcor moulding trial showing >95% pin formation due to vacuum

Further trials were conducted into the de-moulding temperature of the castings, with the results demonstrating that a de-moulding temperature of less than 100°C should be achieved to avoid damage. Trials were also conducted using various reinforcements to provide greater stability, most of which proved unsuccessful due to the resistance presented by the effective filtering of the reinforcements. An example of this is shown in Fig. 3.13 where steel gauze was utilised for reinforcement but prevented the formation of pins in a large central region due to flow restriction.



Fig. 3.13: Reinforced Ceramcor moulding showing flow issues caused by change in permeability

Through further adaptation of the mould to improve the vacuum connection, it was possible to produce tooling with 100% pin formation (see Fig. 3.14).

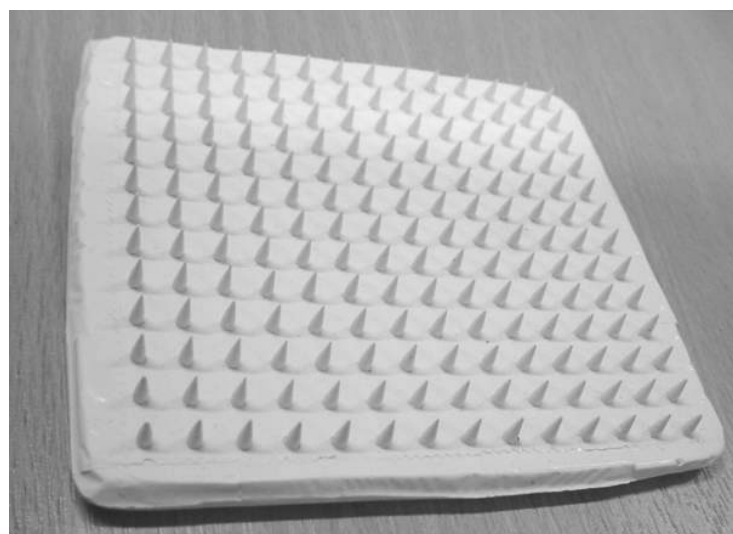


Fig. 3.14: 100% Ceramcor pin formation

Laminating Trials

With a process for casting fully formed pin beds established it was possible to take the development activities with this material onto laminate trials. The first of these used two and four ply stacks of the Saertex 310g/m² 24k T700 bi-axial NCF combined with one and two plies respectively of the 250g/m² M36 epoxy resin film. The first of these trials demonstrated problems with piercing through the peel-ply used in the lay-up and tool damage from vacuuming the laminate stack over the mould. This resulted in a high proportion of pin fracture during the piercing process caused by the tight weave of the peel-ply and the bending force applied from drawing vacuum around the tool owing to a slight curvature in its shape. This curvature was a result of distortion to the rubber mould from the high temperatures used during the moulding process. These problems were overcome through using a micro-porous film in place of the peel-ply and layers of polyester breather to cushion the ceramic against the worktop during vacuum forming. Once a successful procedure for inserting the pinned tools into laminate stacks was established the problem of containing vacuum integrity through a thin membrane over a set of sharp pins arose. Initial approaches to solve this looked at the use of excess breather layers to protect the vacuum bag from the points of the pins. The results of this approach are shown in Fig. 3.15 where the hole quality achieved provided an acceptable starting point. However, the general

laminated quality was particularly poor due to the low compaction force transferred to the laminate through the spring effect of the breather.

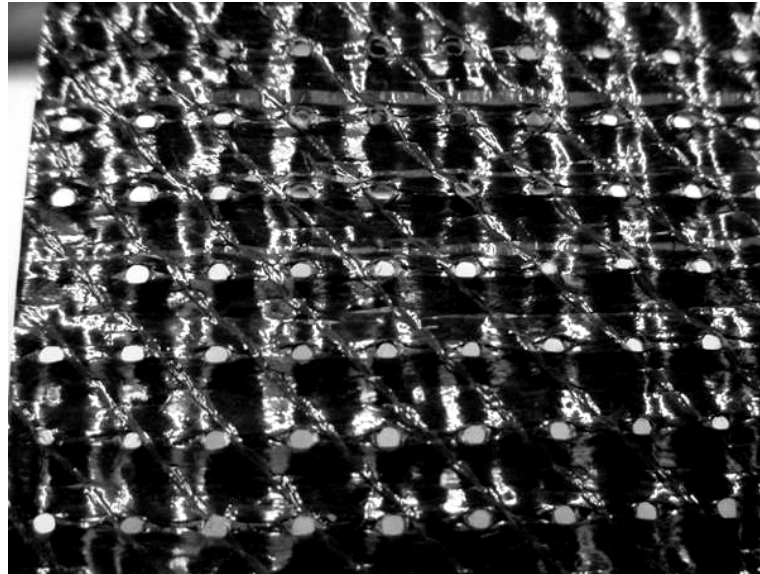


Fig. 3.15: 1st Ceramcor lamination trial

Further insertion trials showed signs of improvement with laminate consolidation as can be seen from Figs. 3.16 & 3.17. These trials achieved an improved level of compaction through the use of honeycomb and rigid foam to consolidate the laminate onto the tool and around the pins.

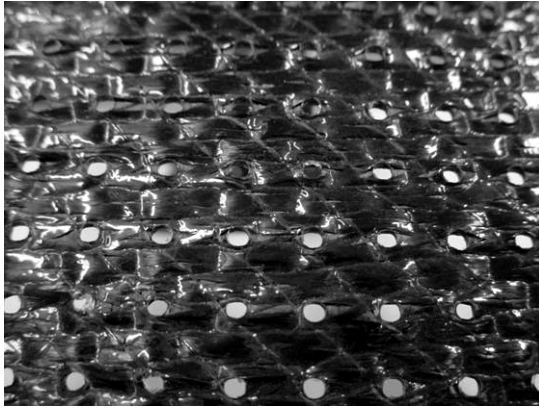


Fig. 3.16: Honeycomb laminate consolidation

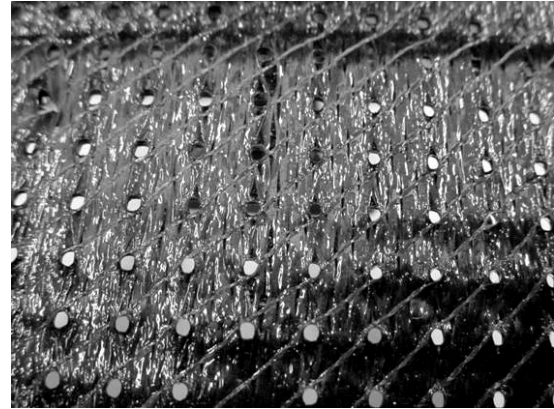


Fig. 3.17: Foam laminate consolidation

Although much improved, the laminate quality of these trials was still found to be unacceptable with the undulating surface showing a high percentage of both in-plane and through-thickness distortion.

To further evaluate the suitability of Ceramcor for the tooling it was necessary to conduct additional development trials because, as the earlier work showed, laminate consolidation over a pinned ceramic tool required significant improvement. The laminate configuration used in these developments were 3 plies of the 24k T700 bi-axial NCF carbon and 2 plies of M36 resin (R) in a sequence of 0/90, R, 0/90, R, 90/0. Four test plaques were manufactured with each using a different type of consolidation medium of low-density (20 kg/m^3) rigid foam and three different thicknesses of pressure strip. The aim of these consolidation materials was to help compact the laminates over the pinned tooling. The results are shown in Figs. 3.18-21.

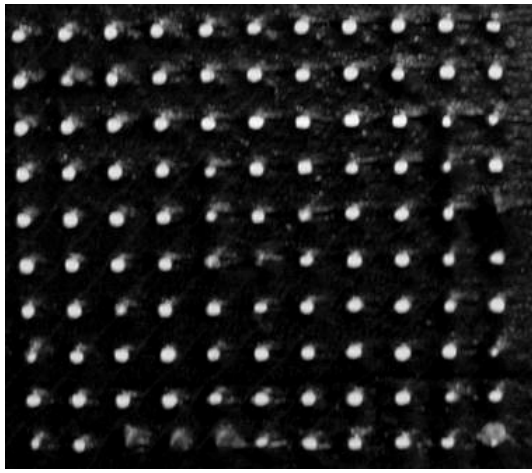


Fig. 3.18: Foam only consolidation

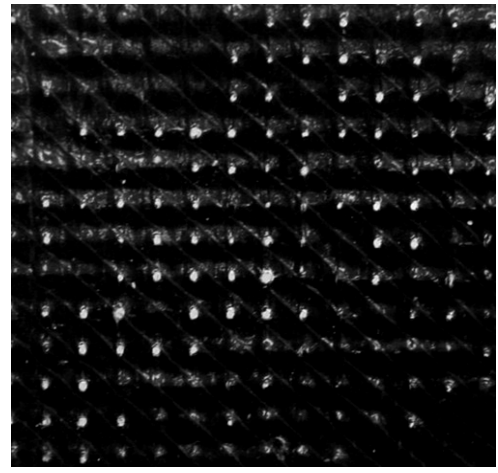


Fig. 3.19: Single layer pressure strip consolidation

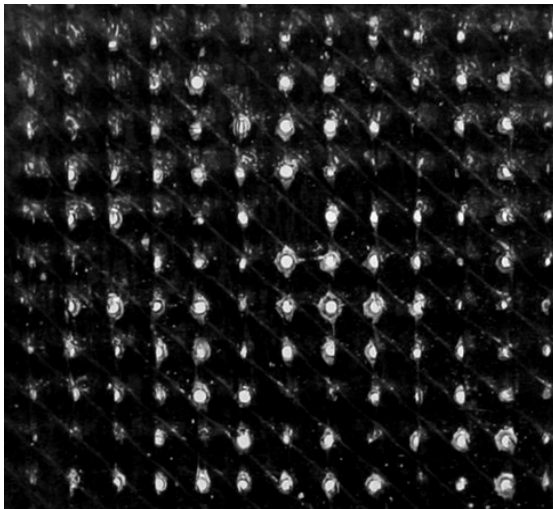


Fig. 3.20: Double layer pressure strip consolidation

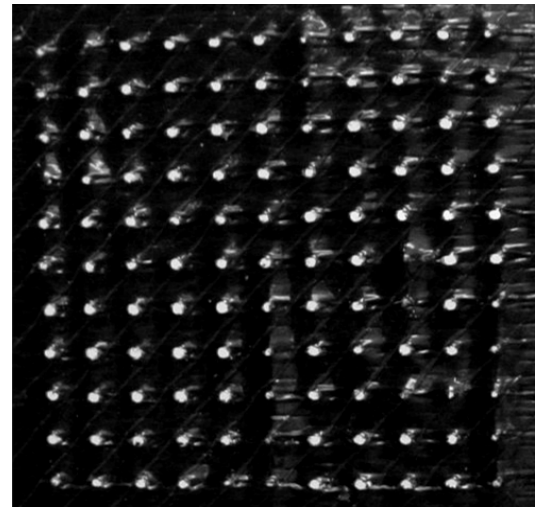


Fig. 3.21: Triple layer pressure strip consolidation

The results of each trial demonstrated that with additional consolidation it was not possible to achieve an acceptable level of laminate quality with vacuum only processing as evident through perforation variation and excessive fibre bridging around perforations. With perforation diameters in the region of 1-2mm, the perforation resistance of the fabric and resin was greater than the load capability of the Ceramcor pins. From these trials it was evident that the low-density foam provided

the highest quality but there was still evidence of penetration failure through the uncured laminate accompanied by a high degree of surface distortion around the holes. With these problems on a 100x100mm laminate containing 121 perforations it was expected that increasing the scale to thousands of perforations and using a curved substrate the processing problems would be significantly amplified.

Conclusion

These trials concluded that for hole diameters on this scale, Ceramcor was not resistant enough on its own and that atmospheric pressure was insufficient to fully consolidate the laminate over such tooling. It was felt that potential existed for this material to be used as a wash off coating for re-usable pins but at the cost of considerable development far beyond the scope of this study. It is for these reasons that this material was not pursued further within the framework of this project.

3.6 Reusable Tooling

The use of re-usable tooling brings with it the obvious benefit of non-recurring costs, where initial outlay is amortised over the life of the programme. There is also a perceived benefit that a process utilising reusable tooling carries the potential for a more streamlined process where

any tool reworking requirements and associated labour costs and energy are minimised in comparison to a tooling system that is moulded for each use.

3.6.1 FlexPerf

The FlexPerf product is a new technology to the aerospace composites market developed by through-thickness reinforcement specialists Aztex Inc. whose z-pinning technology permits through-thickness properties to be enhanced through pre-cure insertion of carbon rod stock. The particular process of FlexPerf provides users with a method for perforating un-cured laminates to produce continuous fibre perforated laminates.

The processing equipment used in this process is illustrated in Fig. 3.22.

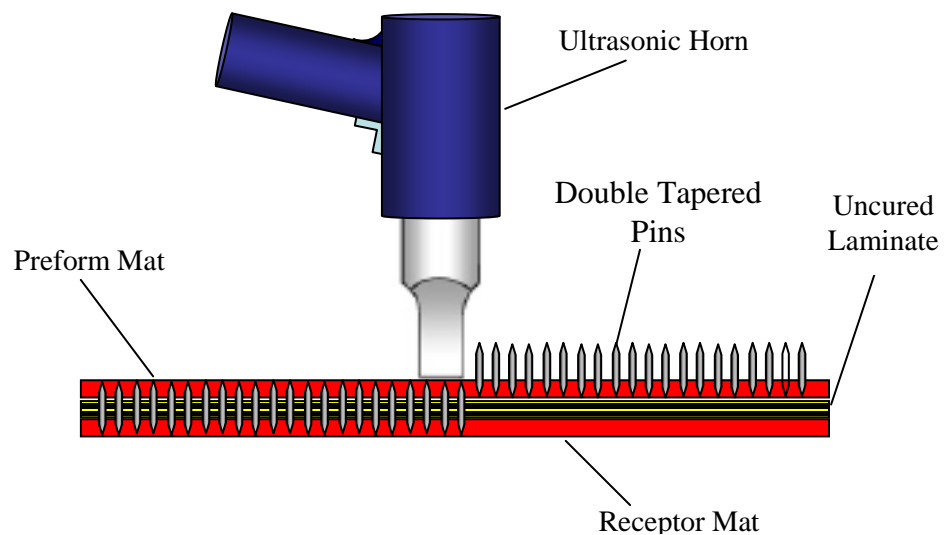


Fig. 3.22: FlexPerf insertion process

The FlexPerf tooling consist of two rubber mats; an upper preform mat supplied with pre-inserted double taper pins, aligned to the required hole pattern, and a lower receptor mat used to sandwich the laminate in place and secure the position of the pins. The pins used are generally available in standard gauge sizes but with additional machinery modifications can be produced to specific design requirements.

With this approach an un-cured laminate is sandwiched between the receptor and preform mats and then consolidated in an envelope vacuum bag (see Fig. 3.23). Although the achievable vacuum during this stage is generally less than 85mb absolute it is still sufficient to hold the tooling in position for pin insertion. From the diagram it can be seen that this is achieved through the use of a double seal in the vacuum bag. The reason for this is that the section of bag covering the insertion pins is removed prior to insertion and without a seal around the perimeter of the preform mat there would be a total loss of vacuum.

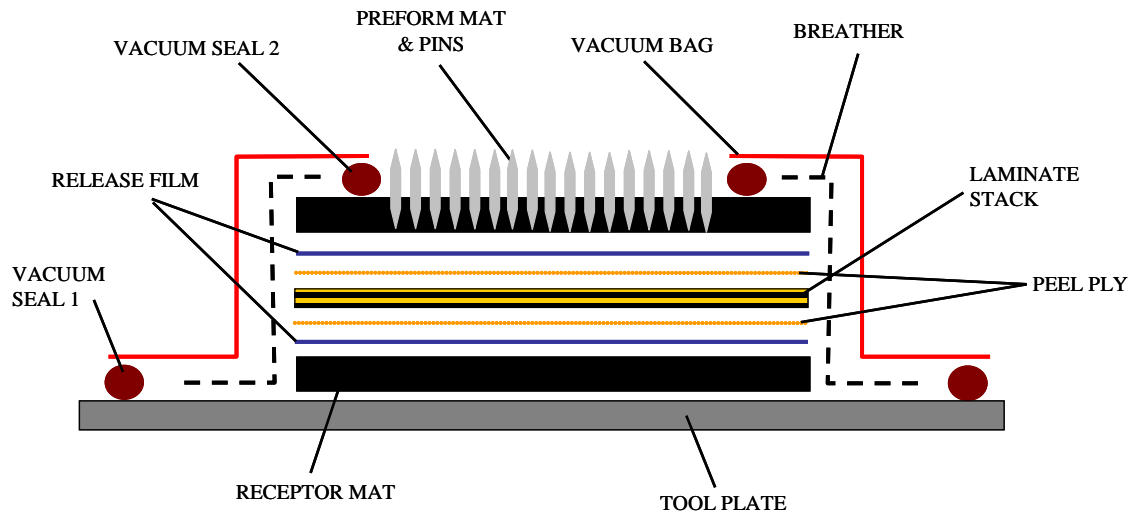


Fig. 3.23: Lay-up configuration for insertion process

The pins are inserted through the configuration using the ultrasonic horn (see Fig. 3.24).



Fig. 3.24: Ultrasonic horn equipment for pin insertion - Branson FS-90

(Branson Ultrasonics Corporation, 1992)

Once all pins are inserted the initial vacuum bag is removed and the sandwiched configuration is vacuum bagged to the required tool plate ready for cure as with a standard composite part.

To de-mould the cured part the receptor mat is first peeled from the pins to reveal the perforated laminate locked to the preform mat. It is then necessary to drive the tapered pins back into the preform mat to their original position; this is easily done using a metallic roller (minimum recommended diameter 100mm) and a scrap honeycomb base (honeycomb was found to provide the least resistant supportive surface). The critical element of the FlexPerf concept becomes apparent during this stage where the length of pin taper against thickness of laminate determines the release of the laminate; i.e. by having a longer taper than the laminate thickness, the pins can be physically rolled from the laminate.

Although these tools are re-usable the mats still have a limited life-span due to the fatigue effects of peeling and the thermal degradation of process cycling, the receptor mats can be expected to last approximately five cycles and the preform mat ten cycles.

Initial Evaluation

Preliminary trials of the FlexPerf process were conducted using six sets of FlexPerf tooling at the Aztex research facilities at Cranfield

University. Each tooling set was 100x100mm and specified to the AS-907 OFD design of a 6% open area utilising a hole diameter of 1.575mm.

During these trials 18 perforated laminates were produced comparing lay-up variations, cure pressure and material types. The first 12 panels again utilised three plies of the Saertex 24k T700 310g/m² bi-axial NCF with two plies of the 250g/m² M36 epoxy resin film in a configuration of 0/90, R, +/-, R, 90/0. The last five panels changed the lay-up to 0/90, 90/0, 90/0 to reflect an equivalent AS-907 design. The final panel then utilised four plies of 8552 pre-preg as per the actual AS-907 acoustic face sheet design (0/90, 0/90, 90/0, 90/0).

The bagging configuration used for these trials is shown in Fig. 3.23, however due to concerns over laminate breathing during cure and the consolidation behaviour of the un-cured laminate in the tooling, variants of this configuration were evaluated as detailed in Table 3.5.

Table 3.5: Summary of FlexPerf trial results

Trial	Process	Pressure	Consumables*	De-bulk	Surface Quality	Laminate Quality
1	RFI	Vacuum	PP, RF	-	100% pitting both sides	3-5% voiding
2	RFI	Vacuum	PP, PPG, RF	-	100% pitting both sides	3-5% voiding
3	RFI	Vacuum	PPG, RF	-	100% pitting both sides	3-5% voiding
4	RFI	Vacuum	PPG, RF	-	100% pitting both sides	3-5% voiding
5	RFI	Vacuum	PP, PPG, RF	-	100% pitting both sides	3-5% voiding
6	RFI	Vacuum	PP, RF	-	100% pitting both sides	3-5% voiding
7	RFI	Vacuum	PP	-	85% pitting both sides	2-3% voiding
8	RFI	Vacuum	PP, G	-	85% pitting both sides	2-3% voiding
9	RFI	Vacuum	PP, G, RF	-	85% pitting both sides	2-3% voiding
10	RFI	Vacuum	PP, GT, RF	-	75% pitting both sides	2-3% voiding
11	RFI	Vacuum	PP, GT, RF	60min @ RT	60% pitting both sides	2-3% voiding
12	RFI	Vacuum	PP, GT, RF	30min @ 60°C	50% pitting both sides	2-3% voiding
13	RFI	Vacuum	PP, GT, RF	20min @ 80°C	50% pitting both sides	2-3% voiding
14	RFI	Vacuum	PP, GT, RF	10min @ 100°C	50% pitting both sides	2-3% voiding
15	RFI	2 bar	PP, GT, RF	-	35% pitting both sides	2-3% voiding
16	RFI	3 bar	PP, RF	-	No defects	<1% voiding
17	RFI	3 bar	PP, GT, RF	-	No defects	<1% voiding
18	P-P	3 bar	PP, RF	-	No defects	+5% voiding
19	P-P	7 bar	PP, RF	-	No defects	<1% voiding

***Left to right equates to laminate surface upwards [PP = Peel-ply HS 013, PPG =**

Peel-ply ‘G’, G = Glass ply, GT = Glass tows, RF = Release film]

The results of these trials established that the FlexPerf tooling required additional pressure, above atmospheric, to achieve an acceptable level of consolidation in an RFI laminate. It was concluded that given sufficient time to conduct a full series of development trials then this process could eventually be adapted for VBO cures. For the purpose of the present study, the test plaques were produced using an autoclave cure where 3 bar of additional positive pressure was applied for the RFI laminates and 7 bar for the pre-preg.

Hole Quality

With acceptable laminate quality achieved by experimenting with the bagging and cure pressure variables the next step in this evaluation was analysis of the achievable hole quality. With samples taken and polished flat-wise for micrographic analysis the holes were found to have clean edges with parallel sides. On closer inspection no evidence of fibre breakout or resin fracture could be found following the pin removal. The laminate did demonstrate a slight increase in thickness around the holes caused by the pin insertion process and probably proportional to the resin pockets created at inter-tow-hole locations. Figs. 3.25-29 show the hole quality achieved in comparison to that of drilling. Fig. 3.25 also clearly shows the tow separation caused by the hole forming process. One effect from this separation is an increased visibility of the polyester stitch used in the NCF textile (depicted by the white lines).

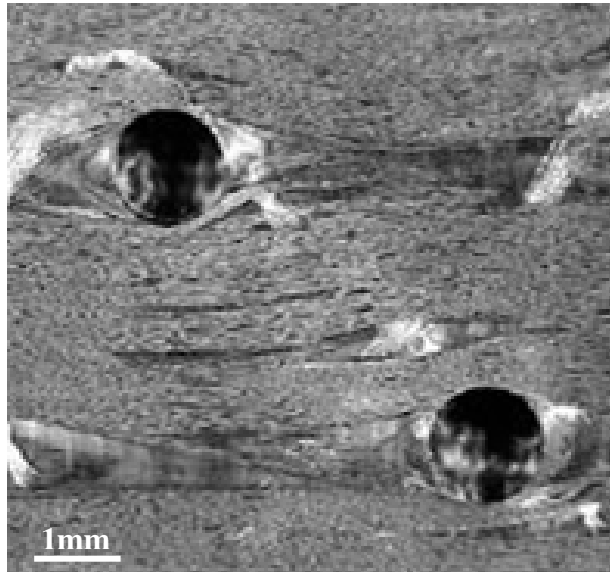


Fig. 3.25: Photograph of FlexPerf moulded hole quality in RFI laminate

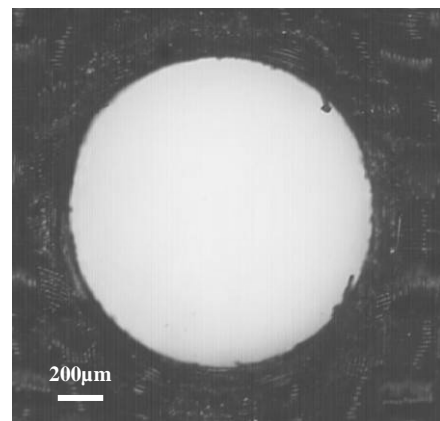
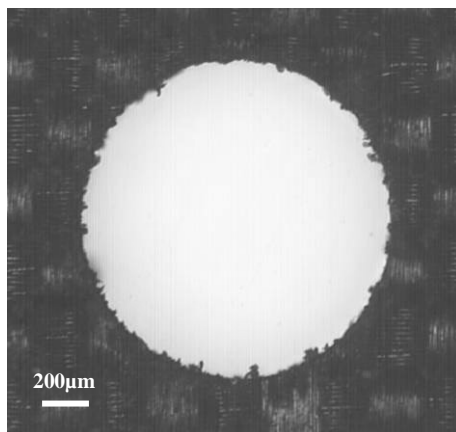


Fig. 3.26: Drilled RFI hole micrograph Fig. 3.27: Moulded RFI hole micrograph

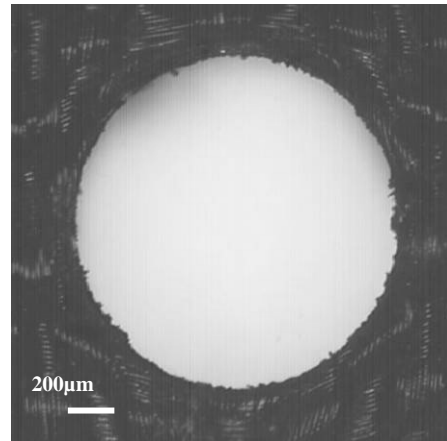
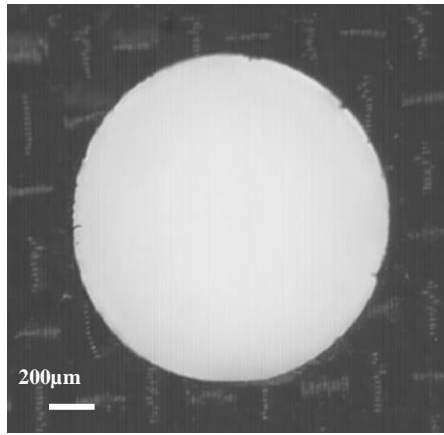


Fig. 3.28: Drilled PP hole micrograph **Fig. 3.29: Moulded PP hole micrograph**

An improvement in moulded hole definition is visible compared with drilling even though there is some evidence of material breakout in the moulded holes; a likely result of the pin removal process. The poorer definition seen in drilling the RFI laminate is probably due to the cutting process (i.e. drill design and cutting speed) being designed for pre-preg acoustic laminates where a much smaller tow size and the use of a structural 2D weave in the fabric allow better resistance to material burring. This is evident in the pre-preg samples where the drilled holes are seen to be clean of any material breakout and again the moulded perforation shows slight signs of material damage during pin removal. At this stage it was thought unlikely that these effects would be visible within the mechanical evaluation of the moulding process but that they would possibly have an effect on the acoustic performance of the configuration. For this reason it was decided to include an acoustic evaluation of the moulding process selected.

Conclusion

These trials established that the FlexPerf product can deliver perforated laminate of acceptable quality with only minor modifications to standard processing methods. Although, disappointingly, the technology could not be used with out-of-autoclave processing, the quality achieved in hole definition means that significant process time savings are still available with this method over a standard drilling approach.

3.7 Pin Material Development Conclusions

The results of these trials demonstrate that for the present study the FlexPerf method is preferable to the washout tooling approach based on its ability to produce laminates of acceptable quality. For this reason the FlexPerf process was selected for full evaluation in the present study through a mechanical evaluation of continuous fibre perforated plates and the investigation of the potential commercial advantages.

3.8 Thin Laminate Testing Trials

3.8.1 Background

As previously discussed, the AS-907 OFD design incorporates a hole diameter of 1.575mm in an open area of 6% in a laminate of approximately 1mm thick. However in order to generate mechanical

property data, specifically compression, on the specific hole pattern, the design thickness should be increased to 2mm as per ASTM D695-02. Unfortunately the processing equipment of Aztex Inc. was unable to machine pins of this diameter suitable for a 2mm thick laminate, i.e. a taper on this diameter greater than 2mm, without significant equipment modifications (costing around \$5000). The closest pin diameter available capable of a 2mm thickness insertion was 1.3mm.

3.8.2 Approach

Without the ability to manufacture 2mm thick test laminates it was necessary to investigate thin test specimens. This meant the four ply pre-preg lay-up, and RFI equivalent, would be used for the mechanical property data generation. The mechanical test specifications used in this project (BS EN ISO 527 for tensile testing, ASTM D 695 for compression testing and BS EN 2563 for interlaminar shear strength testing) call for a minimum thickness of 2mm to be used. With relatively little published on thin specimen testing, an experimental investigation was essential before the project could progress further.

With unidirectional specimens, a thickness of 1mm does not present issues for evaluating tensile performance since the fibres are aligned with the load direction and the failure mode is fibre-dominated. Even in a cross ply configuration a 1mm thickness for tensile testing does not present a

significant concern due to the failure modes expected being dominated by the fibre breaking strain and independent of thickness. However, reducing cross-ply laminate thickness does become a concern when testing for failure modes sensitive to thickness, such as compression and interlaminar shear strength (ILSS). When a thin test specimen is loaded under compression there is a risk of end crushing or buckling prior to ultimate load, hence recording low failure strengths. With ILSS testing the problems lie with the relationship of thickness and span length ($\text{span} = 5 \times \text{thickness}$) that ensures an interlaminar failure; the risk of a flexural failure increases with the span/depth ratio. In addition to the thickness issues associated with compression testing, a further problem was that of the increased gauge length required when testing the perforated specimens. With standard compression testing to ASTM D 695, a 'dog-bone' specimen is required with a width of only 12.7mm in the gauge region. This presented a secondary issue in testing the AS-907 acoustic pattern due to the edge effects expected with holes not positioned half of their pitch distance from the specimen edge. One potential resolution was to adapt a parallel sided specimen configuration but here an increased gauge length between the end tabs would be required to allow the incorporation of sufficient acoustic open area to test the moulded hole theory. This would also further add a requirement for reducing the probable buckling failure modes with an increased gauge size. To investigate these test specimen issues a short

series of testing trials was conducted using a Lloyd test machine with 20kN and 5kN load cells.

3.8.3 Compression Test Trials

Four modified configurations of compression specimens were considered; (1) parallel sided un-tabbed, (2) parallel sided with short end tabs, (3) dog bone with short end tabs and (4) parallel sided with medium tabs and PTFE anti-buckling spacers. Each configuration was prepared from the same RFI processed laminate of 0/90 lay-up of 1mm thickness. Examples are illustrated in Fig. 3.30. The dimensions of the typical ASTM D695 compression dog-bone specimen are shown in Fig. 3.31.

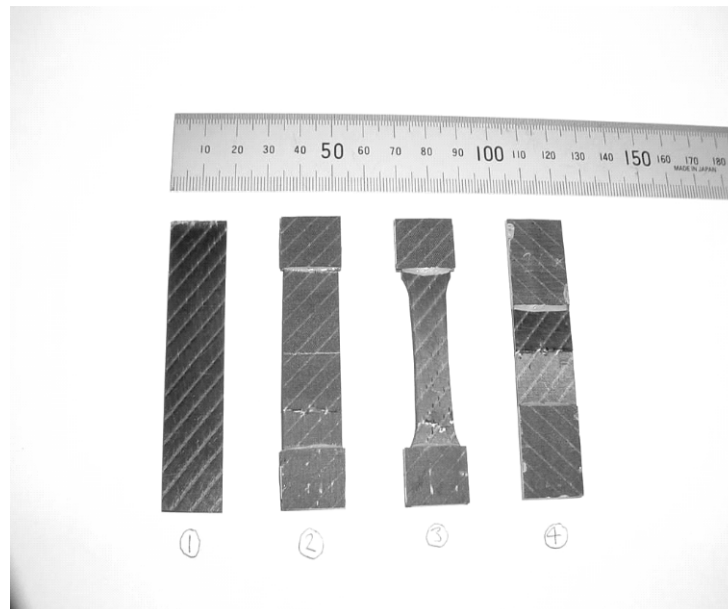


Fig. 3.30: Trial compression specimens with 1mm thickness

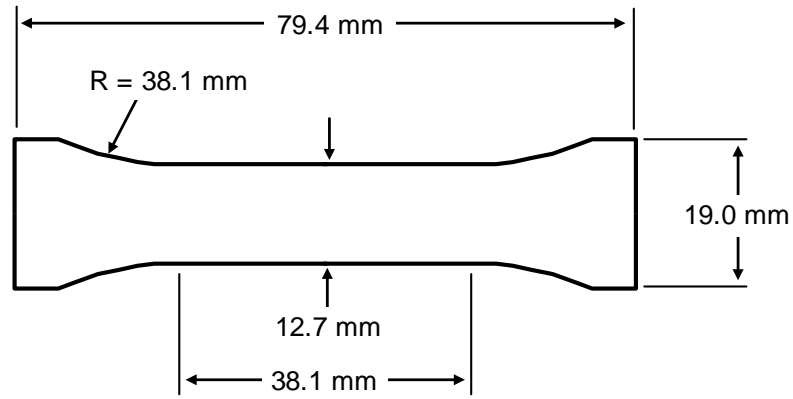


Fig. 3.31: ASTM D 695 compression test specimen

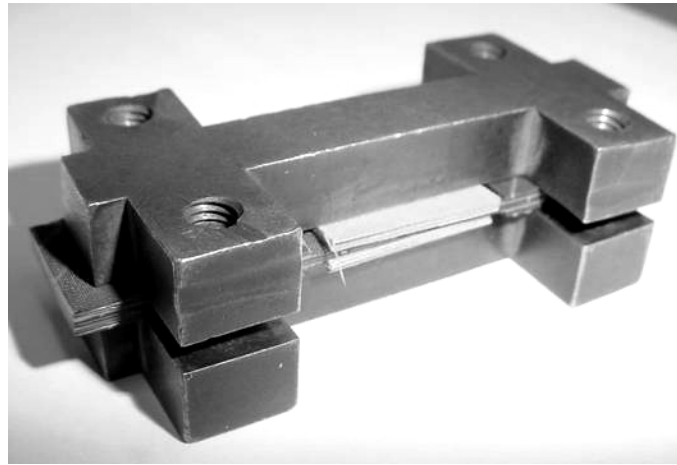


Fig. 3.32: Anti-buckling compression jig as specified for thin laminates in ASTM D 695 (shown with PTFE anti-buckling plates)

Each specimen was jig mounted (Fig.3.32) as per ASTM D 695 for the compression testing of laminates with a thickness less than 3.2mm, and tested using a Lloyd test machine with 20 kN load cell. All specimens were tested as standard non-perforated laminate due to the higher failure loads of the configuration where premature failure is more likely. Each test was conducted with a cross-head speed of 1mm/min and taken to failure to

allow the analysis of each failure mechanism. The test data summary and typical failure mode from each set is shown in Table 3.6.

Table 3.6: Results and failure modes of thin specimen compression trials

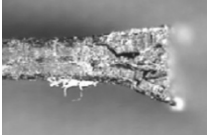



Configuration	1	2	3	4
Description	Parallel sided, un-tabbed	Parallel sided, short end tabs	Dog bone, short end tabs	Parallel sided, medium tabs, anti-buckling spacers
Mean failure load (N)	N/A	3082	2196	7935
UCS (MPa)	N/A	194	213	461
SD	N/A	11.3	26.9	40.2
CV (%)	N/A	5.8	12.6	8.7
Failure type	End crushing 	Buckled 	Buckling/compression at span radius 	Pure compression 

Table 3.6 shows that the Configuration 1 specimens all failed through end crushing and hence no meaningful failure load could be recorded. This established the necessity for the compression specimens to incorporate end-tabs to transfer the loading into the desired failure region. Configuration 2 failed through buckling, indicating these specimens required a change in dimension at the test span or further support to counter the buckling mode. Configuration 3 highlighted the sensitivity of this type of specimen to edge effects and machining quality through failures consistently occurring at the point of curvature of the span. The low-friction support surfaces used in Configuration 4 to counter the buckling

modes in the gauge region provided pure compression failures at the mid-point of the test span. These low resistance anti-buckling supports, when used in combination with the standard anti-buckling jig (Fig. 3.32), showed that the specimen is given enough support in an extended gauge length so that true compression failure is achievable through preventing buckling. This low friction support surface was provided through the use of adhesive backed PTFE stacked to an equivalent thickness of the specimens. Compared to a baseline performance of 434 MPa from a 2mm specimen thickness the Configuration 4 specimens seem to hold great potential for offering a suitable test.

3.8.4 ILSS Trials

With ILSS testing the support roller radii of the available test jig restricted the minimum test span that could be used. As specified by BS EN 2563 the radius of these rollers was set at 3mm giving a minimum physical span of 6mm and a recommended span of 10mm. With an approximate 1mm specimen thickness and the governing test rule ($\text{span} = 5 \times t$) then a 5mm test span was required to achieve true interlaminar failure. However, due to the jig restrictions quoted above this dimensional configuration was impossible to test with standard supports. The testing of a laminate at a span to thickness ratio greater than five results in a higher probability of flexural failure as seen in standard three point bend testing. A proposed solution to this problem, and one investigated here, was to utilise the

bonding of two specimens together to achieve a gross specimen thickness in the region of 2mm. Although this method was not considered suitable for perforated laminates due to adhesive flow, some trials were conducted. Three trial specimen types were manufactured from the same RFI processed laminate by bonding two sections of laminate together using BSL 312/5 film adhesive. The specimen dimensions and results are shown in Table 3.7.

Table 3.7: ILSS specimen dimensions and trial results

Specimen	A	B	C
Width (mm)	13.75	13.75	13.75
Thickness (mm)	2.20	2.20	2.20
Span (mm)	11.00	11.00	11.00
Failure load (N)	1688	1661	1487
Shear strength (MPa)	42	41	37
Failure mode	Multiple shear	Multiple shear	Multiple shear

Although each specimen failed in shear the strengths recorded are likely to incorporate effects of the film adhesive potentially causing test variability. However with the specimens appearing to fail in multiple interlaminar shear it was thought this approach would be suitable for further investigation if the test laminate thickness was restricted by the FlexPerf process. Because the highest shear stress is in the adhesive layer, it is likely that the ILSS values are below the true value, but as the study was not absolute, but comparative this methodology serves purpose. Compared to a baseline performance of 49 MPa there was an obvious

knockdown seen in the bonded specimens. The utilisation of three laminate layers in such a configuration may prove sufficient to place the maximum shear stress back within the laminate and could prove worthy of future research.

3.8.5 Test Trial Conclusion

The results of the compression trials indicated the suitability of testing thin laminates using a modified specimen configuration (i.e. parallel sided, end tabbed, increased gauge length and low friction support). The ILSS results also indicated potential. As this investigation has only tested a limited number of repeats (three) for each method, further investigation would prove beneficial to assess variation with thin laminate testing. The conclusion for this project was to proceed with a perforated open area design of 6%, as with the AS-907 design, but utilising a hole diameter of 1.3mm in order to allow a test piece thickness of 2mm. This decision was based on a need for the test programme to directly compare the two perforating methods rather than the exact acoustic design of the AS-907.

Chapter 4: Mechanical and Physical Material Characterisation

4.1 Introduction

A test matrix was established to evaluate the mechanical and physical performance of moulded acoustic perforations. For data consistency and to permit drawing comparisons the test matrix was also designed to cover the performance of both drilled perforated and non-perforated laminates.

The mechanical properties chosen for evaluating the discontinuous aligned fibre, continuous distorted fibre and continuous aligned fibre configurations were:

Tensile strength and modulus [EN ISO 527-4]

Compressive strength and modulus [ASTM D 695 – 02a]

Interlaminar shear strength [EN 2563]

As with most aerospace material and process evaluations these tests were conducted under dry and wet conditions to take lifecycle performance into account. These environmental tests were conducted for all properties, with the exception of compressive modulus, due to an incompatibility between the available extensometer and the environmental testing chamber. The conditioning used for the test programme was selected to be 1000

hours at 85% relative humidity and 70°C with a subsequent test temperature of 80°C. The moisture absorption was monitored for each laminate configuration.

Maintaining a focus on the primary performance requirement of acoustic attenuation was also necessary with sufficient previous work at GKN establishing a link between hole surface quality and acoustic attenuation performance. In consideration of this and that the initial evaluation into hole quality showed some minor material breakout, a programme of additional testing for acoustic attenuation was undertaken.

The AS-907 design specifies a perforated skin of four carbon-epoxy pre-preg plies in a 0/90 lay-up. The pre-preg ply areal weight is 270 g/m² which gives a cured laminate thickness in the region of 1mm at an approximate fibre volume of 58%. To meet the test specification requirements, and provide a valid reference point for future comparison, it was necessary to adapt this design to obtain a cured thickness of 2mm. As discussed earlier, this was particularly important for the compressive and interlaminar testing to achieve true failure mechanisms. This thickness increase was achieved by simply doubling the lay-up.

With a pre-preg lay-up determined by the existing design, it was necessary to establish an equivalent design for the RFI system to allow a meaningful comparative study. To reduce the impact on future design changes the laminate thickness was taken as a guide in determining an RFI equivalent. As discussed in the previous chapter, the material system

selected for the RFI evaluation was a 310g/m² 24k T700 bi-axial non-crimp fabric incorporating the GKN-qualified 250g/m² M36 epoxy resin film. With this combination, the existing design transposes to three plies of fabric. To achieve the increased test thickness of 2mm this lay-up was simply doubled as with pre-preg.

These modified test lay-ups were:

Pre-Preg 8552-5H-6k-AS4-280: [0/90]_{4S}

RFI M36-BX-24k-T700-310: [0/90]_{3S} – Resin film at inter-ply layers

Laminates of a non-perforated, drilled and moulded hole configuration were then manufactured from both material systems in order to provide the test specimens required to satisfy the test matrix shown in Table 4.1.

Table 4.1: Test matrix

Test	Perforation Type	Material	Test Conditions & No. Specimens	
			Dry RT	Wet 70°C/85%RH 80°C
Tensile strength & modulus [EN ISO 527-4]	Drilled	RFI	5	3
		Pre-preg	5	3
	Moulded	RFI	5	3
		Pre-preg	5	3
	None	RFI	5	3
		Pre-preg	5	3
Jig assisted compressive strength & modulus [ASTM D 695 – 02a]	Drilled	RFI	5	3
		Pre-preg	5	3
	Moulded	RFI	5	3
		Pre-preg	5	3
	None	RFI	5	3
		Pre-preg	5	3
ILSS [EN 2563]	Drilled	RFI	5	3
		Pre-preg	5	3
	Moulded	RFI	5	3
		Pre-preg	5	3
	None	RFI	5	3
		Pre-preg	5	3
V _f [ISO 11667]	Drilled	RFI	5	
		Pre-preg	5	
	Moulded	RFI	5	
		Pre-preg	5	
	None	RFI	5	
		Pre-preg	5	
CPT	Drilled	RFI	5	
		Pre-preg	5	
	Moulded	RFI	5	
		Pre-preg	5	
	None	RFI	5	
		Pre-preg	5	

4.2 Hole Pattern Design

With the perforation diameter restricted to 1.3mm with FlexPerf and the acoustic open area (AOA) set at 6% by the AS-907 design it was necessary to determine a new hole pattern. The AOA is determined as the percentage of total pattern area that falls on the holes themselves. The style

of pattern used was a staggered triangular hole spacing as with the AS-907, the method to determine this is set in Appendix B from the details of Fig. 4.1.

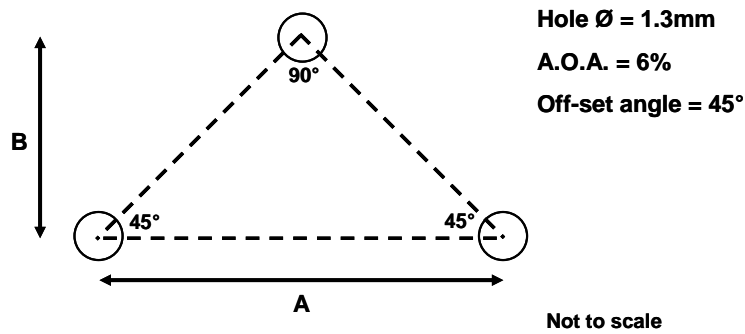


Fig. 4.1: Triangular area of hole pattern used for pitch calculations

Following the analysis in Appendix B this then provided a hole pattern as shown in Fig 4.2.

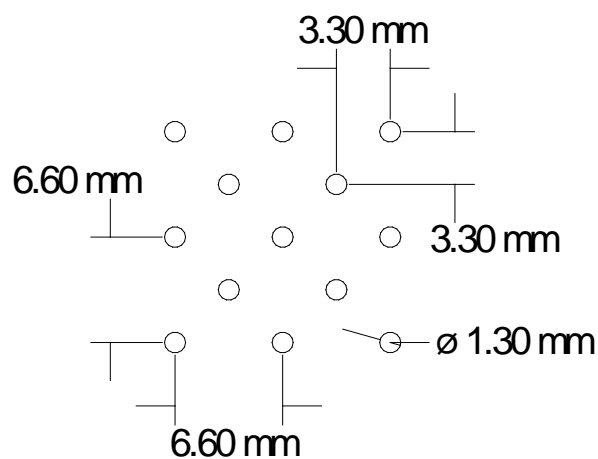


Fig. 4.2: Hole pattern for test pieces

This pattern was aligned to occur full-width in the central section of the specimen length with dimensions as determined by the relevant specifications; these are illustrated in Figs.4.3-4.5.

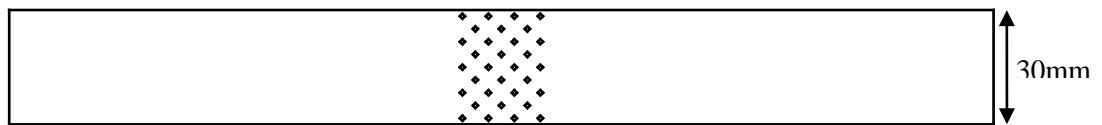


Fig. 4.3: Tensile specimen BS EN ISO 527 (250 x 30mm)

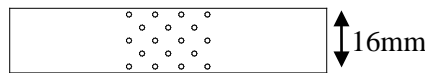


Fig. 4.4: Compression specimen ASTM D 695 (80 x 16mm)

The compression specimen is illustrated in Fig. 4.4 without end tabs. During testing each specimen used 25x16x2mm bonded tabs to avoid end crushing.

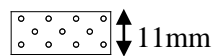


Fig. 4.5: ILSS specimen BS EN 2563 (25 x 11mm)

Specimen edges were set at the midpoint of hole rows to simulate each specimen being an acoustic skin sample and minimise the influence of edge effects on the failure modes achieved.

With the specimen dimensions established, the FlexPerf hole pattern tooling was designed to provide all of the test specimens from a single laminate. This design was then used for the moulding and drilling patterns to provide:

10 tensile specimens

12 compression specimens

12 ILSS specimens

6 V_f specimens

Additional specimens were produced in the event of any re-test requirements. As with the compression and tensile specimens, strips of perforations were used to cover only the gauge lengths so as to reduce the manufacturing costs for each approach. The final design is illustrated in Fig. 4.6 and shows the extra material available between specimens for the physical test requirements of differential scanning calorimetry (DSC) and dynamic mechanical analysis (DMA).

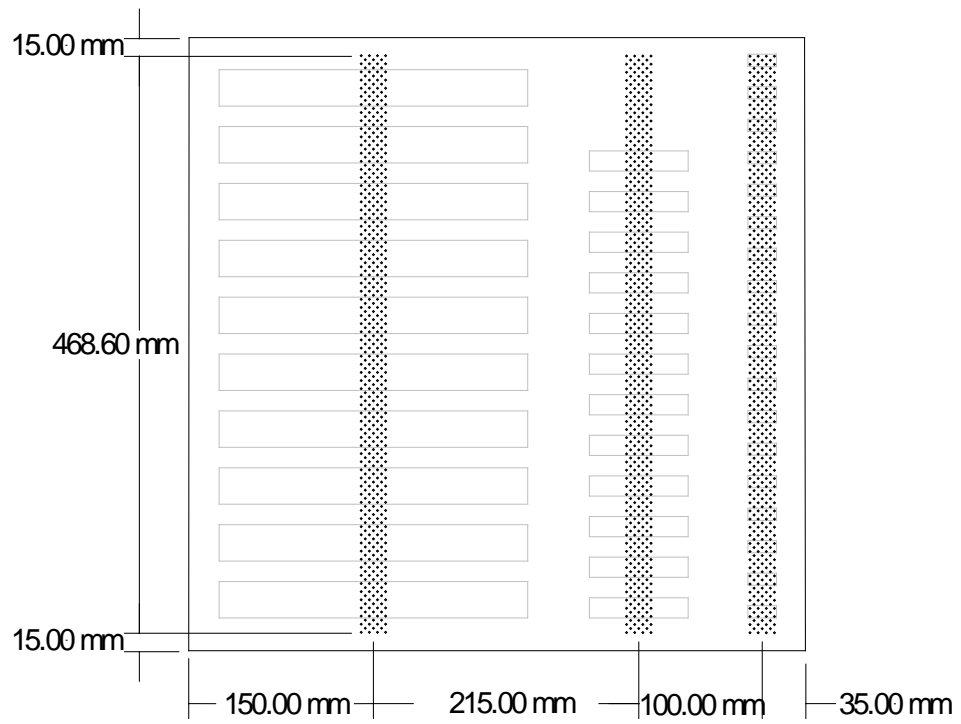


Fig. 4.6: Final design for FlexPerf tooling and 5-Axis machining pattern

**[First column = Tensile specimens, Second column = Compression specimens,
Third column = ILSS & Vf specimens]**

An example of a plaque drilled and CNC machined to this design is shown in Fig. 4.7.

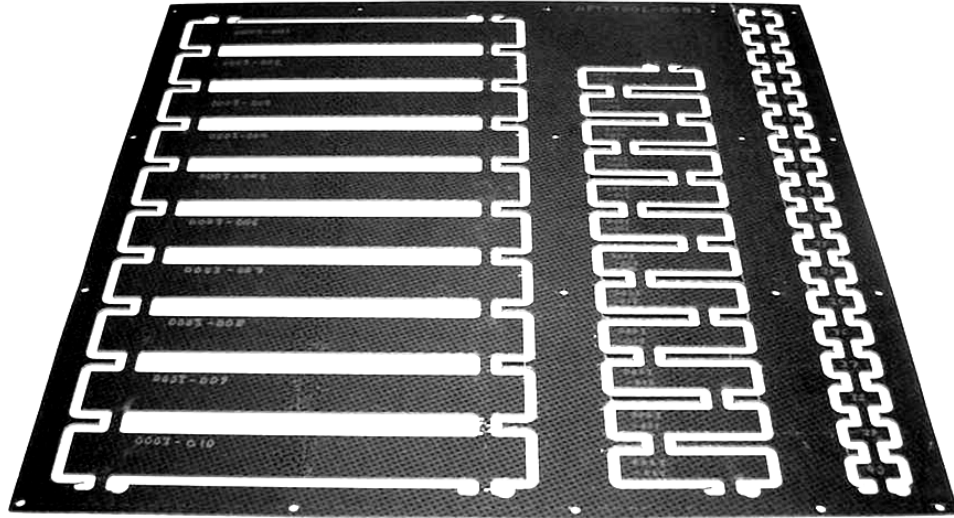


Fig. 4.7: Post machining of test plaque 0003

Each plate was machined to the cutting pattern utilising a 5-axis router. Individual specimens were then removed from the plate using a diamond coated circular saw and the specimen edges polished to the relevant specification requirements with 600 and 1200 grit paper.

4.3 Predictive Methods

Godage's (2002) predictive study of the mechanical impact of acoustic perforation patterns focussed on the stress concentrations generated from a face-centred square/hexagonal array pattern. This piece of work discusses a closed loop evaluation where a model is built empirically from test data and then re-calculated based on a coefficient approach for the relation of the net-section isotropic stress concentration factor (K_{tni}) to the net section composite stress concentration factor (K_{tnc}). While this

approach is useful for building an empirical model to predict changes to the array dimensions it does not offer any overall benefit for use in the present study where a single hole pattern is explored with varying material forms and hole forming methods. However, one useful aspect explored with this approach was the value in calculating the stress concentration effect from the data of this study with the modified hole pattern and evaluating if predictions could be made for the baseline AS-907 OFD acoustic pattern dimensions. Calculating the dimensional contributions to the model proposed by Godage of both the modified and original patterns returns the same factor of 0.721.

The geometrical factor (GF) is calculated from:

$$GF = 1 - 2 \frac{d}{I} \cos\theta$$

Where :

d = Hole diameter

I = Hole pitch within row

θ = Hole offset angle

With the resource and time restrictions of the industrial research phase there were no real possibilities to attempt to model the moulded and drilled behaviours in detail. Utilising the available GKN laminate data on the base-line pre-preg material it was possible to run some basic strength and modulus reduction calculations for the presence of the perforations

based on area reduction. While far from a perfect predictive analysis and unlikely to capture the performance of the moulded perforations, it was a method that provided some insight into expected performance drops. The calculations of the approach are detailed in Appendix C while the resulting predictions are shown below in Tables 4.2 & 4.3.

Table 4.2: Area reduction tensile predictions

Specimen	Strength (MPa)	Modulus (GPa)	Reduction (%)
Non-perforated	800.2	71.3	-
Failure at off-set 9 holes	488.1	43.5	39
Failure at full 5 hole row	626.8	55.9	22
Failure at intermediate 4 hole row	661.5	58.9	17

Table 4.3: Area reduction compression predictions

Specimen	Strength (MPa)	Modulus (GPa)	Reduction (%)
Non-perforated	697.1	59.4	-
Failure at off-set 5 holes	413.9	35.3	41
Failure at full 3 hole row	527.2	44.9	24
Failure at intermediate 2 hole row	583.8	49.7	16

It was unclear at this stage of the study how accurate the moulded hole perforation predictions would be but it was expected that the off-set failure predictions would replicate those of at least the drilled specimens.

4.4 Test Results

With the laminates manufactured and specimens prepared the test matrix shown in Table 4.1 was executed with the data generated presented in Table 4.4.

Table 4.4: Laminate mechanical dataset

Material	Pre-Preg						RFI					
Condition	RT			H/W			RT			H/W		
Type	Non perf	Moulded	Drilled	Non perf	Moulded	Drilled	Non perf	Moulded	Drilled	Non perf	Moulded	Drilled
Panel	0002	0004	0003	0002	0004	0003	0001	0006	0005	0001	0006	0005
TENSION												
UTS (MPa)	800.2	615.6	462.8	866.0	667.7	490.6	1073.8	841.0	674.8	1110.7	837.9	677.2
% Drop		23.1	42.2		22.9	43.4		21.7	37.2		24.6	39.0
SD	18.7	18.7	8.7	16.2	15.5	7.2	25.2	22.2	37.7	45.4	41.7	17.9
COV	2.3	3.0	1.9	1.9	2.3	1.5	2.4	2.6	5.6	4.1	5.0	2.6
E _r (GPa)	71.3	72.5	62.4	63.3	66.1	52.7	60.9	62.6	51.1	58.7	57.8	44.6
% Drop		-1.7	12.5		-4.5	16.8		-2.8	16.2		1.6	23.9
SD	3.3	5.1	1.9	0.2	4.0	0.7	1.4	2.2	1.6	1.8	2.4	3.6
COV	4.6	7.1	3.0	0.4	6.1	1.3	2.3	3.5	3.1	3.1	4.2	8.0
COMPRESSION												
UCS (MPa)	697.1	456.1	371.3	593.0	332.3	349.1	433.7	363.6	315.4	353.2	243.0	269.9
% Drop		34.6	46.7		44.0	41.1		16.2	27.3		31.2	23.6
SD	58.5	29.4	44.4	38.9	43.9	32.5	64.3	30.0	18.6	27.2	20.5	6.8
COV	8.4	6.4	12.0	6.6	13.2	9.3	14.8	8.3	5.9	7.7	8.4	2.5
E _c (GPa)	59.4	58.5	51.7				47.6	48.5	39.4			
% Drop		1.6	13.0					-2.0	17.1			
SD	12.0	9.8	10.5				6.2	6.8	4.8			
COV	20.2	16.7	20.3				13.0	13.9	12.2			
SHEAR												
ILSS (MPa)	78.1	66.0	57.7	62.3	51.2	48.3	48.5	48.2	43.2	35.5	33.9	34.1
% Drop		15.4	26.1		17.9	22.6		0.6	11.0		4.7	4.0
SD	3.5	4.6	2.2	1.7	0.5	2.1	5.6	3.2	1.3	2.8	2.6	0.9
COV	4.5	7.0	3.8	2.8	0.9	4.4	11.6	6.7	3.0	7.8	7.6	2.6
PHYSICALS												
CPT (mm)	0.281	0.294	0.281				0.323	0.360	0.319			
V _f (%)	57.7	56.0	57.7				55.4	50.4	55.4			
ρ _{lam} (g/cm ³)	1.58	1.57	1.58				1.52	1.49	1.52			

NOTES:

- Reduction percentage values relative to respective non-perforated samples
- Tensile and Compression data normalised to 60% V_f through method shown in Appendix D
- Perforate results based on gross cross-sectional area for direct comparison

- Moulded hole values taken using a nominal thickness value based on average of non-moulded areas of plaques
- Hot/Wet values unavailable for E_C due to incompatibility between extensometer and thermal test chamber

4.4.1 Comparing the Baseline Materials

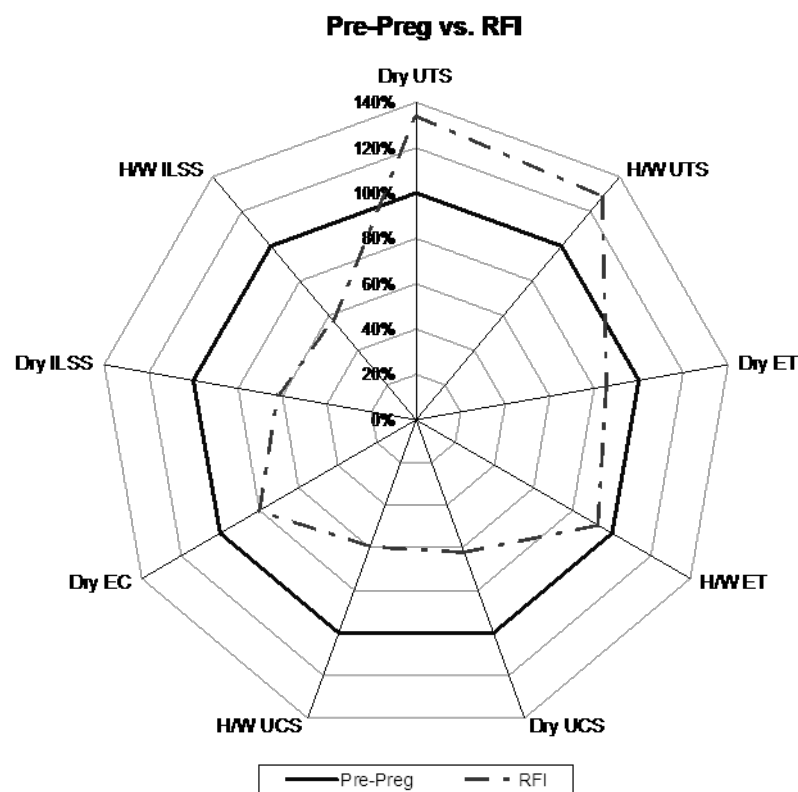


Fig. 4.8: Graphical comparison of the normalised properties for the two material systems (un-perforated)

Although the distinct differences in material forms make a direct comparison difficult it is possible to see some performance differences. In Fig. 4.8 the mechanical evaluation of each non-perforated material system

is compared with the pre-preg performance as the benchmark. The differences in the constituent material properties are highlighted in the previous chapter. These are evident through the improved tensile strength performance of the T700 fibre used in the RFI material along with the effects of reduced fibre crimp in the NCF reinforcement. The higher tensile modulus of the pre-preg material has a small contribution from the higher modulus of the 8552 resin which also shows in the higher compression performance of the pre-preg. The increased ILSS of the pre-preg is likely to be due to a combination of the increased toughness of 8552 resin over M36 resin and the interlocking fibre-ply nesting of the pre-preg weave compared to the relatively smooth NCF inter-ply regions. The following comparisons detail the differences between each test condition, while error bars have been utilised to illustrate the maximum and minimum of each dataset it is important to note that the test frequency in the analysis was limited to five specimens in dry conditions and only three in the conditioned state.

4.4.2 Assessing Pre-Preg Performance

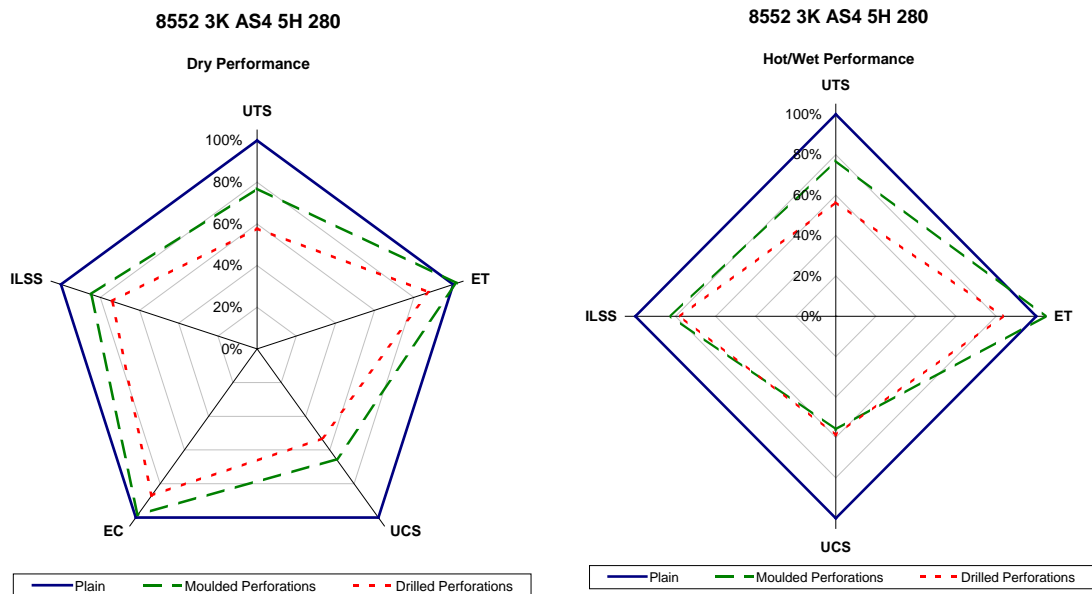


Fig. 4.9: Perforation effects on the pre-preg material system

Fig. 4.9 offers a graphical comparison of the perforation effects on the pre-preg with the plain non-perforated configuration taken as the benchmark level. In the dry performance there is a **knockdown in the moulded perforations yet they still consistently outperform the drilled perforations by 15-20%**. This is still true in the hot/wet condition for the fibre dominated tensile tests, yet in the matrix/fibre related compression and shear tests we see a similar performance for the two perforation types.

4.4.3 Assessing RFI Performance

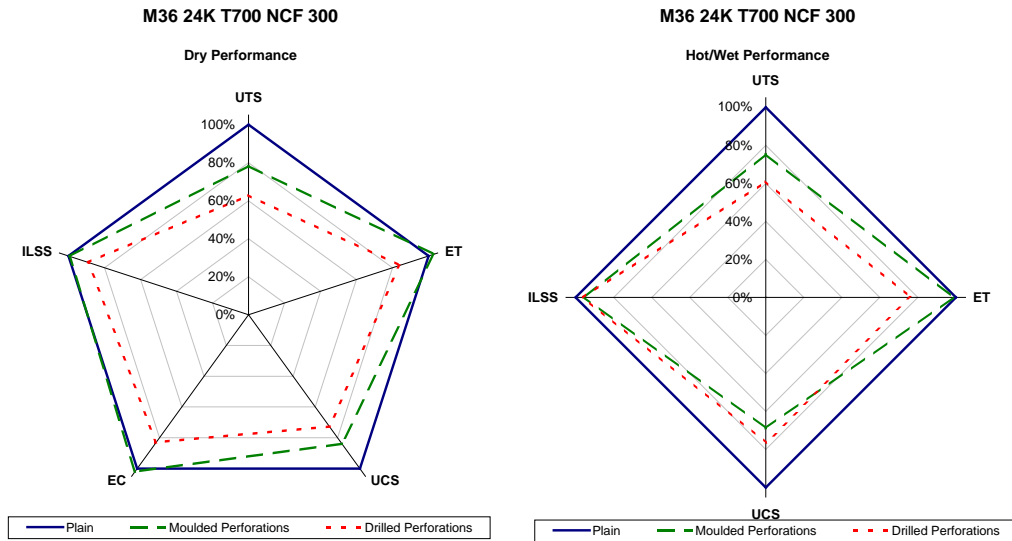


Fig. 4.10: Perforation effects on the RFI material system

Fig. 4.10 shows a similar comparison for the RFI laminates. A consistently **improved performance of the moulded perforations over the drilled configuration** in all but the hot/wet compression and shear conditions can be seen. One clear difference in this dataset is that the stiffness and shear performance of the moulded perforations is at an equivalent level to that of the non-perforated benchmark level. The effects of each perforation type on each property are considered in detail below. Note that when drilling returns a higher parameter value it is only ~5% greater than the moulded hole value.

4.4.4 Perforation Effects on Tensile Properties

There are several conclusions to be drawn regarding ambient tensile properties. The drilled specimens show considerable reductions in strength and modulus attributable to discontinuous fibres. The moulded hole specimens display a reduced strength due to the perforations but a lower reduction in failure stress due to fibre continuity. These specimens also demonstrated a slight improvement in stiffness over non-perforated laminate. This behaviour was consistent in both material types. The environmental tensile results also showed this, but with reductions associated with matrix performance degradation due to moisture absorption. These data are illustrated in Figs. 4.11 & 4.12.

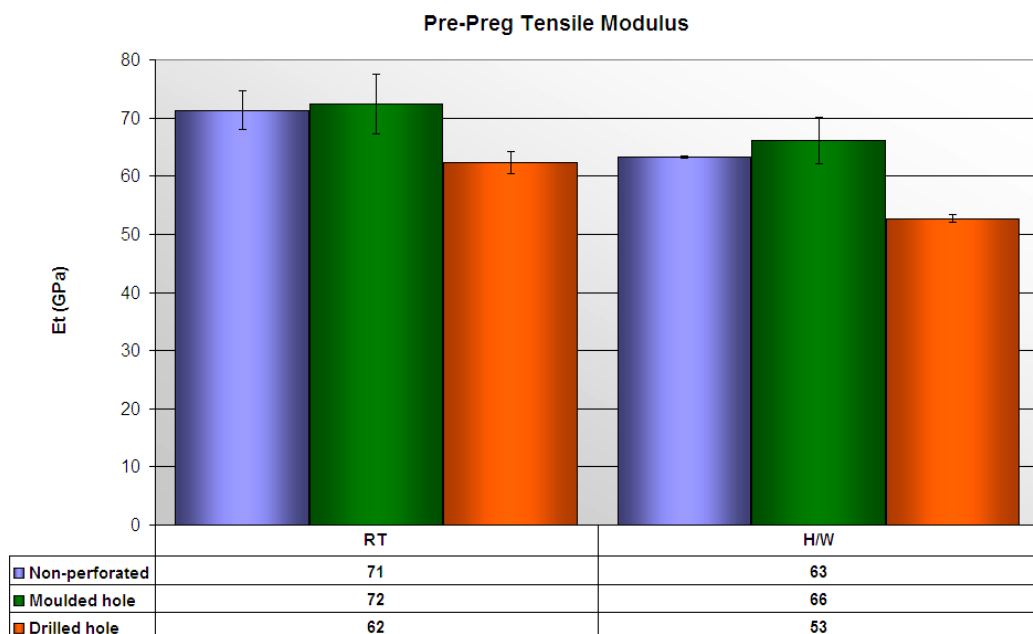


Fig. 4.11: Pre-preg tensile modulus results

Fig. 4.11 illustrates a 12% stiffness reduction related to perforation drilling in dry conditions and 17% after hot/wet conditioning. The corresponding fluctuations in the moulded hole perforations can be taken as equivalent performance to that of the non-perforated material.

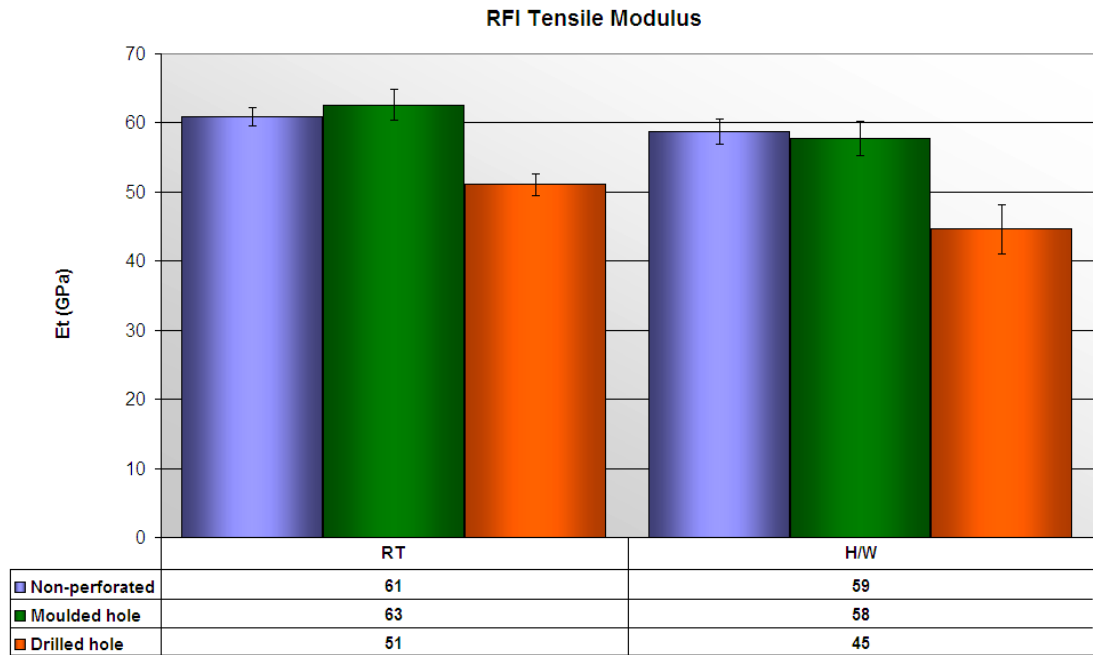


Fig. 4.12: RFI tensile modulus results

The RFI data presents a similar picture to that of the pre-preg. In dry ambient conditions the drilled perforations reduce laminate stiffness by 16% while the hot/wet conditioning results in a 24% reduction. Again the performance of the moulded perforated laminate can be taken as equivalent to the non-perforated base-line.

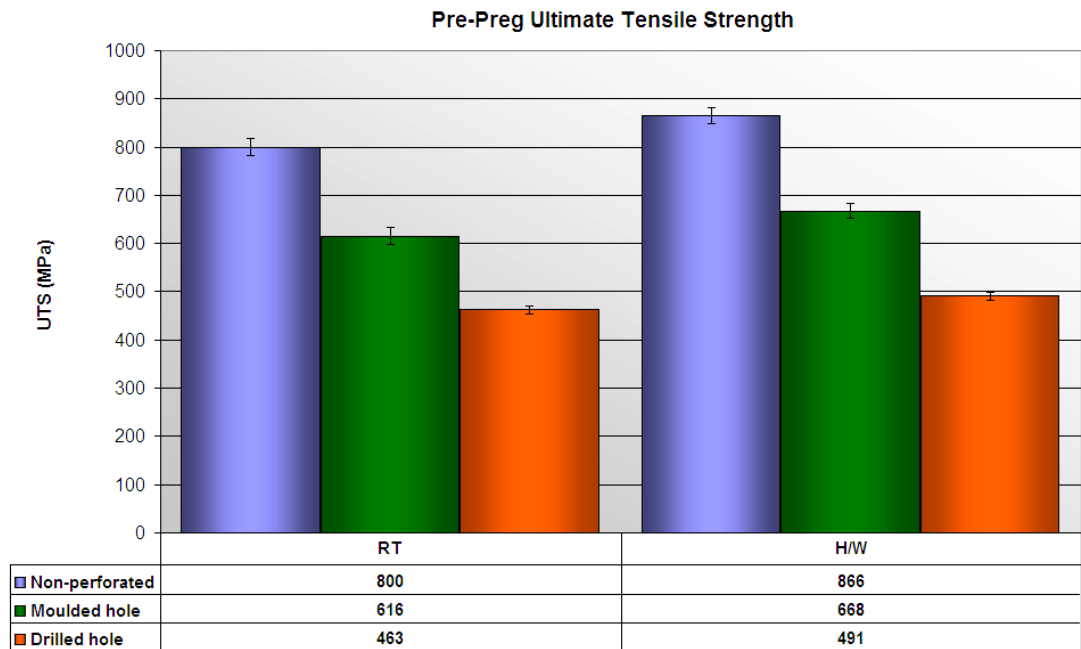


Fig. 4.13: Pre-preg tensile strength results

Fig. 4.13 illustrates the consistent tensile strength reductions in both perforated laminates for the ambient and conditioned pre-preg. Here the drilled perforations have reduced the laminate tensile strength by 42% in ambient conditions and 43% in hot/wet conditions. The moulded perforations showed a similar consistency of reduction where the laminate strength was reduced by 23% in both test conditions. With the reduction in drilled perforation almost double that of the moulded perforations, it can be concluded that the continuous fibres of the moulded holes have offered a significant increase in load bearing capability. This large decrease for the drilled laminates is associated with the combination of broken fibres and the stress concentration of the holes. With the moulded hole laminates, stress concentrations at the holes and the crimping of the fibres around the

holes still cause some strength reduction. The stress concentrations at the moulded holes are likely to be less than those in the drilled laminates as the increase in thickness at the hole perimeter provides geometrical reinforcement to the perforations.

With the conditioned specimens the reductions caused by the perforation remains comparable with the ambient results; overall strengths increase slightly in most of the cases. This slight increase can be attributed to the plasticising of the matrix by the moisture whereby the residual stresses within the matrix are alleviated as the matrix swells from moisture ingress and hence the failure initiation occurs at a higher load.

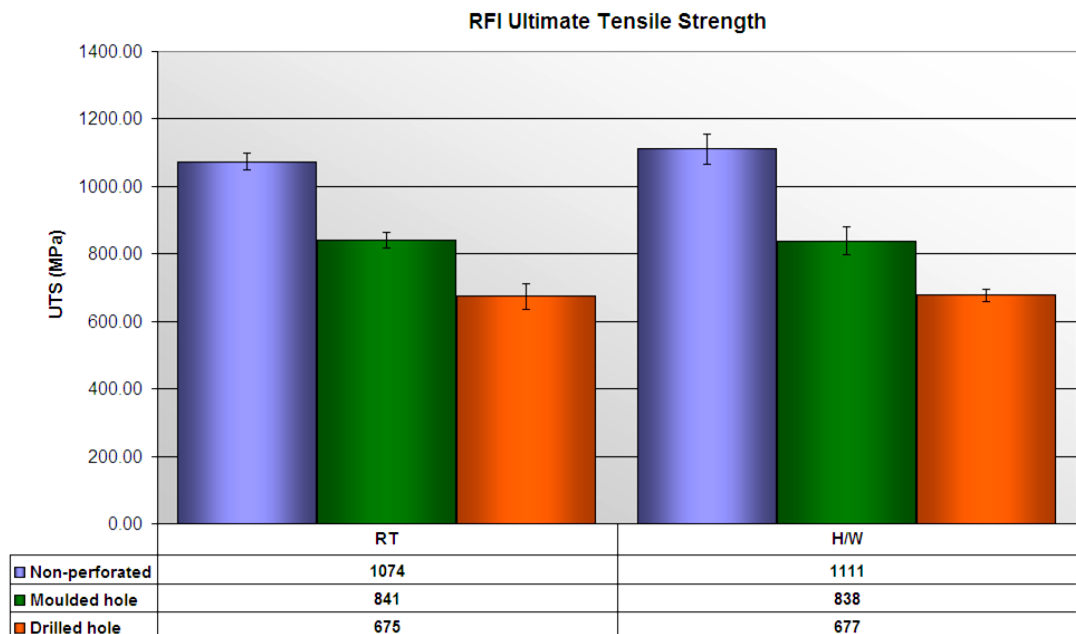


Fig. 4.14: RFI tensile strength results

Fig. 4.14 further validates the relationship shown in the pre-preg data. Here the drilled perforations result in a reduction to the laminate

strength compared with the moulded perforations. The drilled data points to a 37% reduction in ambient conditions and a 39% reduction in hot/wet conditions whereas the reductions for moulded specimens are 22% and 25% respectively.

The perforation effects found on the tensile properties of the material systems are in line with previous studies (Chang et al., 1987) where it was found that moulded holes can provide strength enhancements relative to drilled perforations (up to +22% for certain cross-ply lay-ups). The findings from this particular study found these strength enhancements to be driven by the fibre continuity achieved and localised hole reinforcements obtained through the hole moulding process. These conclusions are further echoed in the study of Ng et al. (2001) where the effects of large single moulded and drilled holes were studied. Here conclusions were drawn on the failure initiation, with initial failure occurring as expected at the hole edge. The fibre continuity of a moulded perforation can thus be seen to provide protection against initial failure compared to the micro-scale damage of both fibre and matrix in the drilling operation. Examples of the failure characteristics observed in mechanisms from the tensile testing are illustrated in Figs. 4.15-20 where all perforated specimen failures occurred in the perforated area and all non-perforated were between (rather than under) end-tabs.

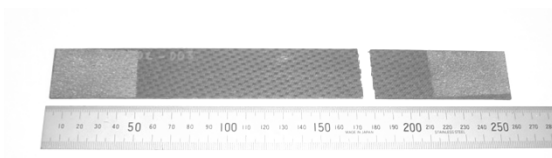


Fig. 4.15: Non-perforated PP UTS

failure

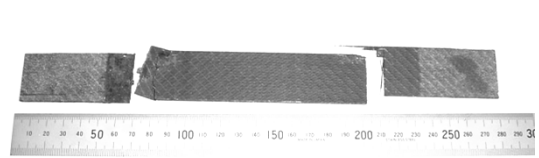


Fig. 4.16: Non-perforated RFI UTS

failure

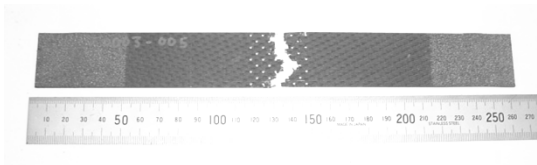


Fig. 4.17: Drilled PP UTS failure

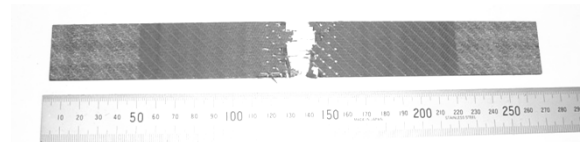


Fig. 4.18: Drilled RFI UTS failure

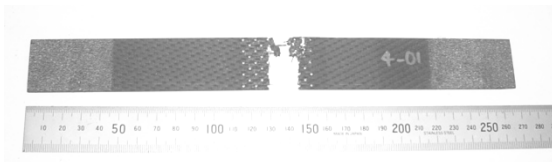


Fig. 4.19: Moulded hole PP UTS failure

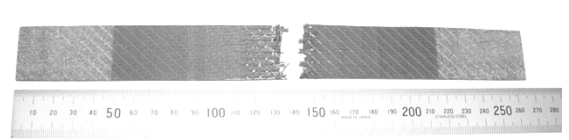


Fig. 4.20: Moulded hole RFI UTS failure

4.4.5 Perforation Effects on Compression Properties

In ambient and hot/wet conditions both the moulded and drilled perforations cause significant reductions in laminate strength. Under ambient conditions the compressive modulus shows no significant difference between the non-perforated and moulded hole configurations while the drilled samples show a clear reduction.

This data also highlights the differences between the woven and non-woven reinforcements. For both material types there is little difference between the ambient and conditioned strength for the drilled perforations.

This shows that fibre discontinuity provides the key failure mechanism in this loading configuration. However, with the moulded perforations there is a lower reduction in ambient laminate strength (consistent with that seen in the tensile data) but an equivalent reduction in both moulded and drilled perforations following hot/wet testing.

The fibre distortion around each hole of the moulded perforations is considered to have the consequence of a pre-buckled state that places a greater reliance on the fibre-matrix interface to resist failure. Taking into consideration the increase in resin content at the moulded perimeters (see Microstructure Analysis, Chapter 5) it is possible to explain why the conditioned specimens show the lower performance after the plasticising effects of the moisture content. The plasticisation of the matrix might be reducing its capacity to resist total buckling of the pre-buckled fibres. This data shows the behaviour pattern to be consistent over both material types. This observation is consistent with previous studies conducted on the hygrothermal effects in carbon-epoxy laminates, where the breakdown of the fibre-matrix interface is a consequence of the increase in moisture content. This has been reported by Candido et al. (2007) where fractographic analysis found degradation of a fibre-matrix interface through moisture absorption. Likewise Selzer et al. (1997) concluded that the presence of moisture in carbon-epoxy composites led to an increase in interface failure due to a softening of the matrix and reduction in fibre-matrix adhesion.

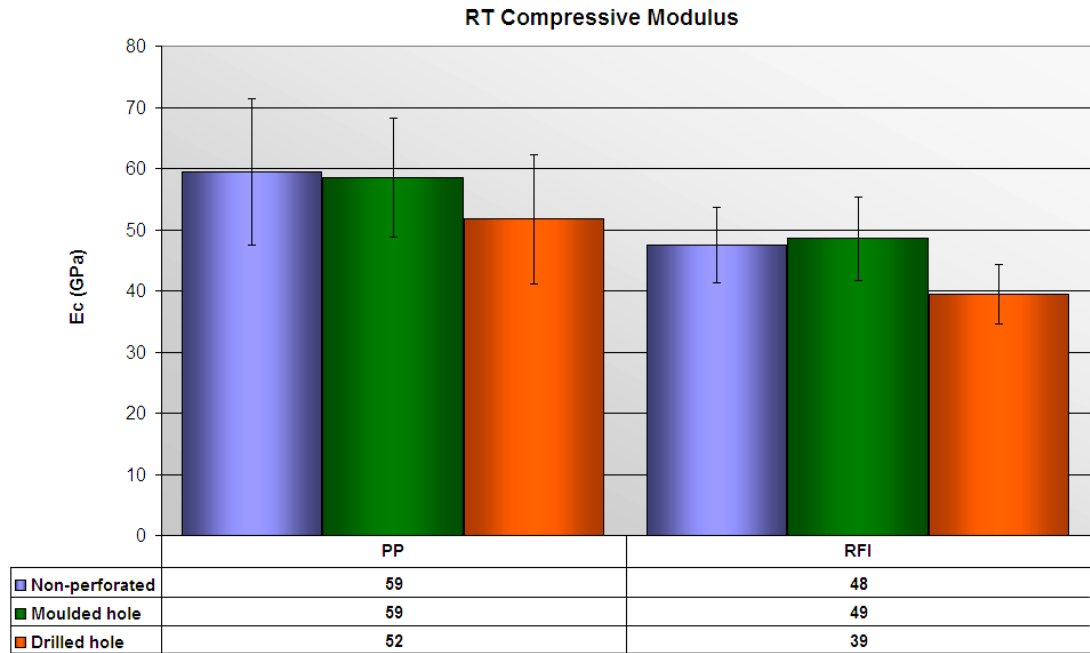


Fig. 4.21: Pre-preg and RFI compressive modulus results

Fig. 4.21 illustrates the same compressive modulus for the standard and moulded perforated laminates. This is attributable to the fibre continuity in each configuration. Equally, the drilled perforation results show the reduction in stiffness caused by the fibre fracture at each hole. In numerical terms the moulded perforation has less than 2% difference in stiffness while the drilled perforations show a 13% reduction.

In addition we see a similar laminate stiffness between the moulded hole RFI laminate and the standard RFI laminate, while the drilled hole samples show a 17% reduction. The probable cause of the stiffness increase between the drilled and moulded perforations (in both material types) is the fibre continuity coupled with geometrical changes seen in the moulded

perforate laminates. In the moulded hole samples an increase in thickness around the holes was observed that would act to reduce the stress concentration caused by the hole itself. This varying geometry can cause significant changes to compressive data and possibly a larger variation will be seen in these tests due to localised buckling effects. The reduction of modulus in the drilled specimens is a further indicator of the discontinuous fibres reducing laminate performance.

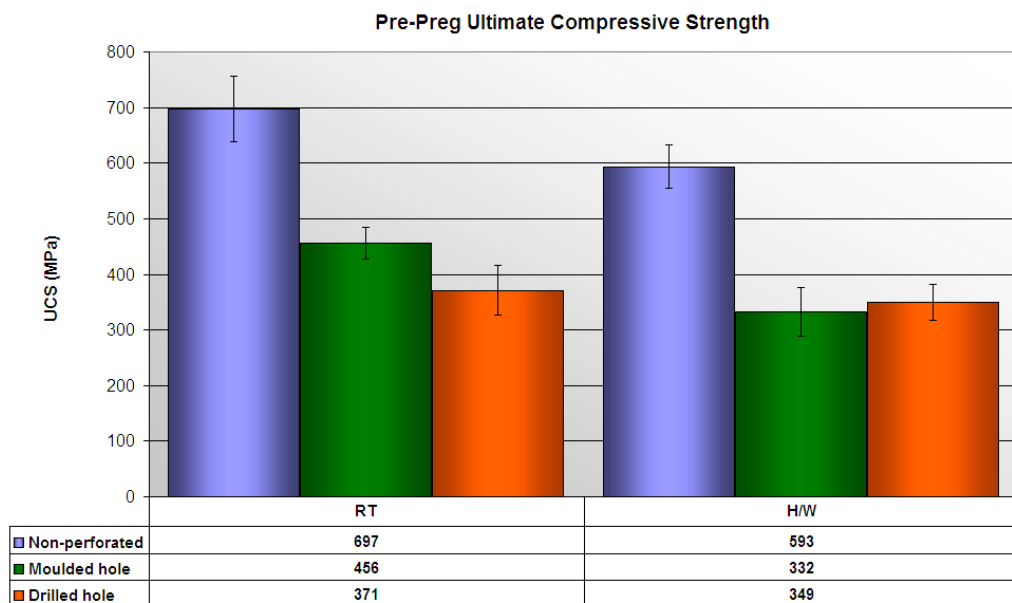


Fig. 4.22: Pre-preg compressive strength results

Fig. 4.22 highlights the differences found between the ambient and hot/wet compressive performance of the pre-preg material. As discussed above, the equivalent environmental knockdown of the moulded perforations compared to the drilled perforations is visible in the data. In ambient conditions, the pre-preg laminate compressive strength reduces by 35% with the moulded perforations and 47% by the drilled perforations.

When environmental conditions are considered, the laminate compressive strength reduces by 41% and 44% with both configurations.

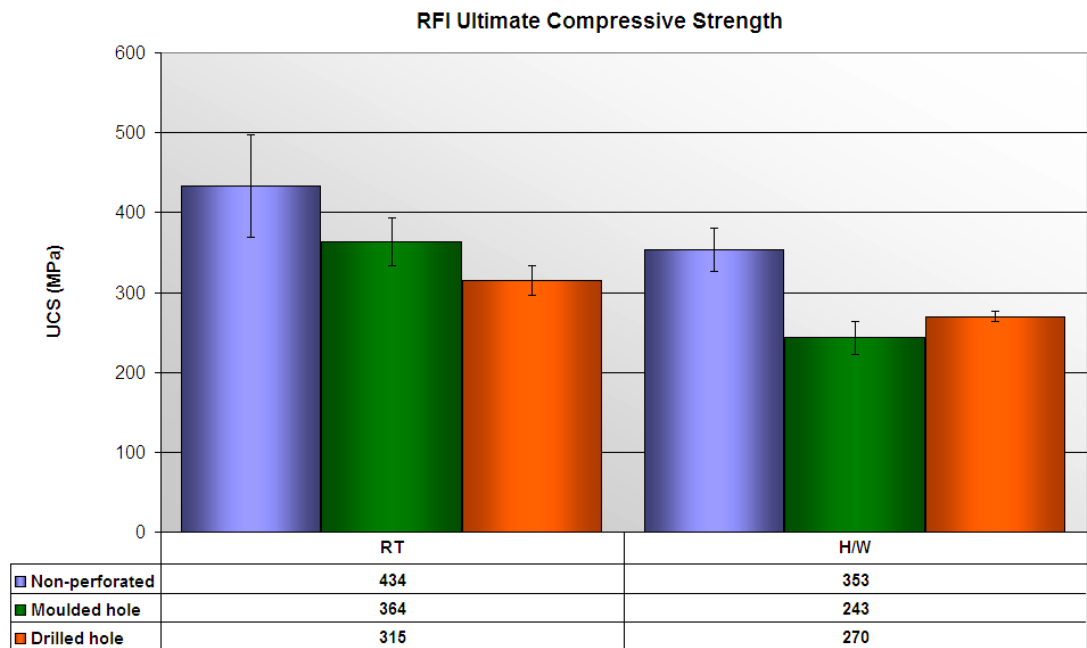


Fig. 4.23: RFI compressive strength results

In Fig. 4.23 the differences between the ambient and conditioned RFI moulded perforation performance are highlighted. In ambient conditions, the laminate compressive strength reduces by 16% with the moulded perforations and 27% with drilled perforations. In considering the environmental conditions, the laminate compressive strength reduces by a further 31% in the moulded configuration and 24% in the drilled configuration. From this data it can be concluded that with the moulded hole configuration, a combination of fibre waviness and resin rich pockets around the stress concentrations leads to failure. This is supported by the

relatively large decrease in strength seen in the moulded hole pre-preg, where the fibres are kinked both in plane (by the moulded holes) and out of plane (by the weave). The contribution of the matrix to the strength of the sample is highlighted by the relatively large decrease seen with the conditioned moulded hole RFI specimens. The RFI moulded hole samples have been seen to have a higher resin content around the holes where failure is initiated.

As illustrated in Figs. 4.24-35, valid compression failures were observed in all specimens for each configuration.

RT Failures



Fig. 4.24: RT non-perforated PP UCS failure



Fig. 4.25: RT moulded hole PP UCS failure

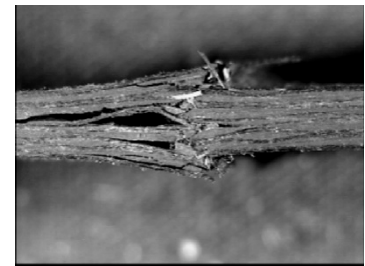


Fig. 4.26: RT drilled PP UCS failure

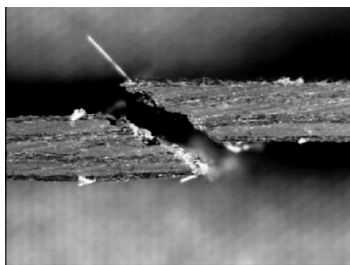


Fig. 4.27: RT non-perforated RFI UCS failure

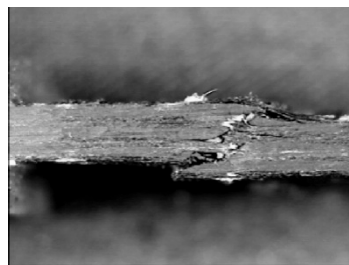


Fig. 4.28: RT moulded hole RFI UCS failure

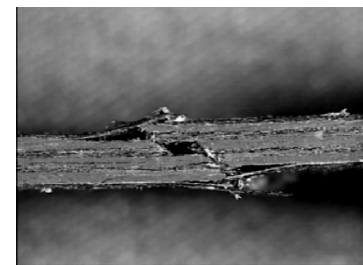


Fig. 4.29: RT drilled RFI UCS failure

H/W Failures



Fig. 4.30: H/W non-perforated PP UCS failure

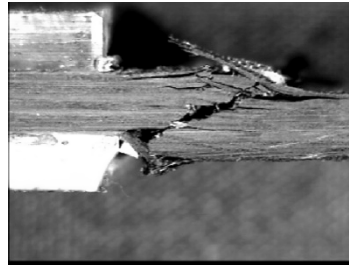


Fig. 4.31: H/W moulded hole PP UCS failure

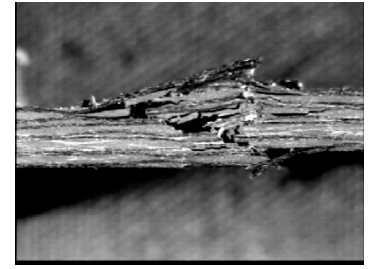


Fig. 4.32: H/W drilled PP UCS failure

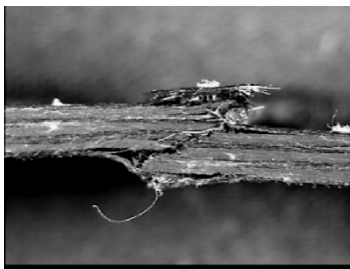


Fig. 4.33: H/W non-perforated RFI UCS failure

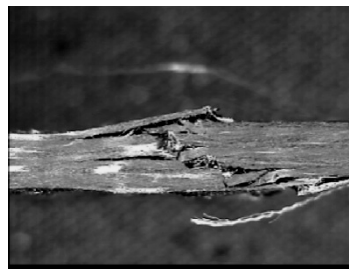


Fig. 4.34: H/W moulded hole RFI UCS failure



Fig. 4.35: H/W drilled RFI UCS failure

4.4.6 Effects of Perforation on ILSS

The ILSS data show an ambient reduction of 15% and a conditioned reduction of 18% in pre-preg performance due to moulded perforations, while in the same material the drilled specimens demonstrate an ambient reduction of 26% and 23% in hot/wet conditions. The RFI material, however, shows similar ambient performance and a conditioned reduction of only 5% in laminate performance due to the moulded perforations. The drilled specimens show an 11% reduction in ambient and a 4% reduction in hot/wet conditions. These results are illustrated in Fig. 4.36-4.37.

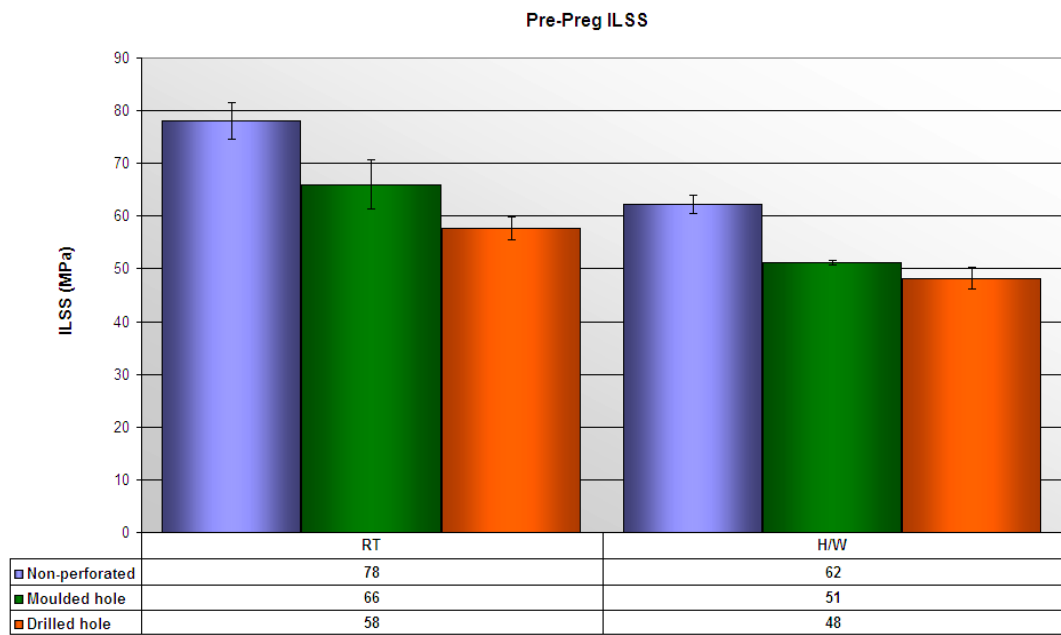


Fig. 4.36: Pre-preg ILSS results

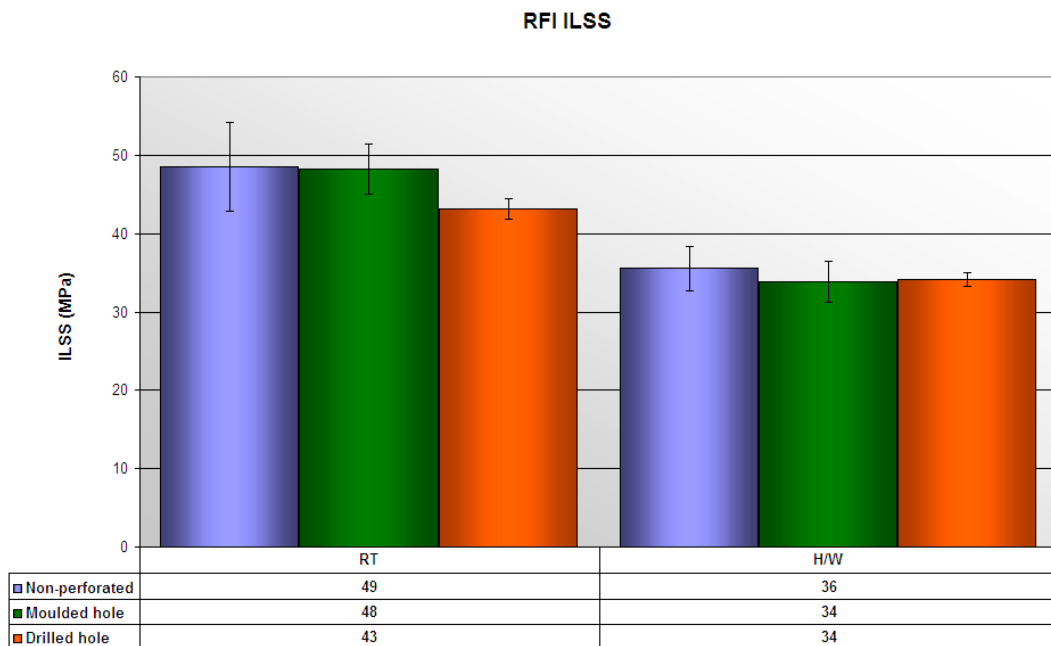


Fig. 4.37: RFI ILSS results

4.4.7 Comparisons to Predicted Performance

With the completion of the test matrix it was possible to refer back to the predicted pre-preg data of Section 4.3 and draw comparisons on the alignment levels achieved.

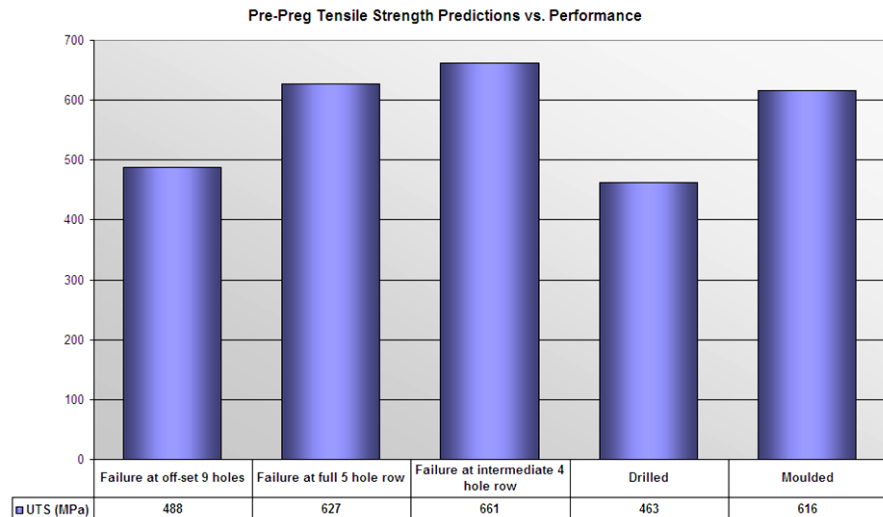


Fig. 4.38: Comparisons of pre-preg tensile strength predictions to actual test data

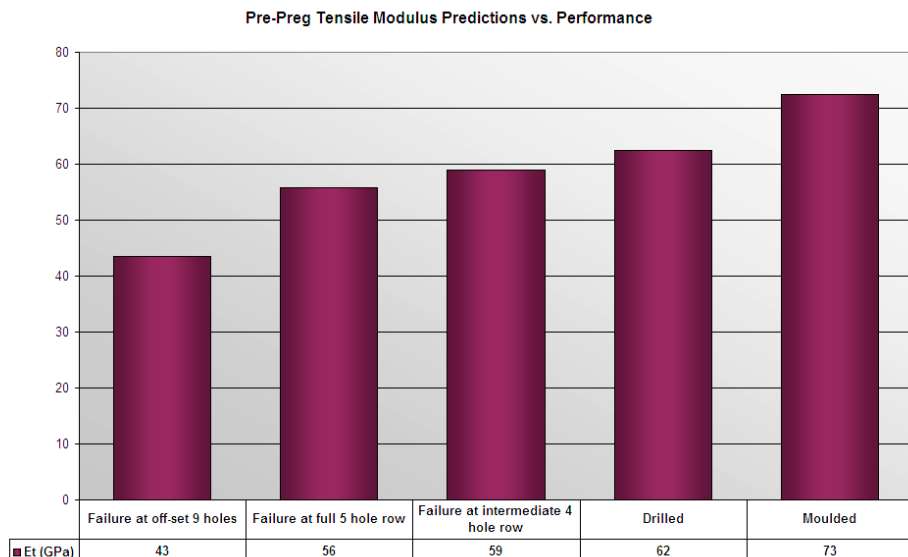


Fig. 4.39: Comparisons of pre-preg tensile modulus predictions to actual test data

It is clear that although the modulus predictions do not show agreement there are some interesting comparable levels in the strength data. There is very good correlation between the failure prediction at the off-set nine hole row with the drilled performance levels. In this case the predicted strength level is observed to be 105% of the actual performance. With the moulded hole performance levels it is the failure prediction at the full five hole row that demonstrates good correlation with the predicted level observed to be 102% of the actual performance.

Validating this retrospectively with the same methods for the RFI performance levels there is an equivalent pattern with a predictive nine hole failure strength of 665 MPa and five hole failure strength of 841 MPa. Comparing with the recorded data we see these predictive performance levels at 97% and 100% of the drilled and moulded tested levels respectively.

Further evidence for these patterns is offered by the failure behaviour witnessed during the tensile testing (see Figs. 4.17-4.20) where a zig-zag failure path was commonly seen in the drilled specimens showing greater influence of the off-set pattern and a straight failure path seen in the moulded specimens where it would be expected that the greater reduced five hole straight path would be the more influential.

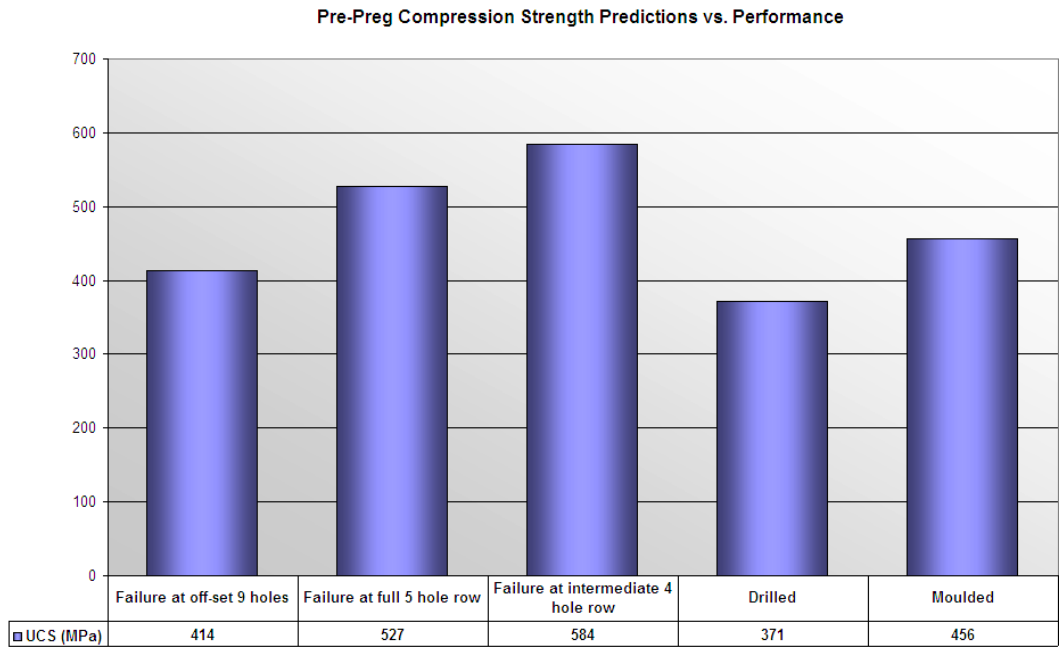


Fig. 4.40: Comparisons of pre-preg compression strength predictions to actual test data

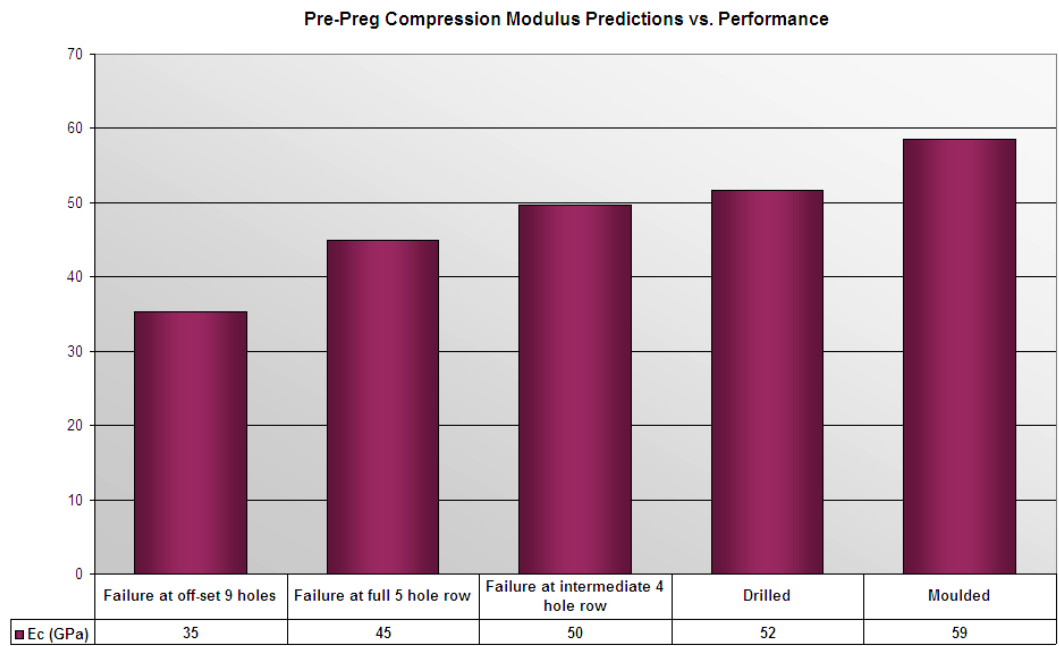


Fig. 4.41: Comparisons of pre-preg compression strength predictions to actual test data

Conducting a similar analysis on the compression based predictions it can be observed that this approach does not offer good alignment in modulus data but does indicate some correlations in strength data. On calculating the correlation levels there is a lower level of alignment than with the tensile conditions predicting at 110% of the drilled performance and 120% of the moulded hole performance. It can therefore be concluded that the compression method returned poorer results due to the increased complexity of the compression failure mode and specifically so with the moulded hole laminates where fibre buckling occurrence will play a key role in the failure mechanism.

While the tensile analysis demonstrates excellent correlation in this study it must still be treated with caution due to the basic nature of the model as highlighted by the compression correlation levels. Further evaluations of this approach for alternative hole patterns with a moulded manufacturing methods may offer further benefits.

4.5 Physical Data

For flat, parallel sided panels cured ply thickness (cpt) is given by:

$$\text{cpt} = \frac{n \cdot A_w}{V_f \cdot \rho_f}$$

Where:

n = number of layers

V_f = fibre volume

ρ_f = fibre density

A_w = fabric areal weight

Evaluation of the physical data shows a localised increase in ply thickness at the hole perimeters due to the perforation process. This variation is illustrated and discussed in detail in Chapter 5. This is evident in both configurations and represents an increase of approximately 4.6% in pre-preg and 12.1% in RFI.

The difference in thickness increases can be associated with the combination of differences in tow size and curing pressures used. In addition, the increase in thickness from standard laminate to moulded hole material is directly linked with two characteristics:

- the displacement of fibres around the holes
- an increase in resin content at the holes due to this fibre movement

This fibre distortion increases the fabric areal weight at the hole perimeters through fibre packing with corresponding gaps appearing between the tows where an increase in resin content can be witnessed. If we consider the relationship above then we can use basic composite theory to investigate this link between fibre distortion and an effective increase in areal weight.

From Appendix E, with $\rho_f = 1800\text{kg/m}^3$, we have:

Table 4.5: Moulded hole perimeter physical analysis

	Pre-preg	RFI
v_f	56.0%	50.4%
cpt	294 μm	360 μm
A_w	296g/m ²	327g/m ²
Deviation from nominal A_w	+5.7%	+5.5%

The respective increases in effective areal weight can be taken as a direct consequence of fibre re-distribution from the 6% open area of the acoustic design as with the similar pre-preg observation.

Although these percentages are slightly lower than the open area specified it can be assumed that this discrepancy is due to the larger tolerances associated with the FlexPerf hole pitch.

The lower fibre volume of the moulded hole laminates can be associated with the resin rich pockets that formed at areas of tow distortion. These were investigated further through microstructural characterisation (see Chapter 5) and reflects the results observed by Mouritz (2007) on z-pinned composites. This particular study found the global fibre volume fraction of a sample reduced due to the laminate swelling that was induced by the z-axis reinforcement to accommodate the additional material. The higher fibre volume of the pre-preg samples are assumed to be due to higher deformation resistance provided by the weave and the increased curing pressure of 7 bar. With NCF type fabrics as used in this RFI process, it is clear from earlier analysis that the stitched fibres distort freely, providing an increased open volume for resin. The values shown were obtained through standard acid digestion and showed the laminates to be of a high quality with low void contents. These tests also provide the values for laminate density, the variation in which is a direct cause of the variation with fibre volume.

The thermal properties tested through Differential Scanning Calimetry (DSC) and Dynamic Mechanical Analysis (DMA) are summarised in Tables 4.6 and 4.7. A TA DMA 2980 was used for the DMA analysis and a TA DSC 2920 was used for DSC. The thermal

performance levels were tested as part of the study to ensure no detriment was seen through the use of the insulating FlexPerf mats. Five samples were tested for each material in both DSC and DMA.

Table 4.6: DSC results for degree-of-cure

% of Cure = $100 \times [1 - (N_c/N_{uc})]$	8552 Laminate (P-P)	M36 Laminate (RFI)	Neat M36
Average	81	60	89
Max	86	67	90
Min	77	52	87

<p>N_c = Normalised internal energy for cured specimen N_{uc} = Normalised internal energy for un-cured specimen</p>

Table 4.7: DMA results for glass transition temperature

DMA Result	8552 Laminate (P-P)	M36 Laminate (RFI)
Avg. T_G - Onset ($^{\circ}C$)	170	176
Avg. T_G - Loss ($^{\circ}C$)	185	194
Avg. T_G - Peak ($^{\circ}C$)	209	221

The values for glass transition temperature and the extent of cure for each of these systems were taken to validate the cure cycles used and were obtained through standard DMA and DSC analysis. The DSC data allow an evaluation of the extent of cure for the systems but true confidence can only be placed in the M36 resin value as this was obtained with cured neat resin. For the composite data the problem lies with determining an exact resin content for each sample tested. The method used

in this project was to normalise the results to 100% resin content through the values obtained for fibre content of un-cured and cured pre-preg. This does not provide an accurate reflection of the actual sample tested but such a study would be beyond the scope of this study and is a topic that would benefit from further investigation.

4.5 Moisture Uptake

One of the main drivers for investigating moulded hole perforated laminates has been the assumption that a moulded hole will have more resistance to in-service weather degradation than a drilled perforate. It is for this reason that the moisture uptake of each configuration was investigated. Perforated specimens were measured for a truer indication of how laminates would perform in component form. In total eight travellers were used, 4 pre-preg and 4 RFI, with each material type having one drilled, one moulded and two non-perforated specimens. Each of the non-perforated specimens was taken from the same laminate as the drilled and moulded samples so as to keep the laminate quality and cure history consistent. The equipment used for this artificial aging was a bench top thermal humidity cabinet similar to the modern Thermotron S-Series type chambers. The parameters for the environmental conditioning were set at 70°C and 85%R.H for a period of 1000 hours with the samples prepared as 50x50mm sections with the cut edges sealed with foil tape to ensure

absorption occurred only through the laminate faces and perforated surfaces. Before the conditioning started the specimens were dried at 110°C for 24 hours and weighed, further weights were then recorded during exposure approximately every 48 hours until the 1000-hour limit was reached and the coupons then tested to failure as per the property matrix shown in Table 4.1. The moisture uptake for each type of specimen and material are shown in Figs. 4.42 and 4.43.

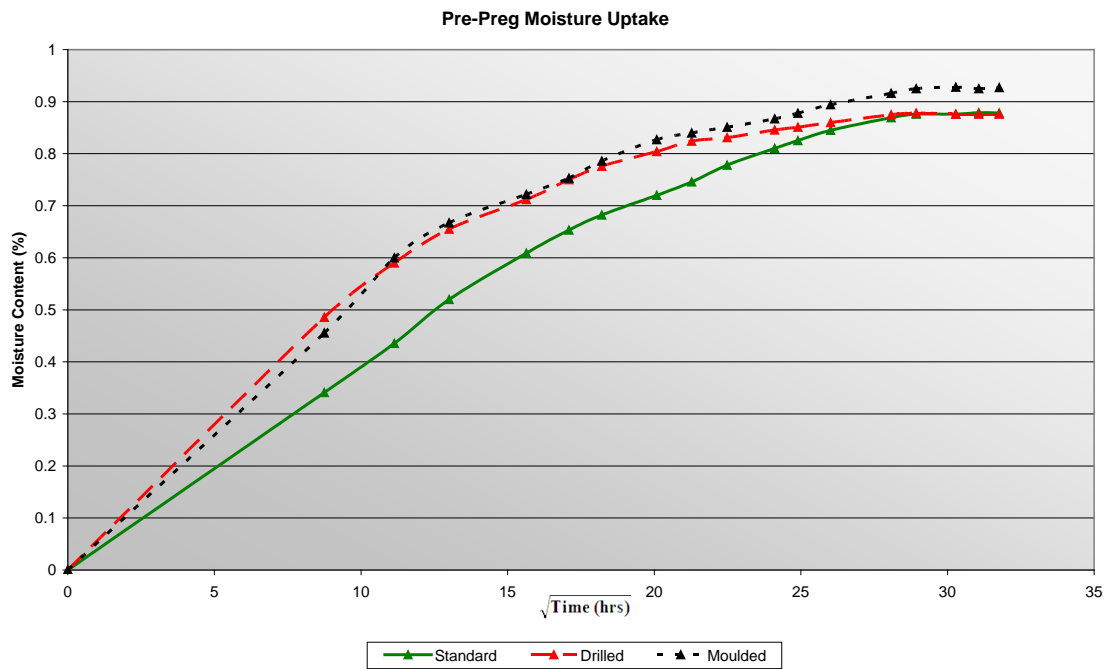


Fig. 4.42: Pre-preg laminate moisture absorption

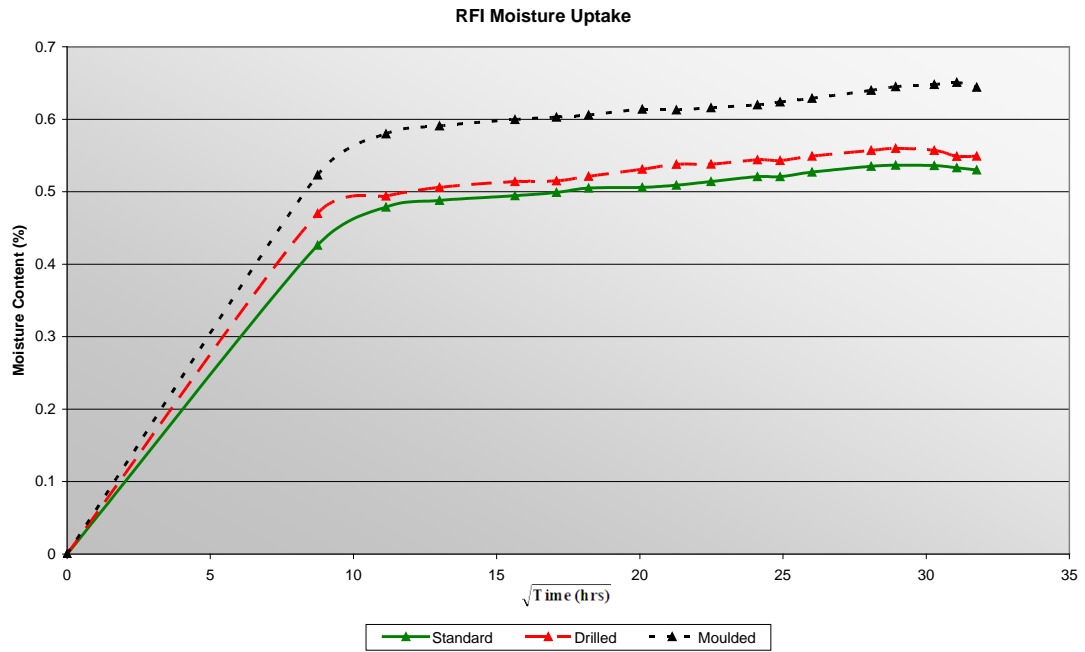


Fig.4.43: RFI laminate moisture absorption

In each material system the perforated samples demonstrate a slightly increased rate of moisture uptake probably due to the higher proportion of surface area present. For the pre-preg uptake curves it can be observed that each configuration type arrives at final values that may be considered equivalent. A distinct difference in the RFI data shows that while this material system in general has a lower equilibrium level (~0.6% vs. ~0.9%) the moulded hole configuration has a higher final value than the drilled and non-perforated RFI configurations. The reason for this slight increase in the moulded perforated RFI is directly linked to the differences in microstructure of each material type. With the exception of the holes there is no difference in microstructure between drilled and non-perforated laminates, as is to be expected. The main difference between the FlexPerf

laminates and the standard laminate structure is the increase in resin volume content and the deformation of the fibres at the perforation perimeters (hole surface). It then follows that by having large resin pockets at the perforation perimeters close to the hole surface gives a larger resin volume in direct surface content for moisture absorption.

The degradation effects of moisture in carbon-epoxy composites are generally a) plasticising of the epoxy resin and b) interface breakdown between the fibre and the matrix. This then gives an explanation of the reduced hot/wet performance of the moulded perforations under compression. This indicates the mechanics of moisture absorption to be predominantly through diffusion as opposed to a wicking effect along the fibres.

Examining the fibre and resin ratio differences of the moulded hole configurations, there are V_f reductions of around 1% for the pre-preg and 5% for the RFI. However if the bulk of this difference occurs solely at the hole perimeters, it is logical to assume that at the surface of the holes the localised resin content of the moulded specimens is considerably higher than at mid hole pitch. It can be expected that the increases in moisture witnessed with the moulded hole laminates will have an effect on the hot/wet mechanical properties of those particular configurations and may even be amplified due to the stress concentrations caused by the perforations. The differences seen between the equilibrium levels of each type of material are linked with the formulation differences of each resin.

The RFI laminates possibly have a higher cross-link density and hence lower free volume for moisture molecules to occupy.

4.6 Acoustic Validation

One of the major differences between the moulded and drilled perforations was found to be the dimensional tolerance of the FlexPerf hole pattern compared with that of the machining pattern. Although FlexPerf provides the same open area as drilling, the hole pitch is likely to be less uniform. There has also been evidence throughout this project that the moulding of holes with this method does not always produce perforations normal to the surface of the laminate. The combination of these reasons raised cause for concern over the acoustic performance of a FlexPerf laminate. For this reason an acoustic validation test was undertaken to evaluate each type of perforation in its role in the conventional Helmholtz resonator setup. The tests were carried out using an impedance tube procedure with the perforate skin bonded to honeycomb cores as per the Honeywell approved test method AS900/MANF/16/0034 with three repeats per configuration. As described by Malmay et al. (2001) the acoustic impedance tube test induces grazing incidence on the sample through the perpendicular generation of an acoustic plane wave. The variations in sound pressure and velocity are then measured to calculate the impedance through two microphones positioned at the acoustic liner surface and at the

extremity of the tube. The data outputs for this particular test method are the reactance and resistance components for the complex ratio of acoustic impedance. The resistive contribution (R) is the real component and represents the ability of the resonator to remove energy from the sound waves at the boundary layer interface of the perforation and air. The reactive contribution (X) is in the imaginary element and represents the ability of the resonator to transfer the sound waves' kinetic energy to potential energy within the cell structure. For these tests it was necessary to manufacture four honeycomb panels, two from each material type and each material having one panel with a drilled skin and one with a moulded hole skin. The method of manufacture for these panels was kept in line with the techniques used in production to keep the panels a close simulation of AS-907 parts. The perforated skins were kept to the same lay-up as per the GKNAS component work instructions, WBA 7271 041-043 and WBA 7271 043-043, utilising the hole design established for this project. For the backing skins, the same lay-up as the acoustic skins was used for simplicity as they had no effect on the comparative results. The core for each test plaque was a 9.5mm thick slotted aluminium honeycomb of 91kg/m^3 and 9.5mm cell size, as used on the AS-907 outer fan duct panels. With these production parts a glass scrim is incorporated into the skin lay-up so as to protect the core against galvanic corrosion. For the purpose of these trials the glass scrim was omitted due to the short lifespan required. The skins were bonded to the core with FM 300-U adhesive with heat induced

reticulation of the adhesive used to reduce the risk of hole blockage. This reticulation process ensures the adhesive separates over the cells of the honeycomb core to form an adhesive bead along the cell walls. The design and construction of the panels are illustrated in Fig. 4.44 with the results detailed in Table 4.8.

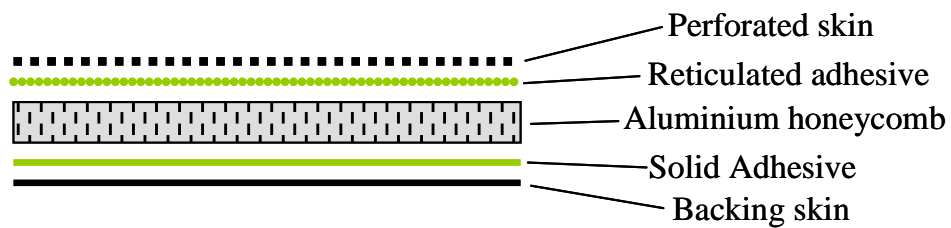


Fig. 4.44: Acoustic test plaque configuration

Table 4.8: Acoustic test results

Laminate Type	Drilled Pre-Preg	Moulded Pre-Preg	Drilled RFI	Moulded RFI
Avg. frequency at minimum reactance (Hz)	2770	2686	2814	2738
Avg. resistance at 3000 Hz (MPa.s/m)	1.23	1.07	1.13	1.14

NOTES (as per AS900/MANF/6/0034)

- Target frequency for minimum reactance is 2350 – 3350 Hz
- Target resistance is 1.10 – 1.70 (MPa.s/m)

The test results show that with the pre-preg specimens the reactance reduces by only 3.0% from drilled to moulded holes so can be taken to be equivalent. The resistance of the moulded hole panel is 13.5%

lower than that of the drilled trial. This reduction indicates that the irregularity of the moulded perforations causes degradation in the acoustic performance. The RFI results again show a 3.0% reduction in reactance from drilled to moulded holes and a 1.3% increase in resistance from drilled to moulded holes. These differences are considered negligible based on the historic knowledge of the test method within GKN.

This difference in the pre-preg and RFI panels can be used to highlight the variation in quality of the FlexPerf process where inconsistent patterns are found when directly comparing the drilled perforations. This variation may be linked with the hole pitch tolerance and would benefit from further investigation. Unless the hole quality variation could be reduced then the FlexPerf method is unlikely to be attractive for aerospace production.

Chapter 5: Microstructure Characterisation

Moulding perforations in fibre reinforced laminates inevitably causes deviation in the normal fibre path and hence the primary load carrying path of each ply. To fully understand the effects this distortion has on the laminate structure it is necessary to investigate how the microstructure varies around the holes. For this reason a series of pre-preg and RFI moulded hole samples were sectioned, prepared and polished for detailed analysis. Sections were taken at various positions across the hole pitch as illustrated in Fig. 5.1.

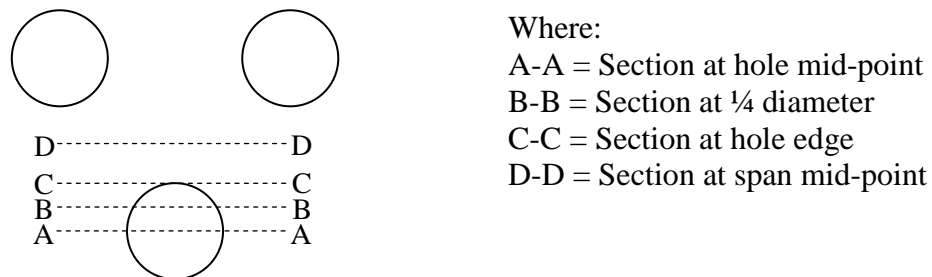


Fig.5.1: Section location in relation to hole position

Analysing these sections from each material type now allows a detailed evaluation of the laminate structure through the hole pitch. This presents an insight into the level of fibre deformation caused by the moulding process at each cross-section in Figs. 5.2-5.11.

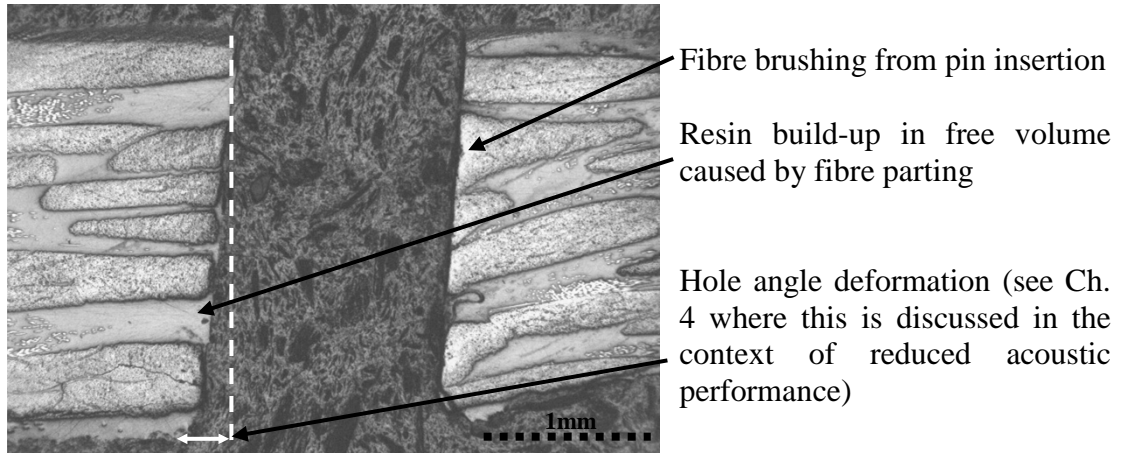


Fig. 5.2: Moulded pre-preg hole at A-A

(Hole diameter 1.3mm)

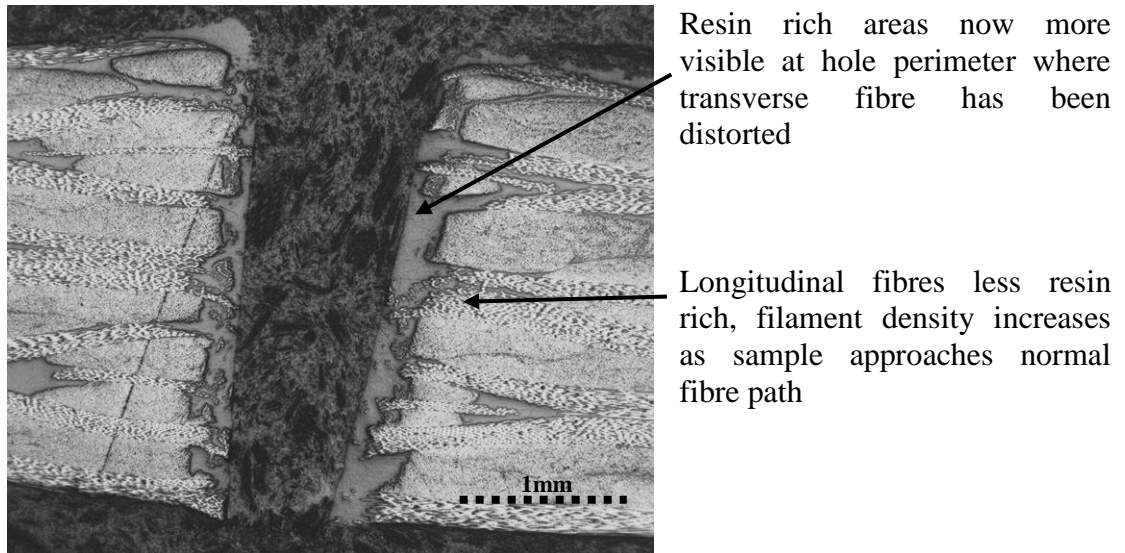
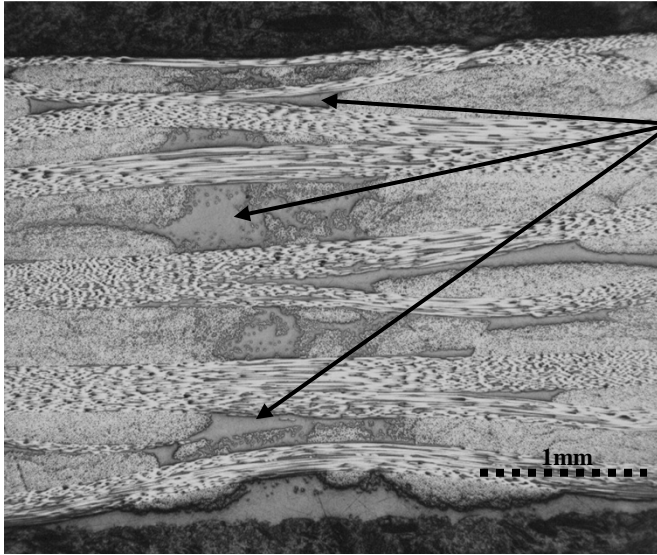
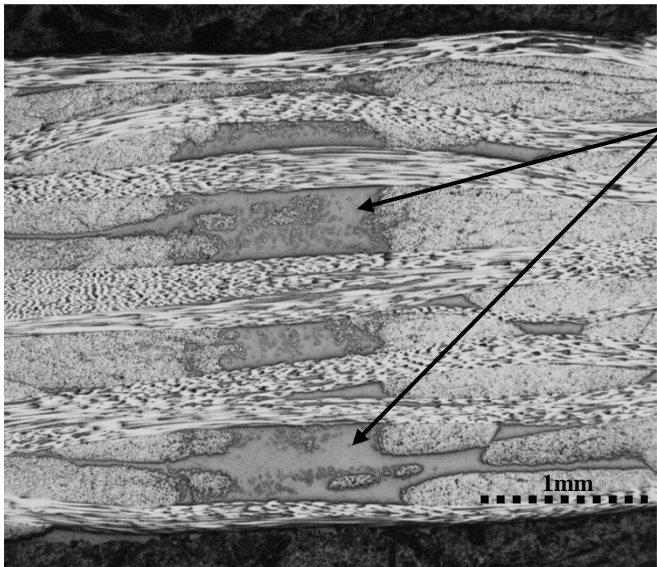


Fig. 5.3: Moulded pre-preg hole at B-B



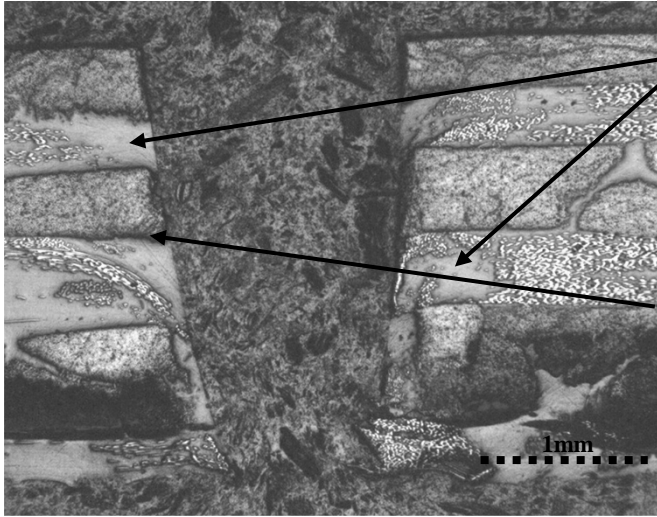
Resin rich areas become more apparent at the point of distortion for the transverse fibres. These are clear resin channels caused through fibre parting of the pin insertion

Fig. 5.4: Moulded pre-preg hole at C-C



Resin rich areas attributable to transverse fibre distortion still visible indicating the depth to which the feature is present. The size of these resin channels indicates the fibre gaps are continuous from hole to hole.

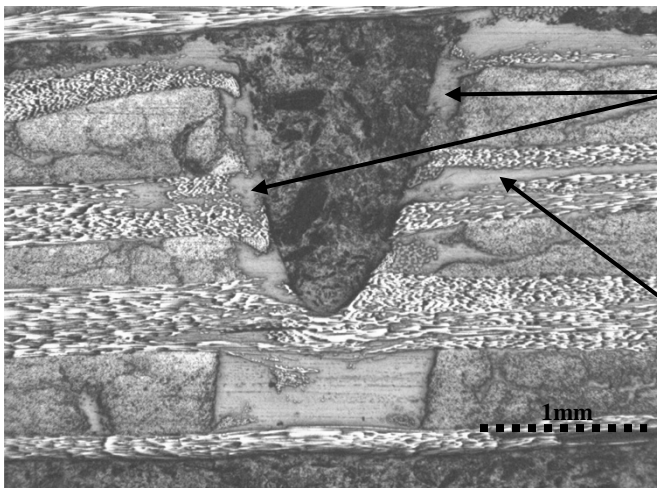
Fig. 5.5: Moulded pre-preg hole at D-D



Resin rich areas where longitudinal fibres are split by pins during processing. In some areas no longitudinal fibre is visible where resin has filled the volume left by fibre movement.

Considerable increase in tow thickness around hole from fibre brushing by pin insertion.

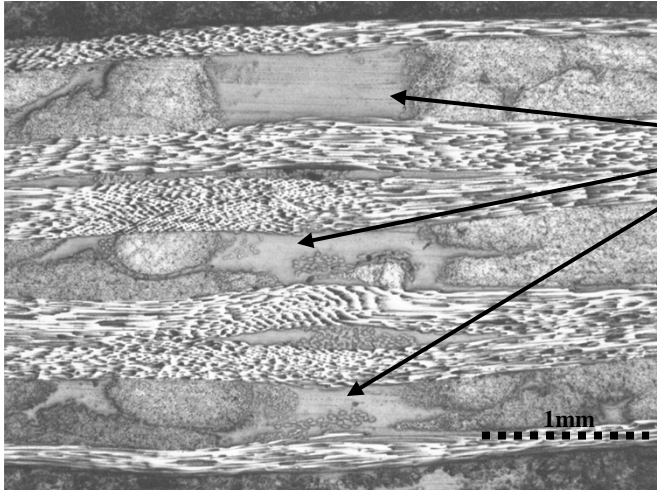
Fig. 5.6: Moulded RFI hole at A-A



Effects of transverse fibres distorting around pin becomes more apparent with appearance of large resin pockets around hole perimeter

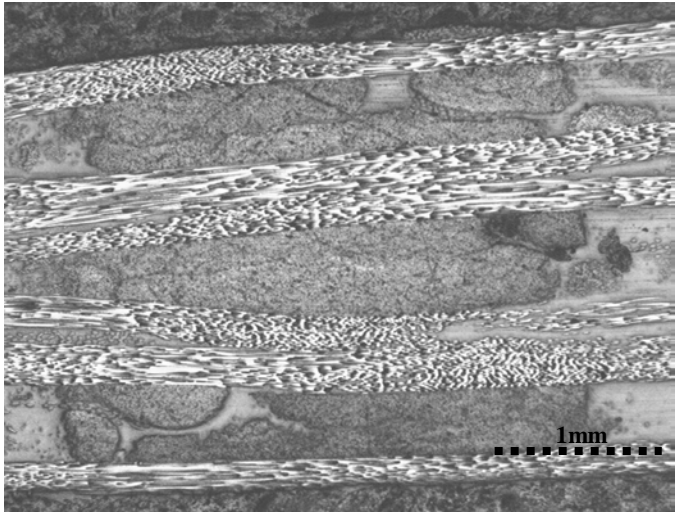
Longitudinal resin richness still visible but reduced in volume as we approach increased density of filaments

Fig. 5.7: Moulded RFI hole at B-B



Transverse resin richness clearly visible indicating the level of progression this feature makes through the laminate

Fig. 5.8: Moulded RFI hole at C-C



Transverse resin richness reduced showing fibre closure after pin distortion

Fig. 5.9: Moulded RFI hole at D-D

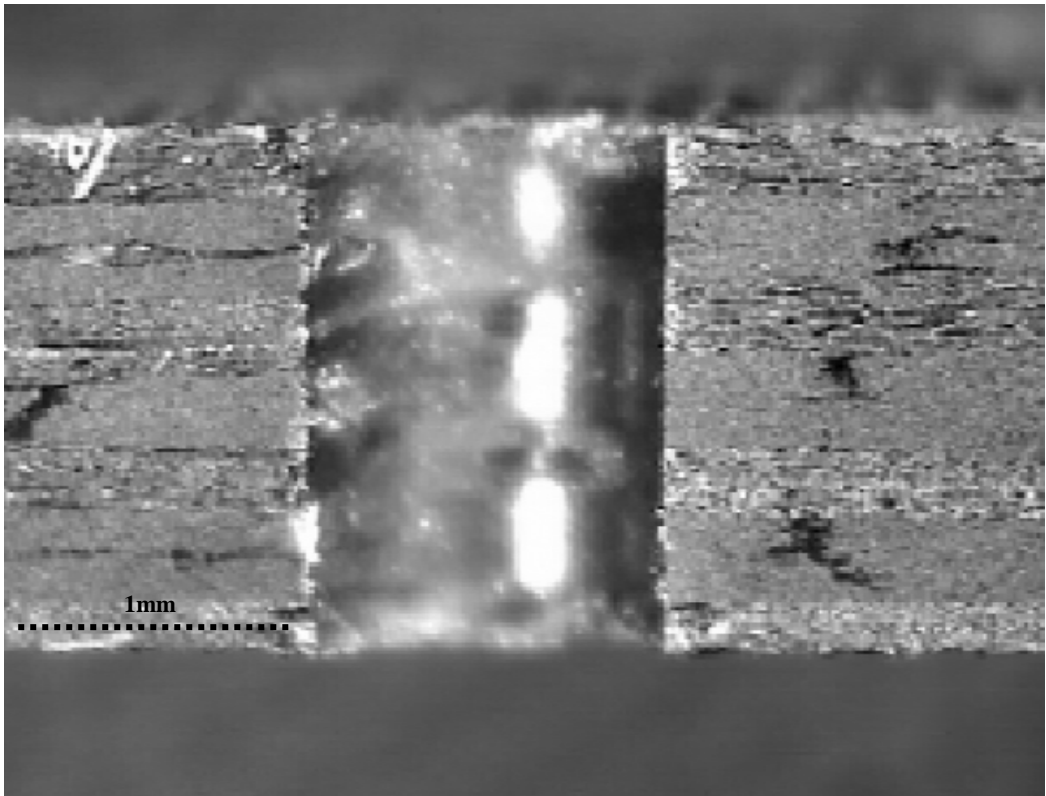


Fig. 5.10: Standard RFI drilled hole

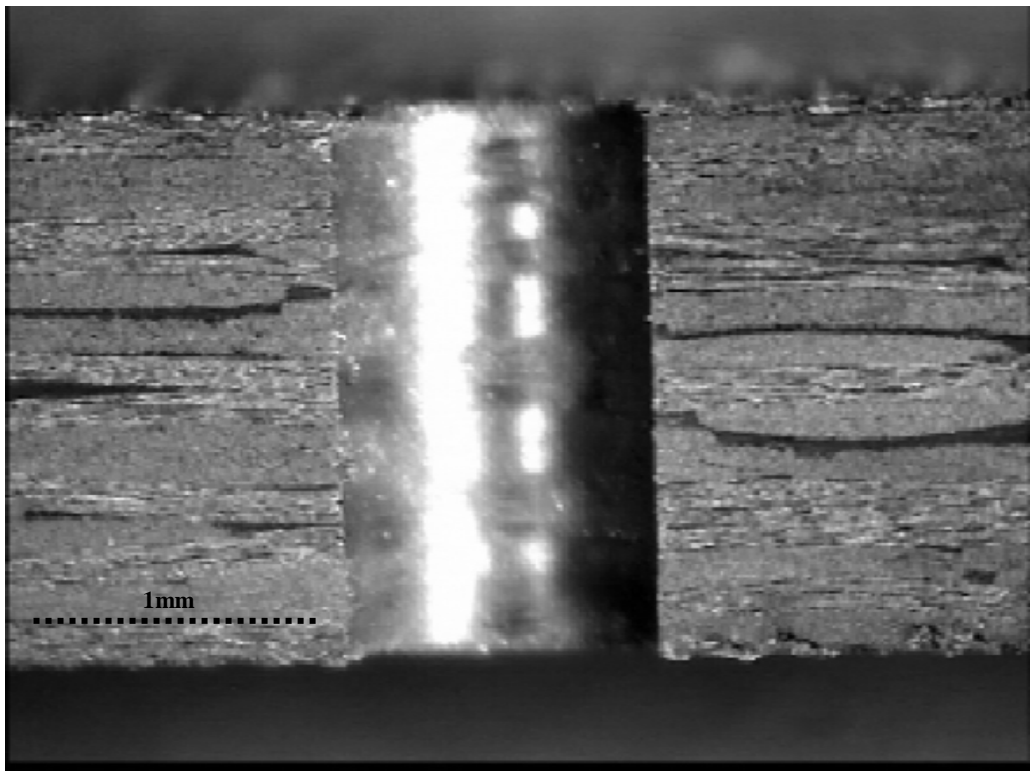
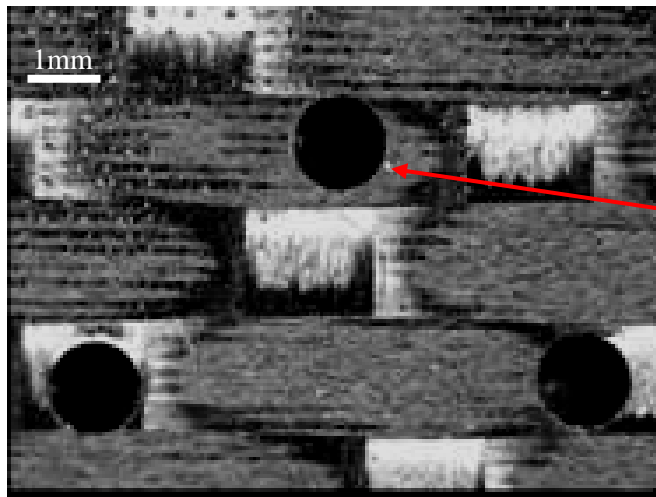


Fig. 5.11: Standard pre-preg drilled hole

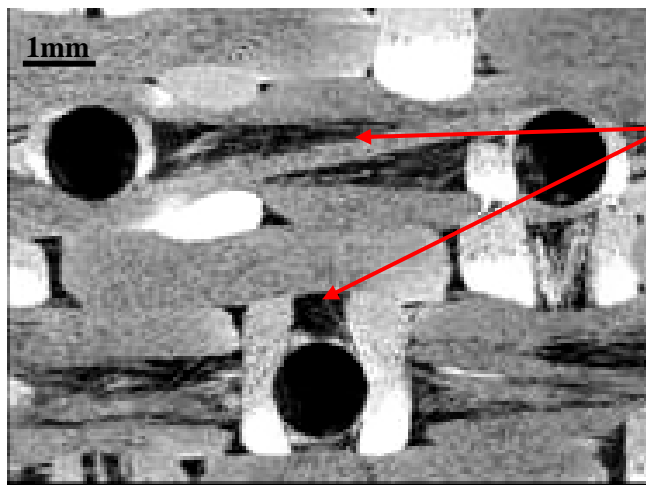
With the drilled hole we now see consistent fibre content throughout laminate and no thickness increase as associated with the moulding process.

In planar view some of these effects are also visible in Figs 5.12-15, at 8x magnification, where samples have been polished in-plane to show the distortion or damage the fibres suffer as they pass the moulded or drilled holes.



Here fibre breakage caused by drilling is visible as a contrasting mark.

Fig. 5.12: Drilled pre-preg planar view



Fibre tows split by presence of moulding pins, upper highlighted area indicates the presence of a single split tow

Fig. 5.13: Moulded hole pre-preg planar view

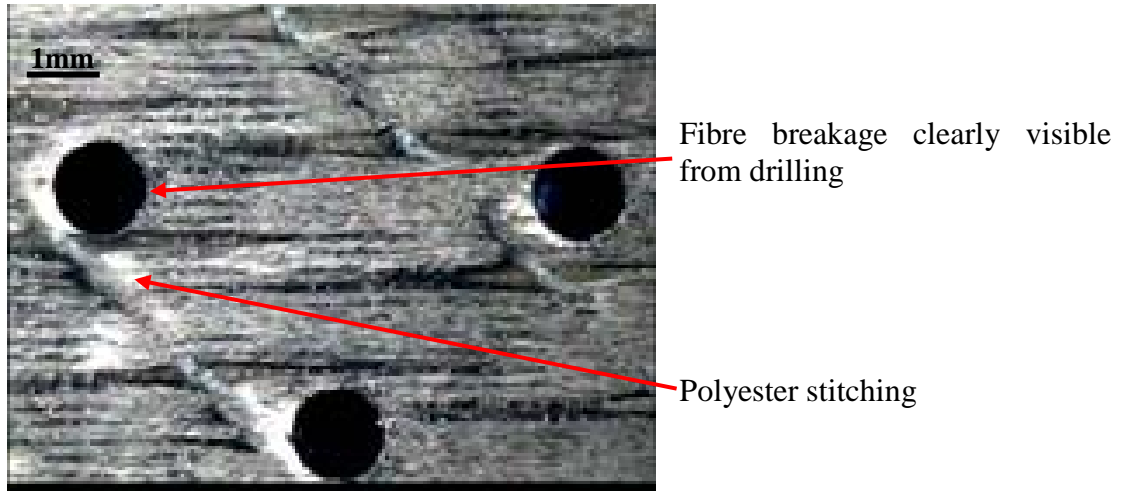


Fig. 5.14: Drilled RFI planar view

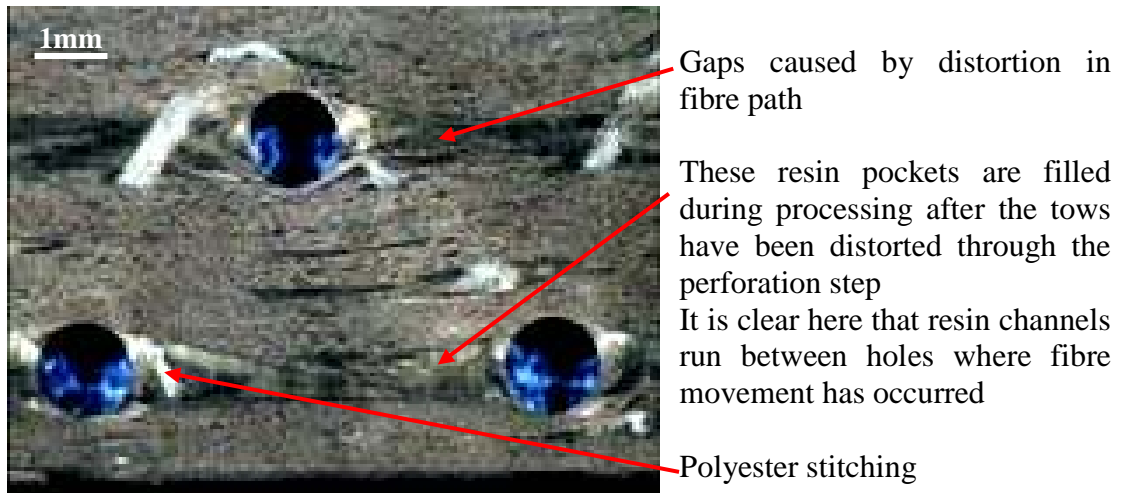


Fig. 5.15: Moulded hole RFI planar view



Fig. 5.16: Hole-to-hole fibre distortion from RFI mouldings

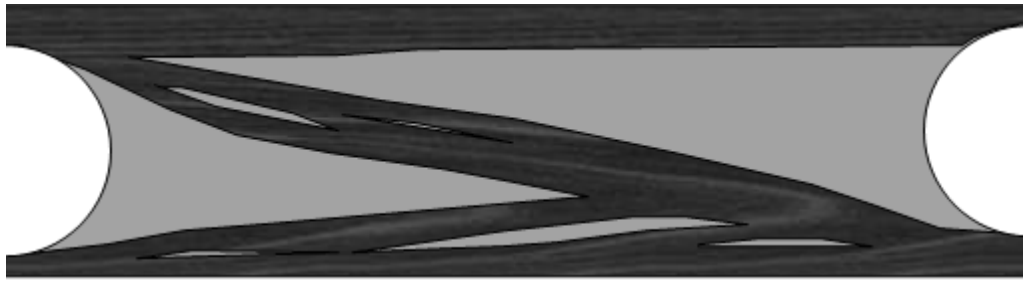


Fig. 5.17: Graphical approximation of fibre distortion from RFI mouldings

Figures 5.16 and 5.17 further illustrate the fibre distortions present in the RFI material. It is clear that the pins are actually displacing the majority of the fibres between the perforations leaving a large resin rich band. These bands of resin richness formed through fibre displacement are evidently located in each ply rotated through 90° and creating a staggered cross of resin richness when observed through the thickness. This has been approximated for a single ply and graphically represented in Fig. 5.18.

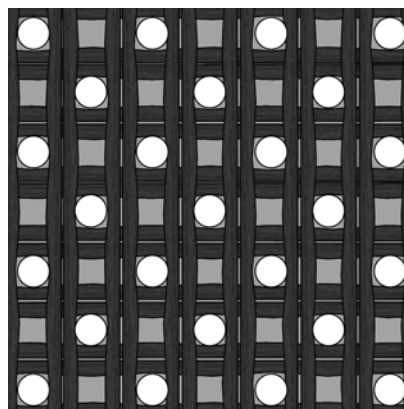


Fig. 5.18: Graphical approximation of fibre distortion throughout single ply from RFI mouldings

Combined with this increase in resin volume, an increase in laminate thickness is present around the hole perimeter as illustrated in the microscopic images. This increase in thickness is directly linked to the higher resin content through the displacement of the fibres as the pins are inserted through the uncured laminate. The degree of this increase in thickness varies between the pre-preg and RFI materials with the RFI laminates showing the greater increase. This is attributed to (a) the weave of the pre-preg providing a resistance to the distortion and (b) the higher curing pressure (7 bar) of the pre-preg laminates. The latter is one factor that can be altered to improve the RFI variation, as any difference in cost between operating an autoclave at 3 or 7 bar is small. It may also be found that an increase in curing pressure would help reduce the amount of through thickness distortion in the RFI laminates.

Typical variations in thickness between holes are illustrated by the graphs shown in Figs 5.19 and 5.20. Here thickness measurements were taken at points between two adjacent holes using a stereo microscope at 20x magnification.



Fig. 5.19: Pre-preg moulded hole to hole thickness variation

The average thickness of the pre-preg laminate with moulded holes is 2.354mm as opposed to 2.248 mm obtained with a standard eight plies of 8552 pre-preg, a thickness change of +4.7%. As is clear from this graph the maximum thickness is at the hole perimeter and the minimum (still thicker than standard laminate) at mid-pitch. This gives a range of +0.071/-0.054mm (+2.9/-2.3%) relative to the average cured ply thickness of the moulded hole pre-preg material.

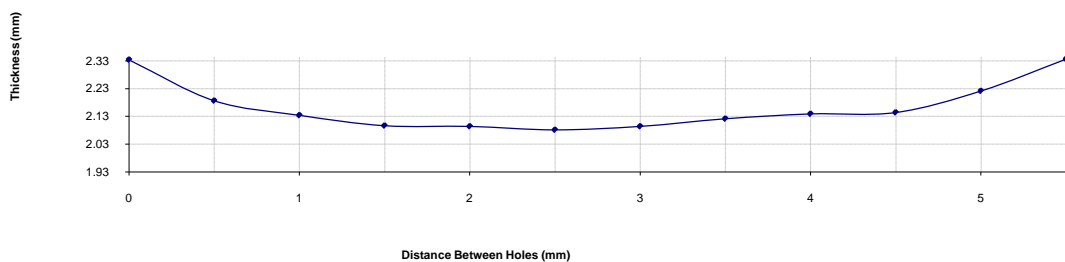


Fig. 5.20: RFI moulded hole to hole thickness variation

The average thickness of RFI perforated laminate is 2.161mm compared to average thickness of 1.926mm obtained with a standard six

plies of 310g/m² NCF and four plies of 250g/m² M36, a thickness change of 12.2%. It is again clear from Fig. 5.19 that the maximum thickness occurs at the hole perimeter and the minimum at mid-pitch. This range gives a thickness tolerance of +0.172/-0.084mm (+8.0/-3.9%) over the average thickness of the moulded hole RFI material.

The increase in thickness at the holes is more severe with the RFI laminates than with the pre-preg. This is a direct result of the increased fibre distortion occurring within the RFI laminates where distinct resin rich bands are induced by the parting fibres as shown in Figs. 5.16-18.

The microstructure analysis helps build a detailed picture of the laminate structure around the moulded holes and aids the understanding of the mechanical properties achieved. In the standard dry ambient conditions these localised laminate thickness increases provide structural reinforcement at the stress concentrations of each hole i.e. at the perimeter. However, in the hot/wet conditions where the resin plasticizes it can be expected that localized fibre buckling is an expected failure mode as the fibres distort around the hole perimeter into the resin rich bands.

Chapter 6 - Industrial Application

As discussed by Bader (2002) economics are critical when considering the application of composite materials. Further, it is imperative to conduct an assessment from a holistic equivalent performance standpoint to ensure the successful implementation of the right solution. The use of such an approach allows a true assessment of performance benefits compared to simple material cost based models where higher performance or quicker process levels are usually not considered within the assessment. Such simple models typically lead to conclusions that higher priced, higher performance materials are economically unviable as aspects such as reduced material use and weight are overlooked. In building an equivalent performance assessment it is important to ensure every performance and cost aspect of the component is captured through a detailed study of the component production cycle. Potter (1997) highlighted this approach for both outline and production costing exercises to ensure the performance-value assessment was conducted parallel with the development cycle.

As part of this study both weight and cost analyses were conducted. These are discussed in this chapter with the weight analysis based on the physical and structural property assessment. The costing analysis is restricted to relative values only to protect proprietary component information but does address a holistic analysis of the production cycle. For

this evaluation the current industry standard component weight saving cost of \$1000/kg was used as supported by Bader (2002).

6.1 Weight Impact

From the mechanical data discussed in Chapter 4 the conditioning of moulded hole laminates results in lower compressive failure strength than that of conditioned drilled laminates. As the certification for in-service performance of composite aerospace parts is critical, this raises a considerable question over moulding perforations as opposed to drilling them. A further implication of this reduced mechanical performance is the loss of potential weight savings, as reduction in strength requires thickness increase for equivalent failure load. Therefore a moulded perforate skin would have an increase in material volume and an increase in overall mass where any increase directly translates to increased acquisition and operating costs. For nacelle applications these points are particularly important due to the typical thermal exposure levels during operation and the direct effects on engine efficiency from any mass increase. To analyse the weight implications of a moulded hole pre-preg laminate an evaluation of the comparative component attributes was conducted.

Utilising the physical properties identified in previous chapters and the calculations in Appendix F, the laminate areal weights for the various pre-preg configurations were established as:

- 4 ply non-perforated laminate = 1.76 kg/m²
- 4 ply laminate with 6% drilled open area = 1.66 kg/m²
- 4 ply laminate with 6% moulded open area = 1.74 kg/m²

However the moulded hole laminate would have a 5% decrease in compressive strength and a 36% increase in tensile strength compared to its drilled equivalent. If it is considered that the load carrying capabilities must at least remain equivalent for the component then an analysis of the hot/wet compression performance of the base-line configuration against the moulded hole laminate is necessary.

Summarising from these calculations (see Appendix G), it can be seen that by moulding the holes and taking the hot/wet compressive failure load as the critical loading case the laminate design would carry a weight increase of 0.516kg/m² and provide an increase in tensile load carrying capability of 80.6%.

Due to the lower compressive performance of the RFI laminates there would be further weight implications through such a design with the same critical failure load. This is confirmed by repeating these calculations with the RFI properties. Again the laminate ply count increases resulting in a weight increase of 0.864kg/m² over the base-line drilled pre-preg design but with an increase to tensile load capability of 144.4%.

6.2 Cost Analysis

The AS-907 has a total of 6 carbon perforates located on the fixed and removable acoustic panels. Working from the existing component drawings, and the 2004 production forecast of 32 aircraft sets comprising 64 nacelles, gives a total of 256 removable and 128 fixed panels totalling 384 with each having a surface area of 0.163 m².

In analysing the cost structure of the Outer Fan Ducts (OFDs) it was necessary to capture all of the relevant processes related to the production and certification of the components. For ease of assessment the component was broken into the distinct task sub-groups of:

- Composite Materials
- Certification
- Labour
- Non-Recurring Costs (NRC)
- Other Materials
- Assembly
- Other Details
- Weight Cost

In assessing the constituent groups each cost element was broken down into a \$ cost per part in order to capture the elements attributable to single investment points (e.g. certification costs, equipment installations, etc.). It was also feasible to conduct this assessment for both the perforated skins and the doors themselves. The results of these evaluations are represented in Figs. 6.1 and 6.2 respectively.

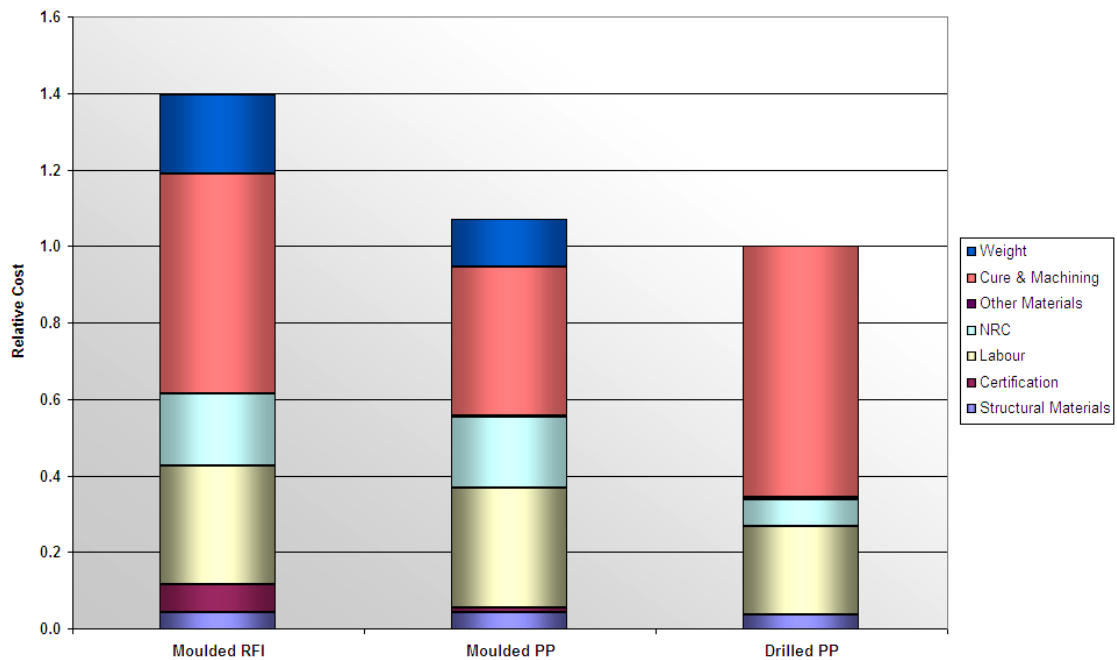


Fig. 6.1: Relative cost structure of acoustic liner panels from OFD

First looking at the cost structure of the perforated panel itself it can be observed that the moulded approach increased component cost in addition to the added weight. A surprising observation from this analysis is the relatively small contribution that the actual material costs have on the component. Due to the reduced cost of creating the perforations through

FlexPerf the contributions from the certification costs are off-set but the implicit increases in labour and tooling cost remove the benefit. From this analysis the panel costs are shown to increase by 40% for the moulded hole RFI and 7% for the moulded hole pre-preg. The main difference between the pre-preg and RFI solutions with the FlexPerf process are the increased cure and certification costs of the RFI material coupled with the weight penalty implications of the RFI design adjusted to provide equivalent hot/wet compressive performance.

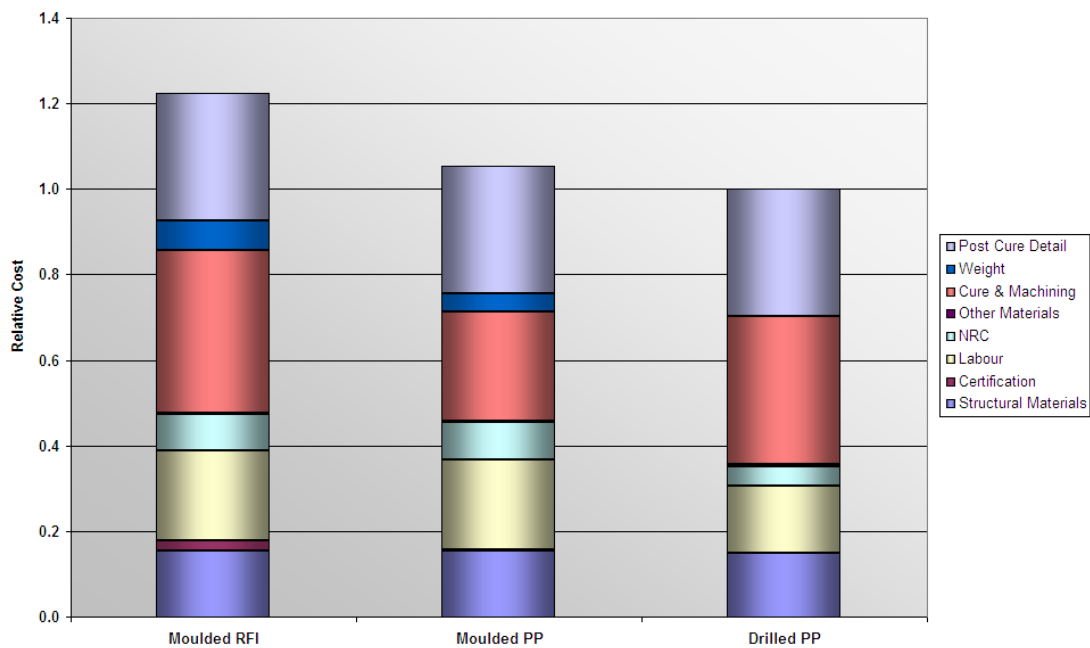


Fig. 6.2: Relative cost structure of OFD component

Taking a similar approach over the whole OFD component demonstrates the weighting effect that the acoustic panel has on the component costs. This analysis shows that the relative contributions of the

NRC and added weight are reduced due to the inclusion now of post cure detail costs (i.e. assembly, painting and quality control). Although the cost differences between each approach do reduce when the component view is taken, the FlexPerf process is seen to significantly increase the component cost of the OFD. One beneficial aspect of the FlexPerf process in the cost structure was a reduced perforation cost highlighting that for larger nacelles, such as those found on the large twin aisle commercial jets; this may offer a route to reduced component costs.

Chapter 7 - Conclusions

This thesis reports a study into alternative moulding technologies for commercial moulding of multiple perforations in composite structures. Two approaches were considered: castable soluble pins and an adaptation of z-pinning technology. The composites produced using these techniques were subjected to mechanical testing (tension, compression and interlaminar shear) both dry and after exposure to hot/wet conditions. The laminates were also characterised for thickness variation, fibre volume fraction, degree-of-cure, glass transition temperature and acoustic properties (reactance and resistance). Further a preliminary weight and cost analysis are included.

During the development phase of the study a number of moulding approaches were considered and evaluated for their feasibility with the component configuration. An extensive evaluation of suitable materials and processing techniques was undertaken incorporating some novel approaches to overcome the identified problems. From this some encouraging results were achieved with water soluble tooling that, although ultimately proving inappropriate for acoustic level perforations, did demonstrate promising characteristics for alternative applications. The method found to give the most suitable approach was that of the reusable FlexPerf process. Along the way to establishing this process as the most appropriate, the process limitations of the materials selected were also explored with significant work accomplished in demonstrating the

flexibility of the GKN RFI process to varying the resin-fibre laminate configuration. The selection of the FlexPerf manufacturing route also provided its own significant challenges for performance characterisation with initial limitations on laminate thickness potentially affecting the available analytical methods. In response some preliminary work was undertaken investigating the use of non-standard test specimen geometries for mechanical testing. While ultimately the work was not required for the programme it did demonstrate some potential routes for thin specimen testing worthy of a fuller and more detailed assessment elsewhere.

From the mechanical evaluation of moulded versus drilled perforations it was found that while the dry performance of the laminates could be improved through the moulding process it was in the hot/wet test conditions where the configuration suffered in compression. On analysis of the microstructure it was found that increased levels of resin richness dominated the perforation edge leaving the pre-buckled distorted fibres susceptible to failure through matrix plasticization from the presence of moisture. The basic predictive methods employed demonstrated an excellent correlation with the tensile performance levels of both the drilled and moulded specimens. Somewhat surprising was the apparent high correlation of the moulded hole performance to failure initiation at the maximum straight hole path. This behaviour would benefit from further assessment using different moulded hole patterns for detailed validation. As expected the attempted predictive modelling of the compression

behaviour was shown to be inappropriate, given the more complex nature of compression behaviour. Analysing the physical nature of the moulded perforations demonstrated a geometrical reinforcing behaviour from the moulding process. Localised thickness increases were found at the hole perimeters which are expected to contribute to reducing the stress concentrations induced by the perforations themselves. From this phase of the study it was shown that the moulded perforations induce a reduced in-service performance level (structural and functional) and increased weight due to fibre volume reductions.

From an analysis of the weight and cost implications it was shown that the reduced hot/wet compressive performance required an increase in component weight for equivalent performance. This was found to increase the component cost through weight penalties of in service performance. During this evaluation a holistic approach was taken to understand the contributions and effects of each production stage ensuring that not only were material cost and labour usage levels taken into account but also consequent component weight, certification, assembly and post production machining.

While this study highlighted the process of drilling perforations to be more suitable than moulding with the materials evaluated, and on OFD's of the relatively small AS-907 nacelle. Further potential is expected if the study were to be extended in the future to analyse the larger structures of the single and twin aisle large commercial aircraft and resolve the issue of

acoustic performance impacts from hole quality variations in the moulding process.

Appendix A: Publications

A1: Low Cost Manufacturing Using Novel Preforming and Resin Infusion Technologies (30% contribution)

26th SAMPE Europe International Conference, PARIS, 5-7 April 2005

Carmelo LoFaro, Marc Doyle, Rob Blackburn, Robin Maskell*

Cytec Engineered Materials Ltd., Wrexham, LL13 9UZ, UK

*Cytec Engineered Materials Inc., Tempe, AZ 85284

Abstract

Liquid moulding methods, particularly VARTM, offer a potential lower cost alternative to conventional pre-preg processes (hand lay up, fibre placement, etc), for the fabrication of high performance composite structures. The utilization of such manufacturing methods for primary structural aerospace applications to date has, however, been reasonably limited. The major reasons for the limited usage of resin infusion methodologies have been both the poor resin properties typically attained (particularly toughness and FST) and the unsuitability of the preforming and infusion processes employed.

New material and process technology developments related to the PRIFORM™ technology offer potential solutions to the aforementioned problems.

KEY WORDS: Materials – Fabric/Textile Reinforcement, VARTM, Preforming, toughness, FST

Introduction

Fiber reinforced polymer composites have been increasingly used in the aerospace and automotive industries due to their high strength, stiffness, low density and resistance to fatigue and corrosion. Historically the vast majority of advanced composite structures for aerospace applications were manufactured by the hand lay-up of pre-preg plies. The advances in automated fabrication processes, such as automated fiber placement and automated tape placement, has provided significant opportunity to reduce manufacturing costs and to improve quality. However all these methods are reliant on pre-preg as the “starting material” and tend to show high capital and recurring costs.

In recent years new cost-effective fabrication techniques have been investigated and developed including pre-preg-alternative methodologies such as liquid resin infusion. A multitude of liquid molding processes has emerged, differentiated by several alternative forms, many with confusing

acronyms. The various process variations have different methods for controlling the flow of resin through the reinforcement and the air removal and may use different tooling materials, however the majority of liquid resin infusion processes share a common format: the fiber reinforcement (the preform) is placed in a mold, injected or infused with resin, and subsequently cured.

The following discussion concerns the utilization of the PRIFORM™ technology and in particular a novel textile product form to manufacture VARTM components for aerospace primary structures applications.

VARTM Process

The VARTM (Vacuum Assisted Resin Transfer Molding) process involves the injection of a low viscosity thermosetting resin under vacuum into a pre-placed fiber preform positioned beneath a transfer media and a flexible vacuum bag, and subsequent curing of the resin to form a composite part.

The VARTM process has the potential to become an attractive manufacturing approach for producing large composite structures due to advantages such as low capital cost (no need for autoclave or automatic fibre placement machine), lower recurring costs and reduced cycle time as compared to conventional autoclave cure pre-preg lay-up. Furthermore the

benefit of using a single-sided tool results in a lower non-recurring cost compared to other resin infusion processes such as matched-mould RTM and eliminates the product's size limitation originated by autoclave size.

VARTM has been used in the marine industry ever since it was first conceived in the 50's, however poor mechanical properties of the resulting composites and preforming difficulties have so far limited the use of the process for aerospace applications. In particular, these limitations are related to the poor toughness of the infusion resins used, the process quality and repeatability and difficulties in achieving sufficient fibre volume fractions to meet stiffness and strength requirements.

The PRIFORM Concept: Toughness and Preforming

The Epoxy soluble thermoplastic fibers¹ (PRIFORM™) technology continues to show broad utility for the manufacture of resin infused composites in primary structural aerospace applications.

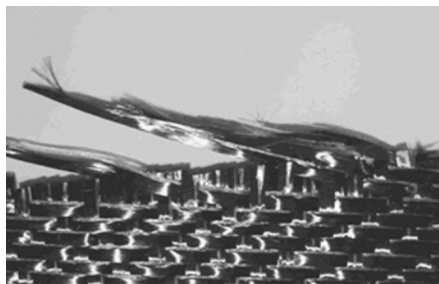
Typically, pre-preg resins utilized for primary structures need high toughness and damage tolerance and are modified by the incorporation of tougheners. For pre-preg resins, such modifications are accompanied by significant increases in resin viscosity. In contrast, resins suitable for liquid resin infusion processes necessitate low viscosity, and as such, these resins, being largely unmodified, are typically brittle in nature. The transposition of the toughening agent from the resin matrix to the reinforcement allows a

decoupling of the problematic viscosity/damage tolerance interdependency. Specifically, in the PRIFORM technology, the thermoplastic toughener used in the Cycom 977-2 pre-preg is spun into a fibre and then incorporated into the structural reinforcement using standard textile processes. This transposition of the toughening agent, from the resin matrix to the preform, allows the resulting resin system (Cycom 977-20 i.e., Cycom 977-2 without the thermoplastic) modifier to be easily injected at low temperatures and pressures. The materials formulation stays the same and the mechanical performance of the resin + hybrid reinforcement material combination is equivalent to that of the pre-preg system Cycom[®] 977-2 thus affording high toughness and damage tolerance. Also the material exhibits the same excellent FST properties that are unique to the 977-2 system, thus further extending the potential material applications to primary structures that need FST compliance (rear pressure bulkhead, fuselage frames and skins, floor beams, etc.)

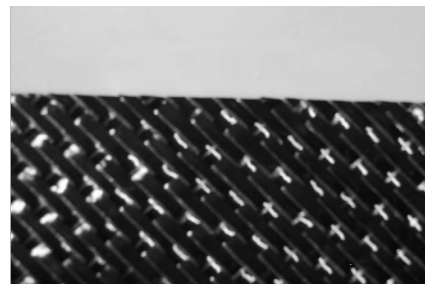
Another advantage of the PRIFORM technology is the ‘self binding’ behaviour of the reinforcement. Preforms for resin infusion can be stabilized and assembled by thermoforming processes that include the application of a binder or fleece on to the surface of the dry fibre reinforcement. The binder softens during the thermoforming process, fusing the fibre reinforcement together, and hardens upon cooling. The resulting stabilized preform has enhanced handling characteristics and can undergo cutting or further assembly steps. However, the use of binders is

not without its drawbacks. The utilization of binders can affect both permeability and fibre wetting of the preform during the resin injection process. Additionally, incomplete compatibility of the binder and the injected resin matrix can lead to diminished mechanical performance in the cured composite part.

The PRIFORM soluble thermoplastic fibres, which are incorporated into a hybrid reinforcement, soften when exposed to elevated temperatures, and thus act as a binder. This property of the fibres can be used to stabilize a single reinforcing ply (Fig. 1), join several plies together, or create a complex 3D preform (Fig. 2) without the need for secondary processes such as binder or fleece coating. In contrast to the use of conventional binders, the PRIFORM self binding technology provides a long out-life (no special storage conditions are required).



Unstabilized Fabric



Stabilized Fabric

Fig. 1: Stabilized fabric showing improved edge quality and minimised distortion.

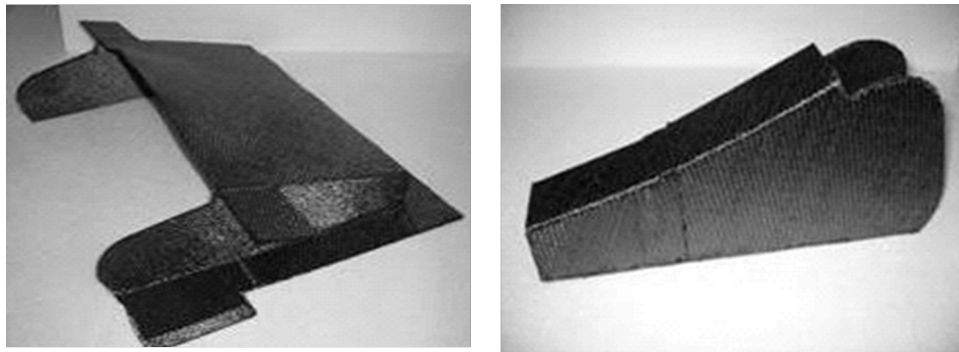


Fig. 2: 3D preforms

The PRIFORM self binding technology affords compaction levels comparable to those achieved with commercial binders and allows to manufacture preforms that match or outperform state-of-the-art manufacturing technologies in terms of quality, dimensional tolerance and ease of production.

PRIFORM High Drape Fabrics

Manufacturing of large contoured parts using composite materials can take numerous routes. Traditionally, hand lay-up of tape pre-preg has been used in virtue of its simplicity as it does not require specialised equipment and its applicability to numerous geometries, however there are a number of associated drawbacks. In particular, it tends to be labour intensive and inconsistency of operator performance leading to rework or scrap has to be taken in consideration. In addition, the hand laid part requires autoclave cure.

In order to minimise the disadvantages of hand lay-up, tape laying machines have been developed and used in the manufacture of large parts. These address such requirements as reduced labour time and reproducibility of the resulting parts. In particular, flat-to-medium contoured parts are well suited for tape laying and the bigger the part and plies the more productive tape layers are. Although successful in some applications, tape layers come with some drawbacks, not least their price. In fact, only simple geometries can be successfully manufactured without the occurrence of phenomena such as tape buckling, bridging and paper breakage that even when addressed, significantly reduce the productivity of the equipment. As per hand lay-up, an autoclave is required to process the part.

A variation of tape layers are fibre placement machines that effectively address complex contouring by automatically laying narrow quantities carbon from a numerically controlled head that can introduce a binder to the fibre tow to maintain its laid position. This manufacturing method has however some drawbacks in that lay down rates are significantly reduced at the detriment of productivity and the presence of an additional binder is required to maintain the laid fibre in position.

A recent development in the manufacture of large contoured parts is resin film infusion of braided or multi-axial preforms and fabrics. In the specific case of multi-axial fabrics, labour is reduced by virtue of the multilayered structure of the fabric that allows for high lay-down rates. The

part can then be processed in an autoclave, where the toughened resin film diffuses through the fabric resulting in a toughened part.

In view of consolidating the advantages and reducing the disadvantages of the techniques described above, a Woven Non Crimp (WNC) PRIFORM fabric has been developed that shows the following characteristics. A biaxial fibre arrangement on two separate planes held together by an array of PRIFORM soluble thermoplastic weave. This fabric offers both high lay down rates and outstanding drapability making it suited to both large and complex geometries. In addition, the fabric is suitable for both closed mould RTM and open mould, out of autoclave, VARTM process while maintaining high volume fraction characteristics and the toughness and FST properties unique to the Cycom 977-2 system. Parts can be manufactured by both hand lay down and by automated gantry positioning depending on part size and complexity.

The following chapter presents process examples using the WNC PRIFORM fabric, while Figures 4 to 6 are an example of the draping ability of the same and of the fabric structure and stability. Figure 5 in particular shows the ability to obtain thermal overlaps. Figure 6 shows a cross section of a laminate showing the lack of crimp in the carbon fibres.



Fig. 4: Drapability test

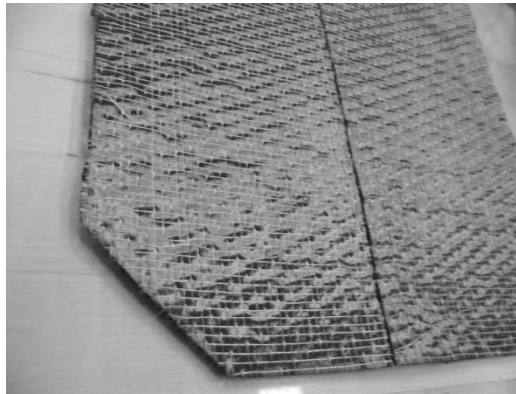


Fig. 5: Thermal overlap

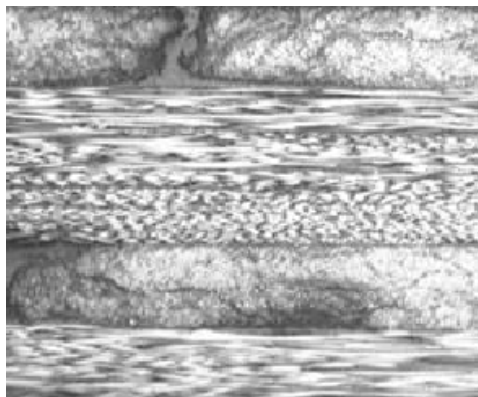


Fig. 6: Laminate cross sections

VARTM Integrally Stiffened Parts

With many aerospace components there is the need for monolithic laminates to be stiffened by using discrete (stiffeners) or continuous elements (honeycomb, foam). Several stiffened structures have been manufactured using the PRIFORM WNC fabric product in combination with the VARTM process. Within these types of structures the resin flow can be very complex and must include both in-plane and out-of-plane paths. By developing an understanding of the flow mechanism at work in a variety of these aerospace configurations and manipulating the key parameters of the process (for example vent and inlet positioning and bagging scheme), complex stiffened structures have been consistently produced. Furthermore the preforming characteristics of the PRIFORM WNC fabric product have been found to aid the consistency of the VARTM process by reducing the effects of intensifiers and sandwich materials on permeability and dimensional accuracy while attaining fibre volume targets of 56-60%.

An example of these stiffened structures is a curved hat-stiffened panel. With this configuration, two different design approaches can be followed: a filled hat section utilizing a solid core (foam) or a hollow section utilizing a removable mandrel. While the first option implies a weight penalty through the use of what is often called a 'fly away tool', both options present the same problem of introducing an impermeable volume into the structure. A further disadvantage of the first option is the

potential for the core material to exhibit significant resin absorption which can introduce further processing problems in the form of resin starvation and reduced bond strength. Cytec has developed a manufacturing approach for hollow structures that overcomes all these problems.

Part of this approach involves the hot compaction of both the base plies and hat structure plies as a preliminary processing stage. The pre-forming process provides the ply stacks with considerable handling stability reducing the level of workmanship required compared to standard dry fabric processing of this structure. Furthermore, through an in-depth understanding of the flow mechanism required for the sections, a novel resin distribution and mandrel concept was developed and the parts were infused with an out-of-autoclave VARTM approach that demonstrated consistent results. Examples of parts are shown in Fig. 7

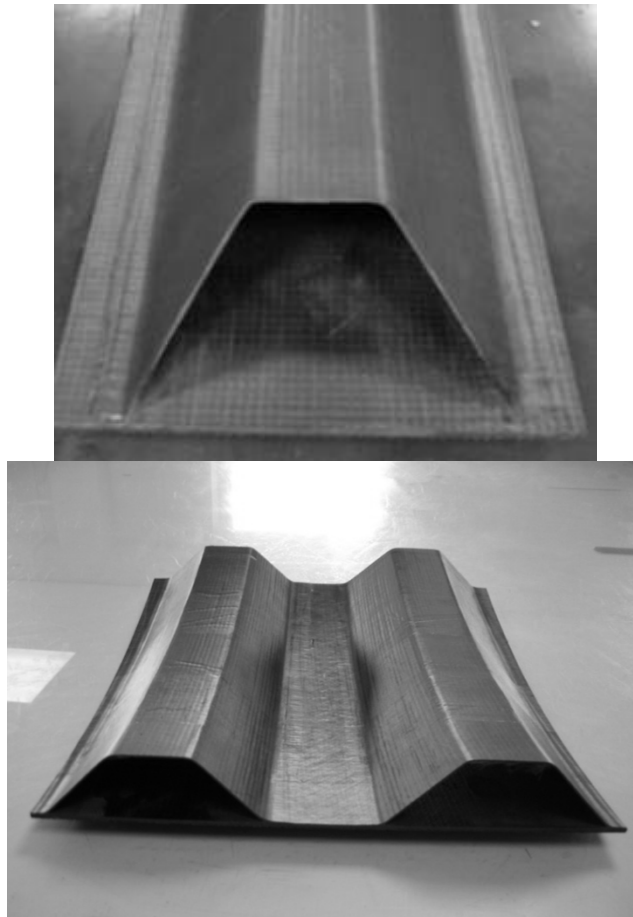


Fig. 7: Curved hat stiffened parts manufactured using PRIFORM with a VARTM process

VARTM Large Curved Parts

In order to test the applicability of PRIFORM WNC fabrics to large curved surfaces, several large dome-shaped parts were manufactured via VARTM with manifold objectives.

Firstly the drapability of the fabric was assessed by laying several plies in a quasi-isotropic configuration that covered the entire surface as well as the return flange of a deep, varying-curvature dome similar to the Rear Pressure Bulkhead of a commercial airliner.

Secondly the as laid preforms were hot compacted under vacuum to achieve a low bulk factor, a uniform thickness distribution and a compaction that would also allow for subsequent handling.

Thirdly the preform was infused with epoxy resin through a standard VARTM process to assess the uniformity of flow front and infusion time. The cured parts were analyzed to assess volume fraction, porosity and ensuring that PRIFORM™ fibre dissolution was achieved thus imparting the toughness and FST properties typical of a primary structure aerospace grade pre-preg material.



Fig. 8: Full ply on dome tool



Fig. 9: Hot compacted dome section preform, showing draped return flange



Fig. 10: Injected and cured dome shaped part

As depicted in Figures 8 to 10, the results of the trials address all the objectives set forth; the part was rapidly manufactured using the WNC PRIFORM fabric without any darts or splices. The return flange of the dome shaped tool was also covered by the fabric in virtue of its excellent drape properties. A hot compacted preform section was successfully handled and showed uniform 110% bulk factor.

The cured dome shaped part was uniformly injected; micrographic sections demonstrated that porosity was absent, and thermoplastic dissolution was complete and uniform thus imparting the desired toughness and FST properties associated with the Cycom 977-2 resin. Volume fractions of the parts manufactured were consistently measured in the 56 to 60 % range.

Conclusions

The combination of the VARTM process and the PRIFORM technology can offer significant savings to the aerospace industry by enabling the low cost manufacturing of large primary structures meeting toughness, damage tolerance and FST requirements.

The PRIFORM woven non crimp fabric allows the end user to obtain high lay down rates and outstanding drapability making it suited to both large and complex geometries.

Large high curvature parts using a toughened material and showing fiber volumes in the 56-60% range including state of the art stiffening concepts can be manufactured for a fraction of the cost of pre-preg based processes.

Acknowledgements

The authors would like to acknowledge the contributions made by the following individuals: Nick Evans (CEM - Wrexham), Stefano Cosentino (CEM - Wrexham), Jason Scharf (North West Composites, US), Jerry French (North West Composites, US)

References

1. LoFaro, C., Aldridge, M. & Maskell, R. (2003). Epoxy Soluble Fibers: Enabling Technology for the Manufacture of High Toughness Aerospace Primary Structures via Liquid Resin Infusion Processes, SAMPE Europe 24th International Conference, PARIS.
2. LoFaro, C., Aldridge, M. & Maskell, R. (2004). New Developments in Resin Infusion Materials Using Priform[®] Technology: Stitching, SAMPE Europe 25th International Conference, PARIS.

**A2: Recent Developments in Preform and Resin Infusion Technologies
for Primary Structural Aerospace Applications (30% contribution)**

37th SAMPE Technical Conference, SEATTLE, 31 October – 3 November
2005

Rob Blackburn, Marc Doyle, Carmelo LoFaro, Robin Maskell*

Cytec Engineered Materials Ltd., Wrexham, LL13 9UZ, UK

*Cytec Engineered Materials Inc., Tempe, AZ 85284

Abstract

The utilization of resin infusion methodologies for the fabrication of high-performance composites for primary structural aerospace applications continues to gain acceptance. These liquid-moulding processes are generally considered to be lower cost alternatives to conventional pre-preg processes, offering the potential for significant cost reduction in the manufacture of composite parts. In addition, the advantages of liquid resin infusion-type processes include the manufacture of complex shapes, part integration, design flexibility, dimensional tolerance, and part reproducibility.

An overview of the most recent developments in resin infusion will be presented; with particular reference to a new resin infusion product form

suitable for the realization of toughened primary structures for commercial air transports, such as rear pressure bulkheads, hinge fittings, fuselage frames, etc. More specifically, an example of the manufacture of a highly contoured aerodynamic fairing will be presented.

Introduction

Pre-pregs continue to be the prevailing product forms utilized for the fabrication of high performance composite parts. Unidirectional tapes (of varying fibre areal weights) and fabrics (in a host of different weave styles) have been the dominant “starting materials,” particularly for primary structural aerospace composite applications. These carbon fibre reinforced materials, have very recently, made significant inroads into applications which have historically been the domain of metals; the wing and fuselage of commercial air transports.

A good deal of work has been performed in the course of the past two decades concerning advances in automated processes for the fabrication of composite parts. Most notably, automated fibre placement and automated tape placement have significantly reduced manufacturing costs and improved product quality and reproducibility. More recently, a multiplicity of resin infusion methodologies has emerged for the low cost manufacture of advanced composite parts. These liquid-moulding processes are a clear departure from conventional pre-preg materials;

however, they potentially offer significant advantages, including low cost manufacture of complex shapes (part integration), dimensional tolerance, part design flexibility, and high deposition rates.

These emerging resin infusion methodologies are commonly referred to by a host of confusing acronyms which include RTM (Resin Transfer Moulding), VARTM (Vacuum Assisted Resin Transfer Moulding), SCRIMP (Seeman Composite Resin Infusion Moulding Process), etc. However, each of these processes shares a common processing characteristic: a dry fibre reinforced shape (a preform) is injected or infused with resin, and subsequently cured. The adoption of such manufacturing methods for primary structural aerospace applications has been reasonably limited to date. The most significant constraint has been that for the most part, the rheological profiles of typical damage-tolerant resin systems do not readily lend themselves to these necessarily low viscosity processes.

The combined use of preforms and resin infusion processes offers the potential for significant composite part cost reduction. Preform assembly, an often overlooked but critical aspect of this technology, can be achieved in a number of ways; hot preforming (which generally involves the application of a binder to the dry fibre reinforcement) or stitching. There are, however, certain drawbacks to both these methods (2), particularly to stitching as a preform assembly method: in view of the fact

that current stitching technologies are based on matrix-insoluble stitching threads, such as polyester or nylon.

In previous papers, (1-3), we have described the development of Cytec Engineered Materials' PRIFORM™ technology, a novel resin/preform technology enabling the lower cost manufacture of high toughness structures via liquid resin infusion processes. The technology relies on epoxy-soluble thermoplastic fibres which are incorporated appropriately within the preform. These soluble fibres, which remain insoluble at the resin injection temperature, dissolve and diffuse throughout the matrix during the cure cycle producing a composite part with high damage tolerance. In addition to providing a resin infusion route to primary structural aerospace applications, the technology also provides methods for preform stabilization and assembly. Composite parts with inherent FST properties can also be manufactured via this soluble fibre methodology. The following discussion provides the most recent developments with regard to the PRIFORM technology including a novel biaxial non-crimp fabric, its mechanical properties and microstructure and a case study for an aerospace application comparing it to pre-preg and standard non-crimp fabrics.

Introduction to Woven Non-Crimp Fabrics

Woven Non-Crimp Fabrics (WNCF), also known to the composites marketplace as scaffold weaves, are a class of biaxial textiles non-crimp fabrics comprised of two distinct fibre tows; a main reinforcing fibre and a scaffolding fibre that differ in linear density and/or type.

The main reinforcing fibre, (e.g. a standard or intermediate modulus carbon fibre), is found in the 0° and 90° directions on two non-interlacing layers. On the other hand, the scaffolding fibre, typically a fine glass or polyester yarn also running in warp and weft, interlaces the reinforcing fibre layers holding them together in two adjacent and distinct planes – hence the seemingly contradicting term Woven Non-Crimp.

The fabric is manufactured on standard weaving looms and has the advantage over standard weaves of drastically reducing fibre crimp hence greatly improving mechanical properties; however, the scaffolding fibre acts only as a non structural, weave-aid fibre. This impairs further improvements to material performance in much the same way that stitching reduces material performance on multi-axial Non-Crimp Fabric (NCF) manufactured on warp knitting machines.

With this challenge in hand, Cytec Engineered Materials has developed an advanced WNCF that utilizes its exclusive toughening PRIFORM Soluble Fibre Technology to substitute the scaffolding yarn,

thus allowing for the mechanical performance of the WNCF to closely approach that of unidirectional pre-preg tape.

In addition, this novel WNCF brings significant processing advantages and innovative characteristics that render it a preferred choice over standard weaves and some multi-axial constructions. In particular, the introduction of multi-functional soluble fibres allows for stabilization and compaction of the fabric, dramatically improving handling characteristics, while the relative arrangement of carbon and soluble fibres allows for unprecedented drapability.

Figures 1 and 2 show examples of a stabilized and a draped fabric. Both these characteristics outperform the behaviour of standard 5 Harness Satin (5HS) weaves that easily fray upon handling and have limited drapability. With respect to multi-axial NCF, the WNCF maintains its advantages in terms of mechanical performance and processing characteristics, however, the comparison can only be done with a [0/90] NCF as the other constructions available from warp knitting machines are not available from standard looms.

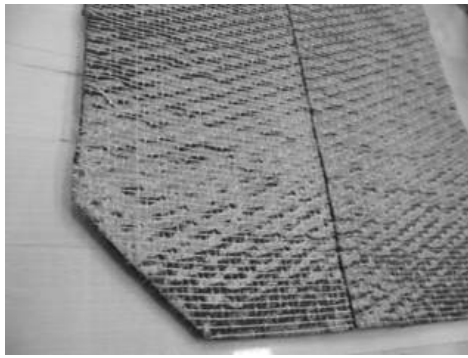


Fig. 1: Stabilized WNCF showing a non-fraying edge and a hot compacted single-ply of WNCF compacted overlap

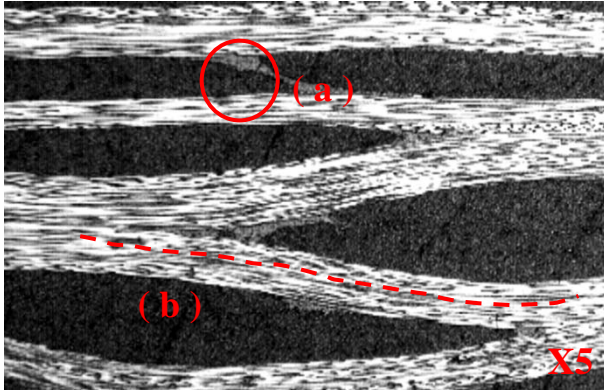


Fig. 2: Draped, single-ply splice free

Microstructure of Woven Non-Crimp Fabrics

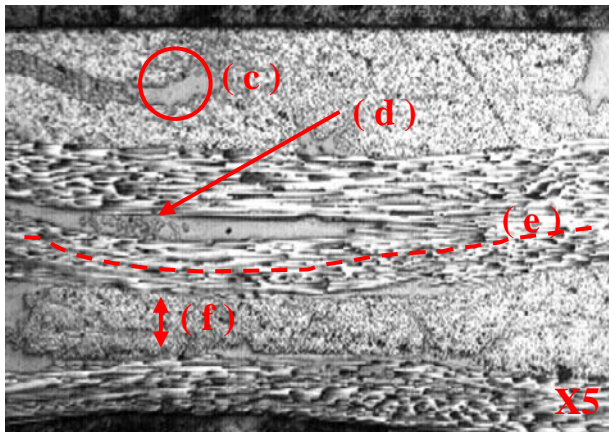
The WNCF takes resin infusion components a step closer to the optimal performance sought by so many end users. These benefits are gained due to the reduced crimp seen in the architecture of the fabric and by the elimination of any secondary stitching materials known to cause fibre distortion and crack propagation. This product still carries the benefit of typical NCFs where heavy tow counts are used enabling processing to become cost effective through an increased deposition rate.

Figures 3 to 5 show a micro-structural analysis of three different fabric forms; a 5 harness satin weave, a biaxial stitched non-crimp fabric and a woven non-crimp fabric respectively.



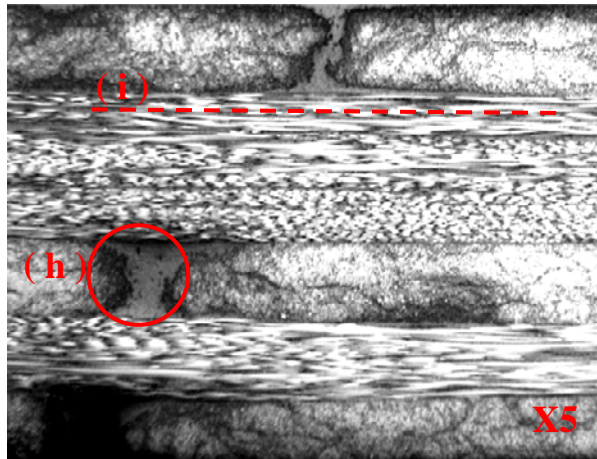
In the common five harness construction each tow continuously interlaces between its perpendicular counterparts causing the presence of localized resin pockets (a) and a constantly deviating fibre path (b). Although small tow counts (3k) is typically used to reduce crimp effects with woven constructions these deviations cause an inevitable knock down in mechanical performance due to fibre micro-buckles.

Fig. 3: 6k HTA 5H with CYCOM® 890 RTM



In this typical non-crimp fabric construction resin pockets (c) are still very much visible and generally increase in size due to the decrease in stability of many stitched technical fabrics. In addition to these, the stitches present (d) invariably cause deviations to the fibre path (e) through the crimping effect (f) of the stitch yarn. Although a crimp effect is still present in non-crimp stitched fabrics their mechanical performance is typically improved over woven equivalents.

Fig. 4: 24k T700 BX NCF with Hexcel M36



With CEM's WNCF the presence of resin pockets (h) is consistent with that found in traditional NCF constructions and is inherent in both fabric types due to tow shape and size. On inspection of the micro-structure the most notable benefits this innovative architecture brings is the in-plane fibre alignment and lack of secondary stitching. These two factors are typically interrelated and through the lack of their presence here allow for an improvement in composite mechanical performance, most notably compression, due to the reduction/removal of fiber micro-buckling generally found in woven and NCF equivalents.

Fig. 5: 24k G50-800 BX WNCF with PRIFORM

In summary; this first generation woven non-crimp architecture provides the processing benefits associated with non-woven fabrics in the form of high permeability, excellent drape and high deposition rates while adding an improved benefit to mechanical performance through reduced out-of-plane fibre deviation.

Mechanical Properties of PRIFORM WNC

Traditional multi-axial fabrics, also known as Non-Crimp Fabrics, constitute one of the most efficient reinforcement technologies for the production of composite components. Multi-axial fabrics are manufactured using a warp knitting technology that consists in stitching multiple fiber layers together in multiple directions. The key value proposition of multi-

axial fabric is the ability to achieve a high Areal Weight (AW) single-ply preform with an oriented reinforcement (for example, quasi-isotropic); this improves manufacturing efficiency and significantly reduces labor time. However, the use of stitching technology to manufacture the fabric causes several disadvantages. The needle used for stitching can damage the structural fibers. Furthermore, if the tension in the stitching thread is too high the surface loop of the stitch can crimp the fibers in the out-of-plane direction. Finally, the stitch pattern also causes in-plane undulations of the fibers. All these issues have a negative influence on several mechanical properties of the cured composite. For this reason, it is well known in industry that stitched multi-axial fabrics show significant reductions in compression strength, open hole compression, in-plane shear strength and bearing strength compared to unidirectional tapes as shown in **Table 1**.

Table 1: Typical reduction factors for matrix dominated properties of NCFs vs. pre-preg.

Property	Reduction Factor
Unnotched Compression	-20 % to -25%
Open Hole Compression	-5% to -10%
Inplane Shear Strength	-20% to -30%
Bearing Strength	-20% to -25%

The WNC fabric has the same structure of a stitched multi-axial without the stitching thread and, based on the microscopy evaluation, it would be expected that the lack of crimp evident in the microstructure of

the WNC positively affects the mechanical properties of the laminate and reduce the knock-down factor seen in standard stitched multi-axial.

In order to prove this theory, it was decided to carry out a mechanical test campaign aimed at comparing the pre-preg CYCOM[®] 977-2 G40-800 24k 268 g/m² to the PRIFORM WNC 977-20 G40-800 24k 550g/m². The two materials use the same fibres (G40-800 24k) and, as the PRIFORM technology is based on the same formulation as 977-2, the resin used in the two materials is chemically identical. Furthermore, the layer areal weight of the materials is almost identical: the pre-preg has a layer AW of 268 g/m² equivalent to a cured ply thickness of 0.254 mm, while the WNCF has a layer AW of 275g/m² equivalent to a cured ply thickness of 0.260 mm.

The PRIFORM laminates for this evaluation work were produced at Cytec Engineered Materials' Anaheim, CA facility using a standard VARTM process and the following processing parameters:

- Apply full vacuum to loaded tool and heat tool to 75 °C
- Inject resin at 75 °C under vacuum (fill time ~ 10-15 mins)
- Ramp to 125 °C at 2 °C min⁻¹
- Dwell at 125 °C for 60 mins
- Ramp to 180 °C at 2 °C min⁻¹
- Dwell at 180 °C for 180 mins

- Cool to ambient temperature

The pre-preg laminates were conventionally autoclave processed at Cytec Engineered Materials' Wrexham, UK facility using the following cure parameters:

- Apply full vacuum to bag
- Apply 7 bar pressure at 0.5 bar min^{-1}
- Ramp to $125 \text{ }^\circ\text{C}$ at $2 \text{ }^\circ\text{C min}^{-1}$
- Dwell at $125 \text{ }^\circ\text{C}$ for 60 mins
- Ramp to $180 \text{ }^\circ\text{C}$ at $2 \text{ }^\circ\text{C min}^{-1}$
- Dwell at $180 \text{ }^\circ\text{C}$ for 180 mins
- Cool to ambient temperature

All laminates produced were scanned ultrasonically to confirm quality. The carbon fibre volume fraction achieved was 0.59 ± 0.02 for all laminates.

The key mechanical properties evaluated were unnotched compression (UNC), open hole compression (OHC), in-plane shear strength (IPSS), compression after impact (CAI) and Mode I energy release rate (G_{IC}). Properties were tested on five different batches for both the pre-preg and the WNC fabric. Conditions were dry/RT and wet where wet is

defined as saturation at 70°C/85% RH. The impact energy for the Compression After Impact (CAI) test was 25J for the pre-preg and 27J for the PRIFORM material. **Figure 6** and **Table 2** show a summary of the test results and the Coefficients of Variation.

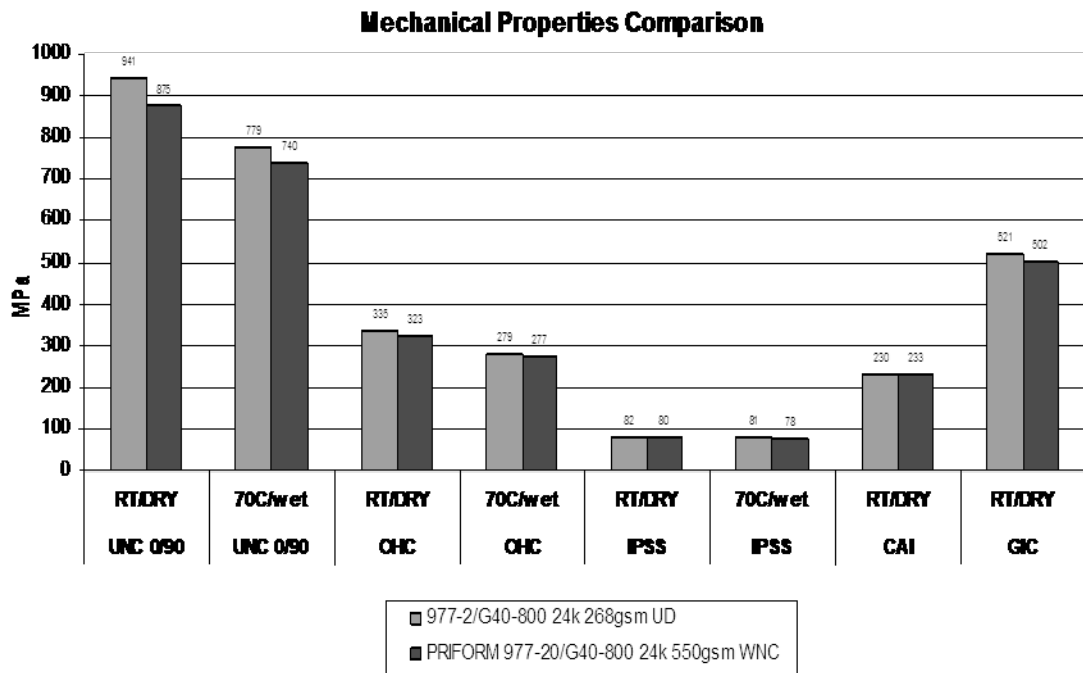


Fig. 6: UD Pre-preg vs. PRIFORM WNCF comparison, mean values and coefficient of variation

Table 2: Coefficients of variation.

TEST	CONDITION	977-2/G40-800 24k 268g/m² UD	PRIFORM 977- 20/G40-800 24k 550g/m² WNC
		CoV (%)	CoV (%)
UNC 0/90	RT/DRY	4.2	3.9
UNC 0/90	70°C/wet	4.05	4.3
OHC	RT/DRY	2.6	2.7
OHC	70°C/wet	2.9	3.8
IPSS	RT/DRY	2.89	2.4
IPSS	70°C/wet	2.5	2.1
CAI	RT/DRY	N/A	3.8
G_{IC}	RT/DRY	8.1	9.4

From the analysis of the data it is possible to draw the following observations:

- OHC, IPSS, CAI and G_{IC} properties are virtually the same for both materials

- A reduction can be observed for UNC, however, the reduction factor is 7% for dry/RT and 5% for 70°C/wet and this is a much lower than what is usually experienced with traditional stitched multi-axial fabrics.

This data proves the theories that the lower degree of crimp in the WNC fabric greatly reduces the knockdown in mechanical properties seen with stitched multi-axial fabrics.

The small reduction in UNC could be due to a residual amount of fibre distortion in the location of the scaffolding soluble thread or to the difference in fibre tensioning between a dry fabric and a pre-preg.

Trade Study

A material and process trade study is presented in this section of the paper for a component that can be manufactured using composite materials and that can be processed through both standard autoclave cure of pre-preg or out-of-autoclave resin infusion processing.

The component of choice is a highly contoured aerodynamic fairing for aerospace use (see **Figure 7**). Measuring approximately 1 m in length, 0.3 m in height, and 0.2 m in width, its geometry is a skewed teardrop shape, showing complex curvatures especially in the region of the sensor opening.

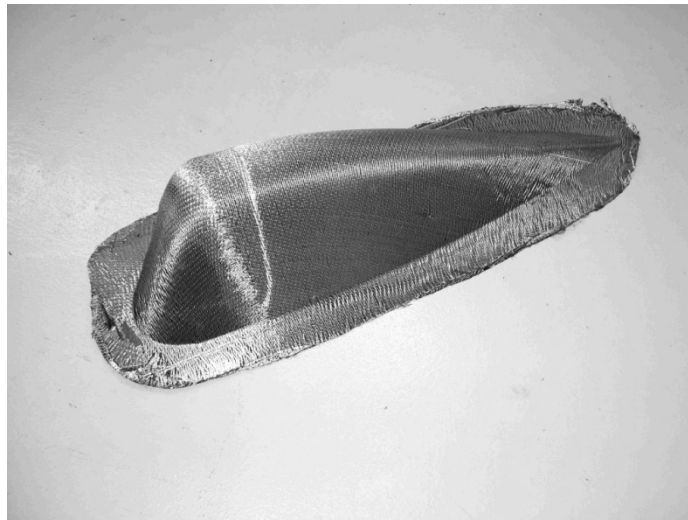


Fig. 7: Aerodynamic fairing – PRIFORM WNC fabric preform.

It is the objective of the trade study to choose the most cost effective solution by considering the following aspects:

Trade Study Assumptions:

- The manufacturer is fully equipped for both autoclave and out-of-autoclave processing.
- Tooling design is identical for both processing options, (i.e. open female tooling).
- The component requires a quasi-isotropic lay-up throughout [-45/+45/0/90]_s.
- The single lamina should be unidirectional, intermediate modulus and approximately 270g/m².

Component Design Drivers:

- Damage tolerant
- Specific Stiffness
- Capability to dissipate electrostatic charges
- Geometrical and Outer Mold Line (OML) accuracy

Sought Material Characteristics

- High compression after impact properties
- Unidirectional or multi-axial fibre arrangement (not woven)
- Intermediate modulus fibres
- Compatible with copper mesh or other electrostatic dissipative material

Candidate Materials

- Toughened pre-preg (5HS fabric, 268 g/m², IM fibre) 5H
- Standard untoughened RTM resin system with a quasi-isotropic NCF fabric (268 g/m²/layer, IM fibre)
- PRIFORM [0/90] WNCF and 977-20 resin (275 g/m²/layer, IM fibre)

All three systems are based on IM fibres, can be combined with an electrostatic discharge layer, and can be moulded on an open female tool; these parameters are therefore discounted as non-discriminating. The trade study is hence based on damage tolerance and process ease.

The main discriminating material property pertinent to the application described is Compression After Impact (CAI); this property has been shown to be equivalent for pre-preg and PRIFORM WNCF, while a drop of 25% is normally found for composites with equivalent fibre arrangement utilizing untoughened RTM resin systems.

This will translate in an identical lay-up for unidirectional tape and PRIFORM WNCF, while the standard NCF will require at least one additional fabric layer to make up for the knock down in CAI properties, therefore increasing the composite fibre weight from 2144g/m^2 to 3216g/m^2 , i.e. a 50 % weight increase.

From a processing point of view, all three systems can be manufactured on a single-sided tool giving OML definition. Also, due to the complexity of the component, hand lay-up is the only candidate manufacturing method. **Table 3** gives a manufacturing time estimate based on previous experience in the lay-up of a similar component.

Table 3: Manufacturing Time Comparison

	Required # of layers	Estimated # of splices / layer	Deposition time** (minutes)	Debulking (Minutes)	Total man hours
5HS Pre-preg	16	5	400	80	8
Quasi Isotropic stitched NCF	6*	4	120	0	2
PRIFORM WNCF	8	0	40	0	0.67

* Extra layers for CAI compliance accounted for

** Deposition rate assumed at 5 minutes / splice / layer

When considering the costs associated to labour and raw materials, the final component cost can be estimated using **Table 4** and represented as a comparison to baseline as per **Figure 8**.

Table 4: Material and Manufacturing Costs

	Man hours	Labour cost / hour	Weight / m ² of composite	Component weight (~0.8 m2)	Indicative Material cost / kg	Material cost / component	Total cost	Notes
PP	8	\$100	4288 g	4.5 kg	\$160	\$714	\$1,514	-
NCF	2	\$100	6432 g	6.7 kg	\$100	\$669	\$869	2.2 kg heavier
WNCF	0.67	\$100	4288 g	4.5 kg	\$130	\$580	\$647	-

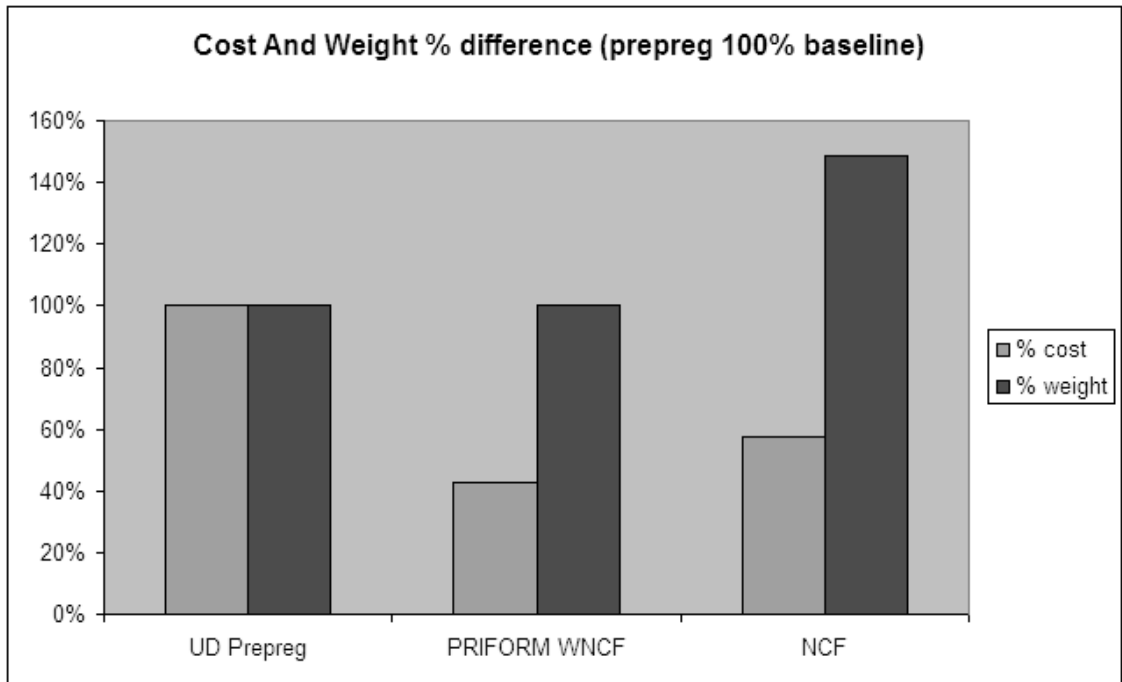


Fig. 8: Cost and Weight Comparison

Conclusions

Unlike standard resin infusion systems, PRIFORM technology combined with VARTM processing can offer significant savings to the aerospace industry by enabling the low cost manufacturing of large primary structures meeting toughness, damage tolerance and FST requirements.

The Woven Non-Crimp Fabric allows the end user to obtain high lay down rates and outstanding drapability making it suited to both large and complex geometries. The mechanical properties of the WNC fabric are very close to pre-preg, thus not compromising performance for cost.

The entire PRIFORM resin infusion product line has a proven foundation in its matrix formulation that is chemically equivalent to the

977-2 pre-preg and 977-2 resin film family, both of which are qualified and long established aerospace products.

Acknowledgements

The authors would like to acknowledge the contributions made by the following individuals: Michael Muser (EADS Military Aircrafts), Bruce Johnson (CEM – Anaheim), Dominique Ponsolle (CEM, Winona) and Nick Evans (CEM - Wrexham).

References

1. LoFaro, C., Aldridge, M. & Maskell, R. (2003). Epoxy Soluble Fibers: Enabling Technology for the Manufacture of High Toughness Aerospace Primary Structures via Liquid Resin Infusion Processes, SAMPE Europe 24th International Conference, PARIS.
2. LoFaro, C., Aldridge, M. & Maskell, R. (2004). New Developments in Resin Infusion Materials Using Priform[®] Technology: Stitching, SAMPE Europe 25th International Conference, PARIS.
3. LoFaro, C., Maskell, R., Doyle, M. & Blackburn, R. (2005). Low Cost Manufacturing Using Novel Preforming and Resin Infusion Technologies, SAMPE Europe 26th International Conference, PARIS.

A3: Process and Performance Enhancements in Resin Infusion Using an Epoxy-Soluble Nonwoven Veil (15% contribution)

SAMPE Europe International Conference, PARIS, 27-29 March 2006

Abdel Abusafieh*, Rob Blackburn[†], Marc Doyle[†], Carmelo LoFaro[†], Robin Maskell[‡], Richard Price*

Cytec Engineered Materials (CEM)

* 1440 North Kraemer Boulevard, Anaheim, CA-92806, USA

[†] Abenbury Way, Wrexham Industrial Estate, Wrexham LL13 9UZ, UK

[‡] 2085 East Technology Circle, Suite 300, Tempe, AZ 85284, USA

SUMMARY

In recent years, one of the major trends in composite manufacturing has been the use of resin infusion processes as lower-cost alternatives to conventional pre-preg processes. While the use of resin infusion has been growing, it has been hampered by two limitations: the low mechanical properties of the resulting laminate and the lack of cost-effective preforming technologies. Cytec Engineered Materials' (CEM) patented PRIFORMTM technology has addressed these limitations by relying on the

co-weaving of epoxy-soluble thermoplastic fibres within a textile reinforcement to provide preform stabilization and assembly and to increase the damage tolerance of the composite.

This paper presents the development of a novel PRIFORM product form, a thermoplastic nonwoven with controlled solubility in epoxy, that allows further improvements over the standard PRIFORM technology.

KEY WORDS: Resin Infusion Processing, Damage Tolerance, Preform Technologies

Introduction

The production of composites via pre-preg presents some well-known disadvantages. While it is generally accepted that pre-preg based composites show greatest benefits for highly loaded parts with large and low curvature shell geometries, manufacturing of complex and integrated parts using pre-preg can cause a dramatic increase in both recurring and capital costs. Resin infusion methods (RTM, VaRTM, etc.) can offer a lower cost alternative to conventional pre-preg processes; but, nonetheless, show some important limitations with regard to the preforming process and the mechanical properties of the composite.

Previous papers, [1-2], described the development of CEM's PRIFORM technology that enables the manufacture of high-performance

structures via liquid resin infusion processes such as RTM, VaRTM, SCRIMP, CAPRI, etc. The technology relies on soluble fibres made from proprietary thermoplastic chemistry tailored to deliver toughness in composite parts manufactured using these techniques. The thermoplastic fibres are engineered to dissolve and diffuse uniformly after the injection process is complete, thus allowing easy injection of the epoxy resin while resulting in matrix morphologies equivalent to those of highly-toughened pre-preg systems used in manufacturing damage resistant composites.

This paper describes the development of a new PRIFORM concept based on a nonwoven veil form of the soluble thermoplastic toughener combined with a 5 Harness Satin (5HS) Carbon fabric to provide toughness via an interleaving mechanism that also facilitates performing and improves design flexibility in composite parts fabricated using liquid resin infusion techniques.

Nonwoven Veil Concept

In the frame of the conventional PRIFORM technology, the epoxy-soluble thermoplastic fibres are inserted alongside structural yarns, usually in a 1:1 ratio in order to maintain an even distribution. This can be achieved by inserting the fibres separately in a textile process or by plying the fibres together prior to the textile insertion. A recently developed novel insertion method consists of an epoxy-soluble thermoplastic nonwoven based on the

same polymer used in the PRIFORM technology. Both these technologies offer the possibility of manufacturing vacuum or pressure assisted infusion of complex components in virtue of their effective permeability. Compared with the conventional technology, the use of a nonwoven as a means to introduce the PRIFORM fibres can offer additional advantages such as flexibility in laminate design, the potential for selective property enhancement (Fire, Smoke and Toxicity surface modification, ply breakout stop etc.) and novel textile forms. Some of these concepts are depicted in Figure 1.

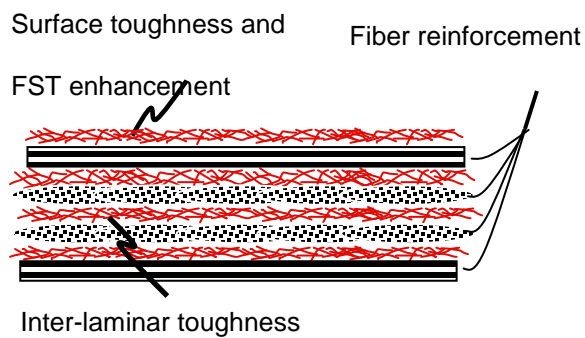


Fig. 1: Potential applications of the soluble PRIFORM nonwoven veil

Nonwoven veils have been used in composites manufacturing for some time. These materials come in a roll form and are used primarily as a preforming aid in resin infusion processes; sheets of nonwoven veil of a rather low areal weight are bonded to a suitable substrate through the application of heat and pressure.

Once combined, the reinforcement and the veil form a dry laminate that maintains some degree of drapability, does not fray upon cutting, is suitable for preforming and for bonding several layers together and retains the permeability required for successful infusions.

Typical state of the art nonwovens are based on carbon, glass, nylon or polyester to enhance thermal, electrical or mechanical properties of a composite laminate. However all these nonwovens are insoluble in epoxy resin and typically cause a reduction in key design properties of the material.

Description of Study

The capability of the new PRIFORM veil technology to enhance processing and performance of resin infused composites is demonstrated through three different characteristics; ease of preforming prior to injection, complete and uniform dissolution in CYCOM[®] 977-20 epoxy resin, and superior mechanical properties. These key aspects of the technology are demonstrated through experimental evaluation and mechanical testing results in the following three sections.

Preforming

When manufacturing components through resin infusion, efficient and high quality preforming is paramount in obtaining high performance

components. The main interest to the process engineer for this step of component manufacture are high precision edges, ease of handling, and the ability to compact several layers together to an acceptable bulk factor prior to infusion. Fibre/fabric and veil combination was successfully tested by running the material through a standard pressure temperature process, thus obtaining a stabilized fabric that promotes handling and cutting.

Examples of the stabilized fabric are shown in Figure 2 where 5HS carbon fabric is bonded to the soluble veil through a temperature and pressure cycle.



Fig. 2: Thermally bonded sample of 5HS fabric and soluble

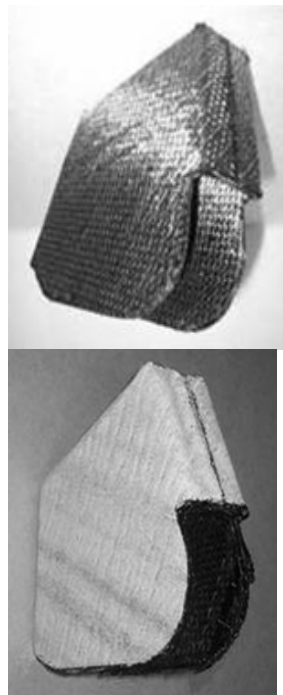


Fig. 3: 16 ply dry preform made using conventional (left) and nonwoven (right)

The 5HS/soluble veil material was cut and preformed in an equivalent manner to standard binder coated and PRIFORM fabrics, i.e., by

shaping it onto a tool and applying a temperature and pressure cycle. The resulting preforms are shown in Figure 3.

As a benchmark to compare the standard preform to the nonwoven preform, edge tolerance was checked against a go/no-go jig. Both preforms were found to comply to the sought $+0 -3$ mm tolerance. The bulk factor was also measured by taking several thickness readings and comparing them to the theoretical cured ply thickness of the final component. Both preforms were also found to be below 115 percent of CPT.

Dissolution in Epoxy

The solubility characteristics of the veil are critical to the practical realization of the technology. An insoluble veil leads to inhomogeneities in the cured resin and negatively affects the thermal and mechanical properties of the composite. In particular, a veil based on a low T_g polymer further lowers the T_g of the composite laminate and affects resin-dominated hot/wet properties.

In order to interrogate the solubility of the PRIFORM nonwoven in epoxy resin, hot-stage microscopy was used. A sample of soluble veil was placed in CYCOM[®] 977-20 epoxy resin and its dissolution behaviour was observed in two distinct situations: an isothermal 1h dwell at 75°C that would mimic the injection of the resin in a preform and a 3°C/min ramp from 75 to 175°C. An equivalent test was carried out with a standard nylon

veil in CYCOM 977-20. Figures 4 and 5 show results for the soluble veil, while Figures 6 and 7 those for the nylon veil.

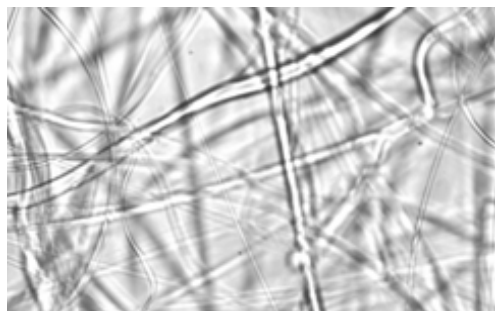


Fig. 4: Soluble veil in epoxy

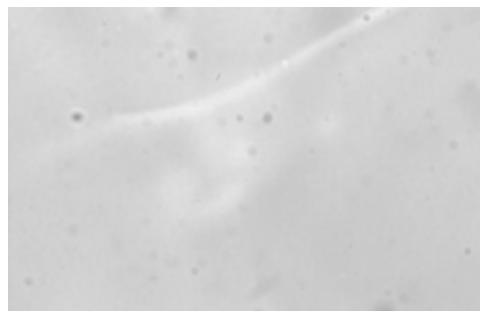


Fig. 5: Soluble veil in epoxy

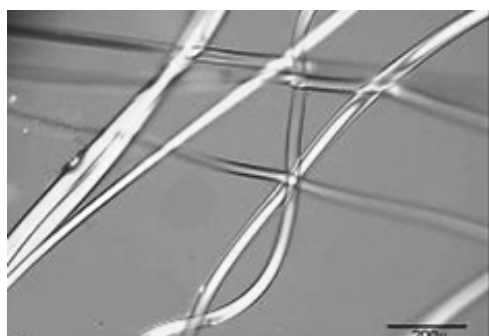


Fig. 6: Nylon veil in epoxy

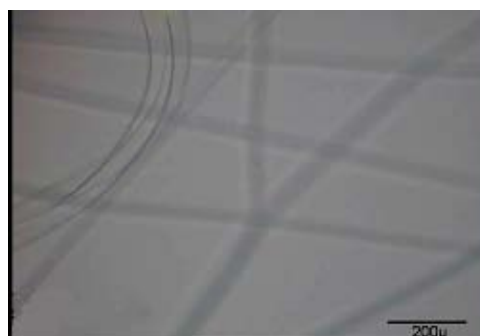


Fig. 7: Nylon veil in epoxy

The isothermal test showed that the neither the soluble veil nor the nylon veil dissolved after the dwell at 75°C. The ramp test showed that a complete dissolution is obtained as soon as the temperature of 105°C is reached for the soluble veil, while the nylon veil showed only optical relaxation and no dissolution.

These results show that the soluble veil behaves in a similar way to the PRIFORM co-woven fibres. Therefore resin injection can be carried out at relatively low temperatures where the solubility of the fibres is minimal. Once the temperature is raised above the injection temperature and below the temperature for the onset of resin advancement, the nonwoven dissolves in the injected resin matrix and the thermoplastic diffuses throughout the part. Lastly, the part can be ramped up to the final cure temperature and held at that temperature until the cure is complete. Figure 8 shows a typical micro section of RTM-cured composite laminate, fabricated using carbon fabric interleaved with the PRIFORM soluble veil. The micro sections reveal complete dissolution of the veil in the epoxy resin.

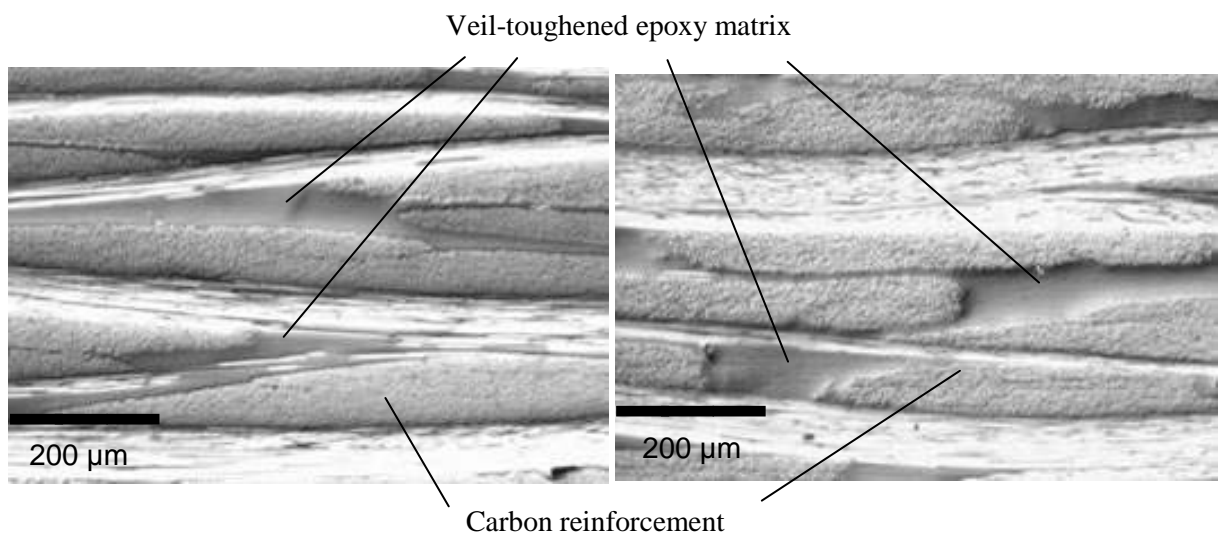


Fig. 8: Micrographs showing complete dissolution of PRIFORM veil in epoxy

Mechanical Comparison

With the preforming and dissolution kinetics of the PRIFORM nonwoven veil characterized and proven, mechanical screening tests have been initiated to compare the soluble nonwoven to nylon nonwoven and standard PRIFORM fabrics. All tests were carried out on 5 harness satin 370 g/m² standard modulus carbon fibre, at Room Temperature Dry (RTD) condition. Results are presented in Figure 9.

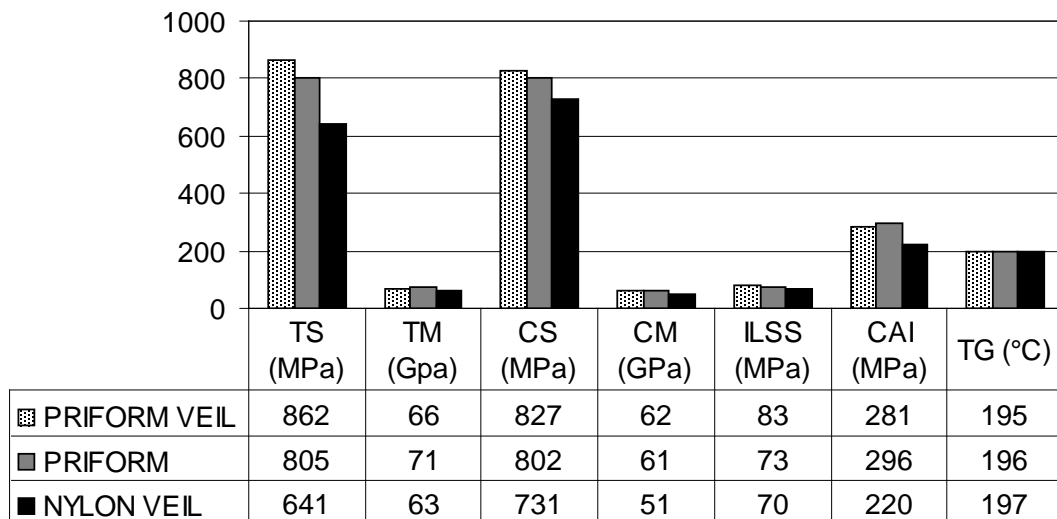


Fig. 9: Comparative mechanical properties for 5HS 6k HTA fabric

In addition to showing equivalency to standard mechanical properties, the PRIFORM nonwoven veil demonstrates a 25 percent increase in Compression After Impact properties over a state-of-the-art conventional nylon veil.

Further hot/wet testing is in progress on this developmental material; and, as such, is not presented in this paper. Data gathered so far, however, demonstrates equivalency to existing material forms. In fact, it is expected that—as with standard PRIFORM systems—the soluble veil will confer hot/wet retention to the mechanical properties of the composite.

Conclusions

The PRIFORM nonwoven technology described in this paper offers a novel approach for manufacturing high performance composite parts using liquid resin infusion processes. In addition to providing outstanding toughness enhancement, the veil can be thermally bonded to various forms of dry carbon reinforcements through a process resulting in self-binding products that can be heat stabilized and preformed at moderate temperatures and that offer the required permeability for successful injections.

Ongoing efforts of scaling up manufacturing, completing characterization and determining new paths for development are directed at offering this innovative material to the aerospace and high performance industry.

Acknowledgements

The authors would like to acknowledge the valuable contributions to this work by Alex Baidak, Stefano Cosentino, Billy Harmon, Dominique Ponsolle, Joe Ritter, Bryan Thai, and Jimmy Quevedo of Cytac Engineered Materials.

References

1. LoFaro, C., Aldridge, M. & Maskell, R. (2004). New Developments in Resin Infusion Materials Using Priform[®] Technology: Stitching, SAMPE Europe 25th International Conference, PARIS.
2. LoFaro, C., Maskell, R., Doyle, M. & Blackburn, R. (2005). Low Cost Manufacturing Using Novel Preforming and Resin Infusion Technologies, SAMPE Europe 26th International Conference, PARIS.

A4: Recent Advancements in Material for Liquid Resin Infusion

Processes (60% contribution)

3rd SETEC Technical Conference, AUGSBURG, 18-19 September 2008

Rob Blackburn[†], Marc Doyle[†], Carmelo LoFaro[†], Rob Maskell[‡],

Dominique Ponsolle*

Cytec Engineered Materials (CEM)

[†] Abenbury Way, Wrexham Industrial Estate, Wrexham LL13 9UZ, UK

[‡] 2085 East Technology Circle, Suite 300, Tempe, AZ85284, USA

* 501 West Third Street, Winona, MN55987, USA

Abstract

Non-Crimp Fabric (NCF) textiles are an established enabling technology for efficient manufacturing with Liquid Resin Infusion (LRI). One limiting factor to the widespread use of this technology in primary structural aerospace applications is the lower performance levels of typical RTM/VaRTM resin systems.

Cytec Engineered Materials' Priform® soluble thermoplastic technology has long demonstrated its equivalence to the industry's heritage

Cycom® 977-2 pre-preg system and the benefits it brings to LRI applications. So far, limited to woven products, this technology is now expanding into NCF and unidirectional dry tapes through the use of a soluble veil.

This paper presents the recent advancements in soluble thermoplastic toughening where the development of a fibrous veil has allowed for the elimination of the intermediate thermoplastic dissolution dwell. Further, it has enabled the development of a toughened NCF with properties matching those of film-infused NCFs and a complementary dry unidirectional tape suitable for LRI processing with performance equivalent to pre-preg tape.

Introduction

As the utilisation of composite materials continues to increase in the aerospace and automotive industries, their application in more demanding and complex structures are observed. This, combined with an ever-increasing focus on production efficiency and total part cost, identifies a real market need for high-performing, yet efficient materials.

In earlier papers [1-2] we demonstrated the suitability of Priform technology for aerospace primary structures. The material performance matches that of toughened pre-preg tape when our Woven Non-Crimp

Fabric (WNCF) is used [3]. WNCF is beneficial where high drape is required, but is restricted by only having 0° and 90° fibre orientations.

This paper exposes the benefits of combining the lay-up flexibility of stitched NCFs and the previously presented soluble toughening veil [4].

The PRIFORM Nonwoven Veil Concept

As discussed elsewhere [4], this novel concept allows a greater degree of flexibility when considering textile toughening. This has normally been achieved through the use of soluble fibres. Our new technology offers benefits when producing stitched materials. These include eliminating the need to control the areal distribution of discrete fibres within a textile. Instead, the interlaying veil provides full-surface cover. This is particularly relevant to stitched textiles where the stitching mechanism can cause bunching to ancillary fibres. Bunching may also significantly affect homogeneity when introducing a secondary resin component to the textile. Another potential benefit of the soluble-veil approach is the added functionality. This may include performance benefits such as added surface or fire smoke and toxicity (FST) protection. In the future design of integrated structures, this discrete interlaminar toughening element could be selectively placed where it is needed within a component.

A significant benefit of the soluble-veil approach to the Priform technology platform is that it removes the requirement for an intermediate

dwell within the cure cycle. The standard soluble fibre requires a dwell for complete dissolution and diffusion (see Fig. 1).

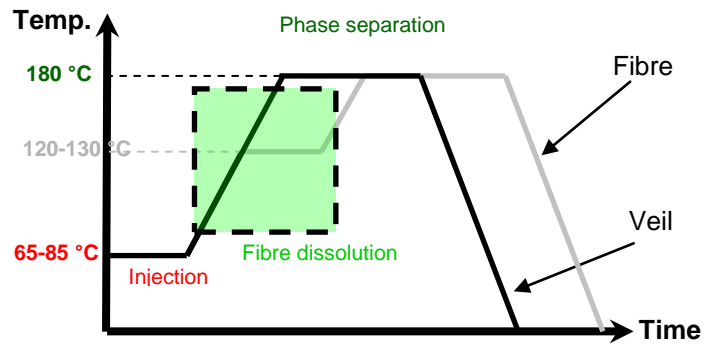


Fig. 1: Priform cure cycle reduction with soluble veil

This reduction has been achieved due to the characteristics of the veil filaments. No premature dissolution is found during resin introduction; but then on starting cure, the dissolution mechanism is initiated and completed during ramp-up.

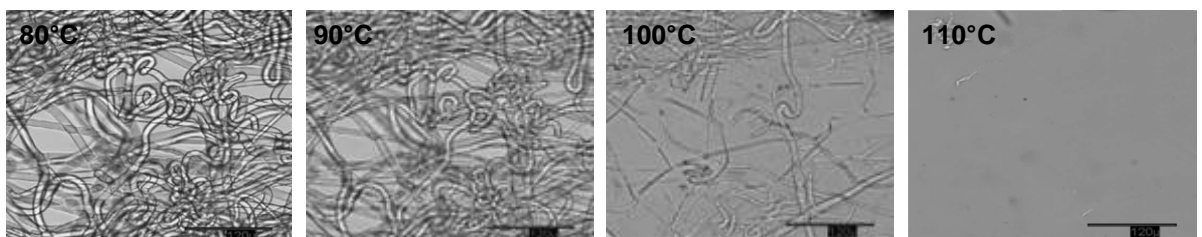


Fig. 2: Controlled dissolution of soluble veil (post-injection)

Veil Interleaved Stitched Non-Crimp Fabrics

The use of stitched non-crimp fabrics in the aerospace industry has been long understood [5]. Although the Airbus A380 aircraft has given NCFs their first commercial aircraft primary structural application [6], it can be argued that they have not been fully exploited in demanding structural applications. This may be due to the typical low performance levels achieved with standard LRI systems. Here, poor damage tolerance and notch sensitivity is a design limitation and the presence of polyester stitching can be an initiator of in-service matrix micro-cracking.

The incorporation of non-woven intermediates in stitched multi-axial textiles is not a new concept. However, the integration of an epoxy-soluble medium into these textiles is and especially when it offers primary structural pre-preg performance. The typical inclusion of non-soluble intermediate layers offers a trade-off in thermal performance against limited toughness gains. The configuration of a veil modified NCF is depicted in Fig. 3.

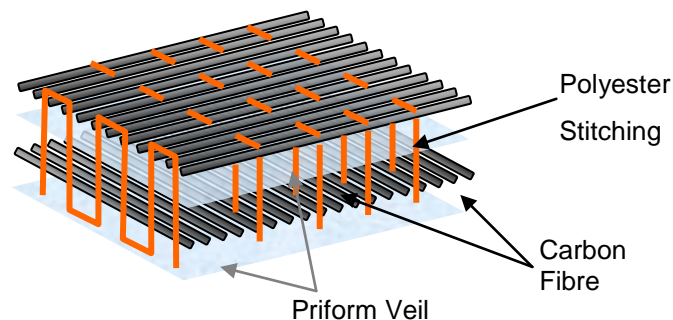


Fig. 3: Construction example of veil interleaved NCF

There have been recent competitive approaches through the use of alternative polymer types or intermediate forms. These are often found to provide a limited level of performance and do not typically offer the balance of toughness enhancement with FST performance and environmental resistance.

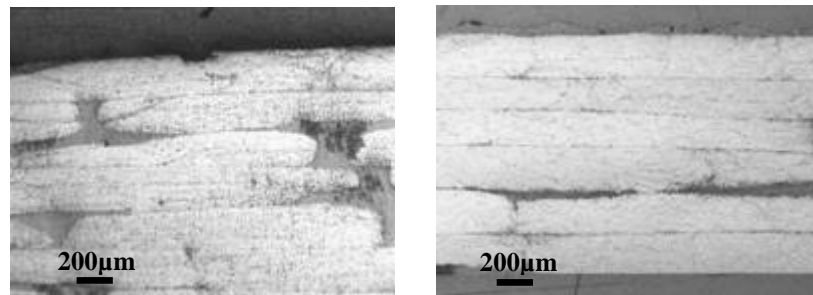


Fig. 4: Cross-section comparison of standard NCF (left) to soluble veil NCF (right)

Fig. 4 shows that the soluble veil NCF provides a comparable cross-section to that of standard NCF.

A further aspect of this material development has been to evaluate the impact-to-drape of the veil inclusion. It has been observed that through managing the stitching patterns used the veil presence has had little effect on the ability of the NCF to drape.

Unidirectional Grades

In addition to the veil multi-axial concept, a stitched unidirectional grade was also assessed. This product sandwiched carbon tows between

glass filaments and a soluble veil and was held in place with polyester stitching. This configuration is displayed in Fig. 5.

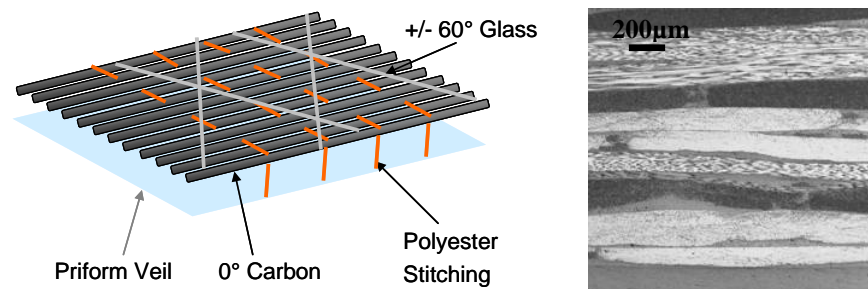


Fig. 5: Stitched unidirectional veil textile construction and cross-section

With glass yarns present in the textile construction, additional non-contributing material is added to the composite. Evaluating the cross-sections of this configuration shows that crimp levels present, from both stitching and the supporting glass filaments, will cause a reduction to plane-laminate performance. The extent of this crimping is illustrated in Fig. 5.

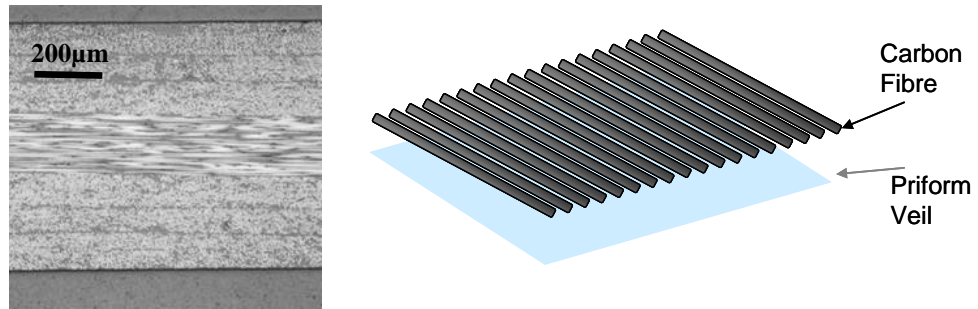


Fig. 6: Bonded Uni-Veil cross-section and construction

The mechanical performance reductions in dry textile configurations are well known and understood within the composites industry. Little progress has been made in closing the gap on axial-performance levels between textile process technologies and those of prepreg tapes. It is typically expected that for 0° axial strength properties reductions of 15-20% are common.

A combination of continuous surface coverage with veil and the ability to self-bind, allows a novel approach to be taken through directly bonding the veil to unidirectional carbon fibres. This removes the need for ancillary materials for stitching and fibre support as with traditional dry 0° textiles. This approach allows a dry tape product form incorporating a soluble substrate that, post-processing, leaves a highly aligned and nested unidirectional ply. This can be observed in Fig. 6 where the significant improvements in fibre alignment are obvious.

Mechanical Comparison

Evaluation of the veil NCF's mechanical performance in key design tests demonstrates the multi-axial product provides an equivalent performance to the heritage Cycom 977-2 toughened pre-preg. The supplementary Uni-Veil product is equivalent to pre-preg tape in providing a significant improvement over the axial performance of standard stitched unidirectional textiles (Fig. 7.).

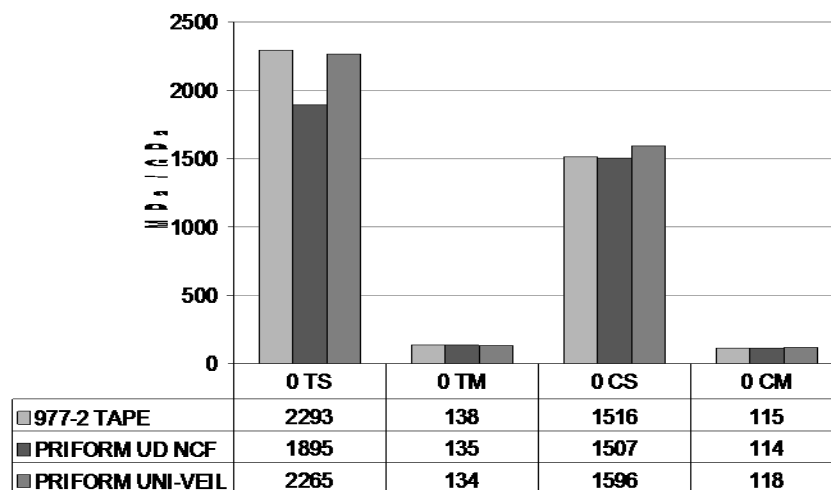
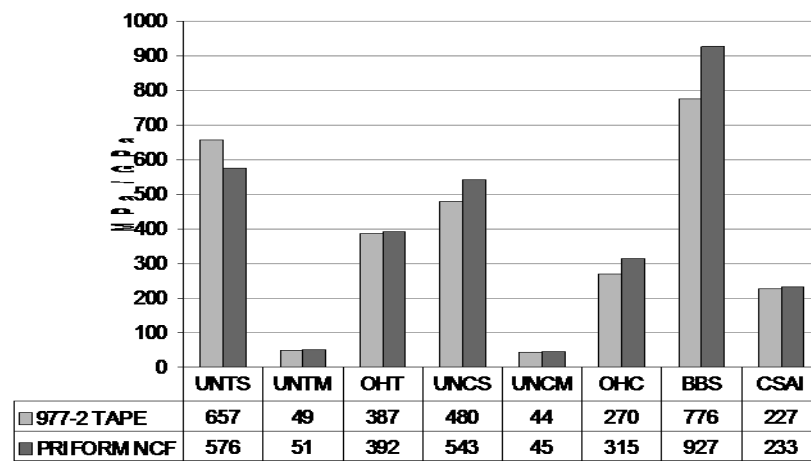


Fig. 7: Mechanical equivalence of Priform Veil Textiles and 977-2 Pre-preg Tape

(all 12K HTS at 268g/m²/layer)

Conclusions

This paper has outlined the processes in advancing Cytec's novel soluble technology platform in Priform through the development of a non-woven veil. The production processes involved with this new technology are well understood and provide filament characteristics with significant benefits in reducing the Priform cure cycle. This paper has shown how the self-binding nature of the technology allows the creation of an optimised unidirectional dry textile. Finally, in both stitched and bonded forms, the equivalent performance of Cytec's heritage Cycom 977-2 pre-preg tape can be achieved with LRI.

Acknowledgements

The authors would like to acknowledge the valuable contributions to this work by Alex Baidak, Robert Parkinson, Rick Price and Mitch Smith.

References

1. LoFaro, C., Aldridge, M. & Maskell, R. (2004). New Developments in Resin Infusion Materials Using Priform[®] Technology: Stitching, SAMPE Europe 25th International Conference, PARIS.

2. LoFaro, C., Maskell, R., Doyle, M. & Blackburn, R. (2005). Low Cost Manufacturing Using Novel Preforming and Resin Infusion Technologies, SAMPE Europe 26th International Conference, PARIS.
3. Blackburn, R., Doyle, M., LoFaro, C., & Maskell, R. (2005). Recent Developments in Preform and Resin Infusion Technologies for Primary Structural Aerospace Applications, 37th SAMPE Technical Conference, SEATTLE.
4. Abusafieh, A., Blackburn, R., Doyle, M., LoFaro, C., Maskell, R. & Price, R. (2006). Process and Performance Enhancements in Resin Infusion Using an Epoxy Soluble Veil, 27th International SAMPE Europe Conference, PARIS.
5. Bibo, G., Hogg, P. & Kemp, M. (1997). Mechanical Characterisation of Glass and Carbon Fibre-Reinforced Composites Made with Non-Crimp Fabrics, Composites Science and Technology, Vol. 57, 1221-1241.
6. Black, S. (2003). An Elegant Solution for a Big Composite Part, High Performance Composites, May, 45-48.

Appendix B: Open Area Calculation Method

In acoustic design one characteristic typically used for classification is percentage of surface area that is open due to the perforations. Where the open area value and hole diameter is given it is feasible to calculate the hole pattern dimensions for this study.

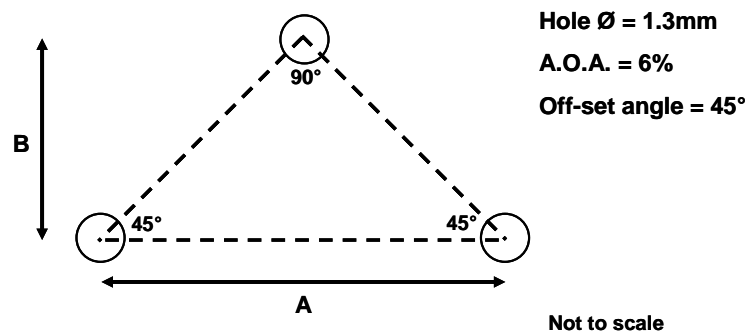


Fig. B.1: Triangular area of hole pattern used for pitch calculations

Triangle area, $A_T = \frac{1}{2} \times A \times B$

And $B = A/2$ (as triangle is right angled isosceles)

Therefore; $A_T = A/2 \times A/2 = A^2/4$

Hole area, $A_H = \pi r^2 = \pi \times 0.652 = 1.3273 \text{ mm}^2$

Only half the surface area of each hole breach triangle perimeter so therefore:

$$6\% \text{ O.A.} = 1.3273 / 2 = 0.6637 \text{ mm}^2$$

$$\text{Therefore } 1\% = 0.6637 / 6 = 0.1106 \text{ mm}^2$$

$$\text{So, } 100\% = 0.1106 \times 100 = 11.0610 \text{ mm}^2$$

$$\text{Therefore } A^2/4 = 11.0610$$

$$\text{So, } A = 6.65 \text{ mm}$$

$$\text{With } B = 6.65 / 2 = 3.325 \text{ mm}$$

Appendix C: Predictive Methods

As this study did not include a finite element analysis of the effects of perforations the methods chosen to evaluate theoretical effects of the perforations were simple area reductions.

Cross-Sectional Area Reduction

Due to the staggered nature of the hole pattern an area reduction assessment can be done from the maximum reduced cross-section through the offset double row of holes (DR), a full single row of holes (FS) and the reduced intermediate row (RS) of holes. These are all demonstrated in Fig. C1.

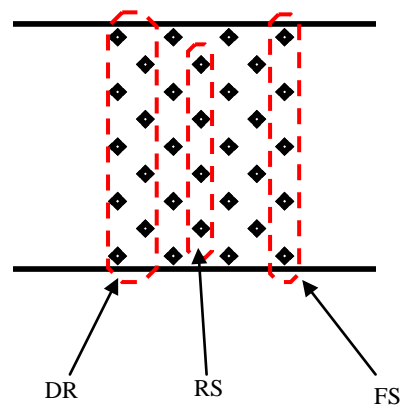


Fig. C1: Row type identification

With the hole diameter, laminate thickness and test specimen width known the area reduction is easily calculated from:

$$AR = \frac{(w \times t) - (N \times \phi \times t)}{(w \times t)}$$

Where :

w = Specimen width

t = Specimen thickness

N = Number of holes in row

ϕ = Hole diameter

AR = Area reduction

Utilising this formula for the given row scenarios the ratio between the gross section area and the reduced net section area (the area reduction factors) can be calculated. This ratio essentially gives the percentage of cross section supporting the load at failure in each case. The reduction factors for the tensile and compression specimen configurations are shown in Table C1. These factors were then applied to the strength value of non-perforated material to assess the potential reduction.

Table C1: Calculation table for reduction factors for application to non-perforate data

Row Type	No. Holes	Hole Diameter (mm)	Thickness (mm)	Effective Hole Area (mm ²)	Width (mm)	Gross Area (mm ²)	Net Area (mm ²)	Reduction Factor
[Tensile Specimens]								
DR	9	1.30	2.26	26.44	30.00	67.80	41.36	0.61
FS	5	1.30	2.26	14.69	30.00	67.80	53.11	0.78
\RS	4	1.30	2.26	11.75	30.00	67.80	56.05	0.83
[Compression Specimens]								
DR	5	1.30	2.26	14.69	16.00	36.16	21.47	0.59
FS	3	1.30	2.26	8.81	16.00	36.16	27.35	0.76
\RS	2	1.30	2.26	5.88	16.00	36.16	30.28	0.84

Appendix D: Normalisation Methodology

For the normalisation of test data to a common fibre volume the following equation is used:

$$\text{Normalised Value} = \text{Test Value} \times \frac{\text{Normalised } V_f}{\text{Specimen } V_f}$$

Where Specimen V_f can be calculated using:

$$\text{Specimen } V_f = \frac{Aw}{100 \times \rho_f \times \text{CPT}}$$

Where:

Aw = Ply Areal Weight (g/m^2)

ρ_f = Fibre Density (kg/m^3)

CPT = Cure Ply Thickness (mm)

Appendix E: Effective Areal Weight Increases

With changes in thickness at the perimeters of the moulded holes it is feasible to calculate the possible contributions to this from the material displaced from the hole moulding process.

For moulded hole pre-preg:

$$V_f = 56\%$$

$$c_{pt} = 0.294 \text{ mm} = 0.294 \times 10^{-3} \text{ m}$$

$$\rho_f = 1800 \text{ kg/m}^3$$

$$\text{Therefore: } A_w = 0.56 \times 0.294 \times 10^{-3} \times 1800 = 0.296 \text{ kg/m}^2$$

It is known from the certificates of conformity that the areal weight of fabric in the 8552 used was 0.280 kg/m^2 so this difference is an increase of:

$$0.296 / 0.280 = 1.057 = 5.7\%$$

Although this 5.7% increase would be close to the typical aerospace areal weight variation of $\pm 3\%$ we can conclude it is a direct consequence of

fibre distortion from the 6% open area of the acoustic design due to the very localised hole thickness increases observed.

For moulded hole RFI:

$$V_f = 50.42\%$$

$$c_{pt} = 0.360 \text{ mm} = 0.360 \times 10^{-3} \text{ m}$$

$$\rho_f = 1800 \text{ kg/m}^3$$

$$\text{Therefore: } A_w = 0.5042 \times 0.360 \times 10^{-3} \times 1800 = 0.327 \text{ kg/m}^2$$

It is known from the certificates of conformity that the areal weight of NCF is 0.310 kg/m^2 so this difference is an increase of:

$$0.327 / 0.310 = 1.055 = 5.5\%$$

This 5.5% value closely matches that observed from the pre-preg calculations further supporting the open are fibre distortion as the main contributing cause.

Appendix F: Performance Derived Weight Calculations

Pre-preg (P-P) standard thickness = 2.230mm [8 plies @ 57.68% V_f]

Therefore standard CPT = $2.230/8 = 0.279\text{mm}$

Standard laminate density, $\rho_{\text{lam}} = 1.58 \text{ g/cm}^3 = 1580 \text{ kg/m}^3$

Areal weight, $A_w = \text{CPT} \times \rho_{\text{lam}}$

Therefore cured ply areal weight = $0.279 \times 10^{-3} \times 1580 = 0.441 \text{ kg/m}^2$

Average thickness for moulded hole laminate = 2.355mm [8 plies @ 56.00% V_f]

Therefore moulded hole CPT = $2.355/8 = 0.294 \text{ mm}$

Laminate density at moulded holes, $\rho_{\text{lam-m}} = 1.57 \text{ g/cm}^3 = 1570 \text{ kg/m}^3$

Therefore cured ply areal weight = $0.294 \times 10^{-3} \times 1570 = 0.462 \text{ kg/m}^2$

4 ply non-perforated laminate = $4 \times 0.441 = 1.764 \text{ kg/m}^2$

4 ply laminate with 6% drilled open area = $1.764 \times 0.94 = 1.658 \text{ kg/m}^2$

4 ply laminate with 6% moulded open area = $4 \times 0.462 \times 0.94 = 1.737 \text{ kg/m}^2$

Appendix G: Calculations for Compression Capability

With the drilled specimens demonstrating a higher hot/wet compression performance it is possible to calculate the increase in thickness that would be required by the moulded laminates to sustain the same compression loads without failure. This increase in thickness can then in turn be used to calculate the weight penalty for this reduced performance level.

Compressive failure load,

$$P_{C-F} = \text{UCS} \times \text{Width} \times \text{Thickness}$$

Average hot/wet UCS for drilled PP = 349 MPa

Average width of drilled compression specimen = 16.08 mm

Thickness for four plies = $4 \times 0.279 = 1.116$ mm

Compressive failure load for 4 ply drilled laminate,

$$P_{C-F} = 349 \times 16.08 \times 1.116 = 6270\text{N}$$

Thickness of laminate to fail at set compressive load, $t = \frac{P_F}{\text{UCS} \times w}$

Average hot/wet UCS for moulded hole PP = 332 MPa

Average width of moulded hole compression specimen = 16.04 mm

Therefore thickness, $t = 6270 / (332 \times 16.04) = 1.177$ mm

However as the CPT of 0.281mm does not give a whole number of plies in 1.177mm it is necessary to adjust the lay-up to ensure the minimum performance levels are achieved. This would then give an unbalanced 5 ply lay-up and thickness of 1.405mm.

Increase in thickness due to moulding holes = $2.355/2.230 = 1.056 = 5.6\%$

Therefore moulded hole thickness of new panel = $1.405 \times 1.056 = 1.484$ mm

Assuming laminate density remains constant:

1.484mm thick moulded hole laminate with 6% open area would weigh:

$$1570 \times 1.484 \times 10^{-3} \times 0.94 = 2.184 \text{ kg/m}^2$$

This therefore represents a weight increase of, $(2.184/1.658) - 1 = 31.7\%$ (0.526 kg/m^2).

While the tensile load carrying comparison would be:

$$\text{Tensile failure load, } P_{T-F} = \text{UTS} \times \text{Width} \times \text{Thickness}$$

Average hot/wet UTS for moulded hole PP = 668 MPa

Average width of moulded hole tensile specimen = 29.79 mm

Standard thickness for proposed lay-up = 1.484 mm

Therefore tensile failure load for 1.484mm thick moulded hole laminate is:

$$668 \times 29.79 \times 1.484 = 29516 \text{ N}$$

For the current drilled design:

Average hot/wet UTS for drilled hole PP = 491 MPa

Average width of drilled hole tensile specimen = 29.84 mm

Standard thickness for current lay-up = 1.116 mm

Therefore giving a failure load of:

$$491 \times 29.84 \times 1.116 = 16337 \text{ N}$$

The ratio of tensile load carrying capability (R_{TL}) of moulded holes over drilled holes is:

$$R_{TL} = \frac{(\sigma w)_{\text{Moulded}}}{(\sigma w)_{\text{Drilled}}} = \frac{628 \times 29.79 \times 1.484}{491 \times 29.84 \times 1.116} = 1.806$$

This represents an 80.6% increase in tensile load carrying capability in hot/wet conditions.

References

- Abaris Training. (2004, July). Abaris Training, Abaris Training Newsletter: Resin Infusion Gains Speed in Aircraft Structures, Issue 6, Retrieved June 20, 2008, from <http://www.abaris.com/Newsletters/NL6-full.pdf>: <http://www.abaris.com>
- Abe, T., Hayashi, K., Takeda, F., Komori, Y., Okuda, A., Suga, Y. (2005). A-Vartm for Primary Aircraft Structures. Proc. 26th International Conference SAMPE Europe, Paris, April. Session B, 379-384.
- Abraham, D., & McIlhagger, R. (1996). A Review of Liquid Injection Techniques for the Manufacture of Aerospace Composite Structures. *Polymer & Polymer Composites*, 4 (6), 437–444.
- Abrao, A. M., Faria, P. E., Campos-Rubio, J. C., Reis, P., & Paulo-Davim, J. (2007). Drilling of Fibre Reinforced Plastics: A Review. *Materials Processing Technology*, 186 (1-3), 1-7.
- Abrate, S., & Walton, D. A. (1992 a). Machining of Composite Materials. Part 1: Traditional Methods. *Composite Manufacturing*, 3 (2), 75-83.
- Abrate, S., & Walton, D. A. (1992 b). Machining of Composite Materials. Part 2: Non-Traditional Methods. *Composite Manufacturing*, 3 (2), 85-94.
- Abusafieh, A., Blackburn, R., Doyle, M., LoFaro, C., Maskell, R., & Price, R. (2006). Process and Performance Enhancements in Resin Infusion

Using an Epoxy-Soluble Nonwoven Veil. Proc. 27th International Conference SAMPE Europe, Paris, April. Session 7B.

Advani, S. (2000). Liquid Impregnation Techniques. In R. R. Talreja, & J. Månson, *Comprehensive Composite Materials Encyclopædia*, Volume 2: Polymer Matrix Composites (pp. 807–844). Oxford: Elsevier.

Åström, B. T. (1997). *Manufacturing of Polymer Composites*. London: Chapman & Hall.

Bader, M. G. (2002). Selection of Composite Materials and Manufacturing Routes for Cost Effective Performance. *Composites: Part A*, 33, 913–934.

Beckwith, S. W. (2007 a). Resin Infusion Technology Part 1 - Industry Highlights. *SAMPE Journal*, 43 (1), 61.

Beckwith, S. W. (2007 b). Resin Infusion Technology: Part 2 - Process Definitions and Industry Variations. *SAMPE Journal*, 43 (3), 46.

Beckwith, S. (2007 c). Resin Infusion Technology Part 3 - A Detailed Overview of RTM and VIP Infusion Processing, *SAMPE Journal*. *SAMPE Journal* , 43 (3), 43.

Beckwith, S. W., & Hyland, C. R. (1998). Resin Transfer Moulding: A Decade of Technology Advances. *SAMPE Journal* , 34 (6), 7–19.

Beier, U. F., Sandler, J., Altstädt, V., Weimer, C., Spanner, H., & Buchs, W. (2008). Evaluation of Preforms Stitched with a Low Melting-

Temperature Thermoplastic Yarn in Carbon Fibre-Reinforced Composites. *Composites: Part A*, 39 (5), 705-711.

Benyus, J. M. (1997). *Biomimicry - Innovation Inspired by Nature*. New York: Perennial (Harper Collins).

Bibo, G. A. (1997). *Deformation and Fracture of Non-Crimp Fabrics*. Submitted for the Degree of Doctor of Philosophy, Department of Materials, Queen Mary & Westfield College, University of London.

Bibo, G. A., Hogg, P. J., Kemp, M. (1997). Mechanical Characterisation of Glass and Carbon Fibre-Reinforced Composites Made with Non-Crimp Fabrics. *Composites Science and Technology*, 57, 1221-1241.

Black, S. (2003, May). An Elegant Solution for a Big Composite Part. *High Performance Composites*, 11 (3), 45-48.

Blackburn, R., Doyle, M., LoFaro, C., & Maskell, R. (2005). Recent Developments in Preform and Resin Infusion Technologies for Primary Structural Aerospace Applications. Proc. 37th SAMPE Technical Conference. Seattle, November, Resin Infusion – Preforms, Part 1 – Session, Paper 3.

Blackburn, R., Doyle, M., LoFaro, C., Maskell, R. & Ponsolle, D. (2008). Recent Advancements in Materials for Liquid Resin Infusion Processes. Proc. 3rd SETEC Technical Conference, Augsburg, October, Session 6, Paper 22.

- Bombardier Commercial Aircraft, Canada. (2008). C-Series Aircraft Specification. Bombardier Inc. Canada.
- Braniff, M. (2002). RTM – A Cost Effective Composite Manufacturing Process for Control Surfaces. Proc. 23rd International Conference SAMPE Europe, Paris, April, 405-414.
- Branson Ultrasonics Corporation. (1992). Datasheet PW – FS-90. Branson Ultrasonics Corporation. USA.
- Candido, G. M., Costa, M. L., Rezende, M. C. & Almeida, S.F.M. (2007), Hygrothermal Effects on Quasi-Isotropic Carbon Epoxy Laminates with Machined and Moulded Edges. Composites: Part B, 39, 490–496.
- Campbell Jr, F. C. (2003). Manufacturing Processes for Advanced Composites. Oxford: Elsevier Advanced Technology.
- Celle, P., Drapier, S., & Bergheau, J.-M. (2008). Numerical Modelling of Liquid Infusion into Fibrous Media Undergoing Compaction. European Journal of Mechanics A/Solids, 27 (4), 647-661.
- Chang, L. W., Yau, S. S., & Chou, T. W. (1987). Notched Strength of Woven Fabric Composites with Moulded in Holes. Composites , 18 (3), 233-241.
- Chen, B., Peng, X., & Fan, J. (2004). Round-Hole-Fiber Distribution in Insect Cuticle and Biomimetic Research. JSME International Journal, Series C: Mechanical Systems, Machine Elements and Manufacturing, 47 (4), 1128-1132.

- Chen, B., Peng, X., Wang, W., Zhang, J., & Zhang, R. (2002). Research on the Microstructure of Insect Cuticle and the Strength of a Biomimetic Preformed Hole Composite. *Micron* , 33, 571-574.
- Ciriscioli, P. R. & Springer, G. S. (1990). *Smart Autoclave Cure of Composites*. Lancaster, PA: Technomic.
- Cripps, D., Searle, T. J., & Summerscales, J. (2000). Open mould techniques for thermoset composites. In R. Talreja, & J. A. Manson, *Comprehensive Composite Materials Encyclopaedia, Volume 2: Polymer Matrix Composites* (pp. 737–761). Oxford: Elsevier.
- Cutler, J. (1999). *Understanding Aircraft Structures*. Oxford: Blackwell Science.
- Dave, R. S., & Loos, A. C. (1999). *Processing of Composites*. Munich: Hanser.
- Elnady, T. (2004). *Modelling And Characterisation of Perforates in Lined Ducts and Mufflers*, Doctoral Thesis. Stockholm: The Royal Institute of Technology (KTH).
- Forbes, P. (2005). *The Gecko's Foot: Bio-Inspiration - Engineered From Nature*. London: Fourth Estate (HarperCollins).
- Godage, I. (2002). *Investigation Of Mechanical Properties Of Perforated Composite Plates Used For Acoustic Attenuation Panels*, Technical Report TR02/05. London: Imperial College of Science, Technology & Medicine.

- Gordon, S. & Hillery, M. T. (2003). A Review Of The Machining Of Composite Materials. Proc IMechE Part L: Journal of Materials Design and Applications, 217(1), 35-45.
- Gunderson, S. L., & Hall, R. B. (1993). Preformed Holes for Improved Mechanical Properties of Laminated Composites with Unidirectional Plies. Proc. 38th International SAMPE Symposium and Exhibition "Advanced Materials: Performance Through Technology Insertion". NB Only abstract seen.
- Gutowski, T. G. (1997). Advanced Composites Manufacturing. New York: J Wiley.
- Han, N. L., Suh, S. S., Yang, J. M., & Hahn, H. T. (2003). Resin Film Infusion of Stitched Composite Panels. Composites: Part A , 34, 227-236.
- Harris, C. E., Starnes, J. H., & Shuart, M. J. (2001). An Assessment of the State-of-the-Art in the Design and Manufacturing of Large Composite Structures for Aerospace Vehicles. Proc. 22nd International SAMPE Europe Conference. Paris, March, 135-146.
- Hawken, P., Lovins, A. B., & Lovins, L. H. (1999). Natural Capitalism - The Next Industrial Revolution. London: Earthscan Publications.
- Heider, D., & Gillespie, J. W. (2001). Compaction Development during Vacuum Assisted Resin Transfer Moulding (VARTM). Proc. 22nd International SAMPE Europe Conference. Paris, March, 101-108.

Hexcel Corporation. (2002). Hexcel Composites, Advanced Composite Applications in Aero Engines. Retrieved June 14, 2004, from www.hexcel.com:

<http://www.hexcelcomposites.com/Markets/Aerospace/Engines.htm>

Hexcel Corporation. (2003, May). Hexcel Composites, HexPly 8552

Product Data Sheet. Retrieved September 1, 2005, from

www.hexcel.com: http://www.hexcel.com/NR/rdonlyres/B99A007A-C050-4439-9E59-828F539B03A4/0/HexPly_8552_eu.pdf

Hexcel Corporation. (2005 a). Pre-preg Technology, Publication No. FGU 017b. Stamford, Connecticut: Hexcel Corporation.

Hexcel Corporation. (2005 b). Advanced Fibre-Reinforced Matrix Products for Direct Processes, Stamford, Connecticut: Hexcel Corporation Publication.

Hexcel Corporation. (2007, March). Hexcel Composites, HexPly M36

Product Data Sheet. Retrieved June 20, 2008, from www.hexcel.com:

http://www.hexcel.com/NR/rdonlyres/4233CAB3-4E46-46A6-8884-5CDD2638A87C/0/HexPly_M36_eu.pdf

Hinrichsen, J. & Bautista, C. (2001). The Challenge of Reducing both

Airframe Weight and Manufacturing Cost. *Air & Space Europe*, 3

(3/4), 119-121.

Hinrichsen, J. (2002). A380 – Flagship Aircraft for the New Century.

SAMPE Journal, 38, (3), 8-11.

- Hubert, P., Khoun, L., Petrescue, L., Gordon, S., & Johnston, A. (2005).
Processing Variability in Low-Cost VARTM Aeronautical Structures.
Proc. 26th International SAMPE Europe Conference. Paris, April, 385-
390.
- Kingsley-Jones, M. (2006). Airbus's A350 Vision Takes Shape. Retrieved
January 23, 2007, from www.flightglobal.com:
[http://www.flightglobal.com/articles/2006/12/12/211028/airbuss-
a350-vision-takes-shape-flight-takes-an-in-depth-look-at-the-
new.html](http://www.flightglobal.com/articles/2006/12/12/211028/airbuss-a350-vision-takes-shape-flight-takes-an-in-depth-look-at-the-new.html).
- Koorevaar, A. (2002). Simulation of Liquid Injection Moulding: Delivering
on the Promise. Proc. 23rd International SAMPE Europe Conference.
Paris, April, 633-644.
- Kruckenbug, T., Qi, B., Falzon, P., Liu, X. L., & Paton, R. (2001).
Experimental and Predicted In-Plane Flow Height Measurements for
Stiffened Structures Made Using the Resin Film Infusion Process.
Proc. 22nd International SAMPE Europe Conference. Paris, March,
77-88.
- Lin, HJ and Tang, CS. (1994). Fatigue-Strength of Woven Fabric
Composites with Drilled and Molded-In Holes. *Composites Science
and Technology*, 52 (4), 571-576.

- Lin, H. J., & Tsai, C. C. (1995 a). Failure Analysis of Bolted Connections of Composites with Drilled and Molded-In Hole. *Composite Structures* , 30 (2), 159-168.
- Lin, H. J., Tsai, C. C., & Shie, J. S. (1995 b). Failure Analysis of Woven-Fabric Composites with Moulded-In Holes. *Composites Science And Technology* , 55 (3), 231-239.
- LoFaro, C., Aldridge, M., & Maskell, R. (2003). Epoxy Soluble Thermoplastic Fibres: Enabling Technology for the Manufacture of Aerospace Primary Structures via Liquid Resin Infusion Processes. Proc. 24th International SAMPE Europe Conference. Paris, April.
- LoFaro, C., Aldridge, M. & Maskell, R. (2004). New Developments in Resin Infusion Materials Using Priform[®] Technology: Stitching. Proc. 25th International SAMPE Europe Conference. Paris, April.
- LoFaro, C., Doyle, M., Blackburn, R., & Maskell, R. (2005). , Low Cost Manufacturing Using Novel Preforming and Resin Infusion Technologies. Proc. 26th International SAMPE Europe Conference. Paris, April.
- Malmay, C. & Carbonne, S. (2001). Acoustic Impedance Measurement with Grazing Flow. *American Institute of Aeronautics and Astronautics*, 2193, 1-9.
- Marsh, G. (2002). Resin Film Infusion – Composites Cost Reducer. *Reinforced Plastics*, 2, 44-49.

- McBeath, S., & O'Rourke, B. (2000). *Competition Car Composites: A Practical Handbook*. Sparkford: Haynes.
- Meyer, R. W. (1985). *Handbook of Pultrusion Technology*. London: Chapman and Hall.
- Morgan, D. (1989). Design of an Aero-Engine Thrust Reverser Blocker Door. Proc. 34th International SAMPE Symposium, Reno, May, 2358-64.
- Mortimer, S., Lo, T., Hillermeier, R. W., & Freidrich, L. (2005). Advanced High Performance Matrices for Liquid Moulding Applications. Proc. 26th International SAMPE Europe Conference. Paris, April, 150-156.
- Mouritz, A. P. (2007). Review of Z-Pinned Composite Laminates. *Composites Part A : Applied Science and Manufacturing*, 38, 2383–2397.
- Ng, S. P., Tse, P. C., & Lau, K. J. (2001). Progressive Failure Analysis of 2/2 Twill Weave Fabric Composites with Moulded-In Circular Hole. *Composites: Part B*, 32, 139-152.
- Noakes, K. (1992). *Successful Composite Techniques: A Practical Introduction to the Use of Modern Composite Materials*, 2nd edn. London: Osprey Automotive.
- Pahr, D. H. (2003). Experimental and Numerical Investigations of Perforated FRP Laminates. *Fortschritt-Berichte VDI* , 18 (284).

- Parnas, R. S. (2000). *Liquid Composite Moulding*. Munich: Hanser Gardner.
- Peters, S. T., Humphrey, W. D., & Foral, R. F. (1991). *Filament Winding Composite Structure Fabrication*. SAMPE, Covina, CA .
- Polland, D., Davis, K., Fawcett, A., Oakes, G., & Marquette, K. (2006). *Advanced Composite Airframe Structures Development for the Boeing 787*. Proc. New Challenges in Aerospace Technology & Maintenance Conference (NCATMC) 2006, Singapore, February.
- Pora, J. & Hinrichsen, J. (2001). *Material and Technology Developments for the Airbus A380*. Proc. 22nd International SAMPE Europe Conference, Paris, March, 123-134.
- Potter, K. (1992). *Design of Composite Products – A Personal Viewpoint*. *Composites Manufacturing* , 3, 173-181.
- Potter, K. (1997). *Resin Transfer Moulding*. London: Chapman & Hall.
- Potter, K. (1999). *The Early History of the Resin Transfer Moulding Process for Aerospace Applications*. *Composites: Part A*, 30, 619-621.
- Qi, B., Raju, J., Kruckenberg, T., & Stanning, R. (1999). *A Resin Film Infusion Process for Manufacture of Advanced Composite Structures*. *Composite Structures* , 47, 471-476.
- Rudd, C. D., Turner, M. R., Long, A. C., & Middleton, V. (1999). *Tow Placement Studies for Liquid Composite Moulding*. *Composites: Part A*, 30, 1105–1121.

- Rueckert, C., & Kupke, M. (2002). New Design Approaches for Carbon Fuselage Structures – Requirements for Advanced Materials, Processes and Manufacturing Technologies. Proc. 23rd International SAMPE Europe Conference. Paris, April, 569-580.
- Rueckert, C., & Kolax, M. (2003). New Design Approaches for Composite Fuselage Structures – Requirements for Advanced Materials, Processes and manufacturing Technologies’. Proc. 14th International Conference on Composite Materials (ICCM-14), San Diego, July.
- SBAC. (2003). UK Aerospace Industry Survey 2003. London: SBAC.
- SBAC. (2006). UK Aerospace Industry Survey 2006. London: SBAC.
- Seferis, J. C. (2000). Chapter 20: Prepregging and Autoclaving. In R. T.-A. (eds.), *Comprehensive Composite Materials Encyclopaedia volume 2: Polymer Matrix Composites* (pp. 701–736). Oxford: Elsevier.
- Selzer, R. & Friedrich, K. (1997). Mechanical Properties and Failure Behaviour of Carbon Fibre-Reinforced Polymer Composites Under the Influence of Moisture. *Composites: Part A*, 28, 595-604.
- Shuart, M. J., Johnston, N. J., Dexter, B., Marchello, J. M., & Grenoble, R. W. (1998). Automated Fabrication Technologies for High Performance Polymer Composites. Proc. Intelligent Processing of High Performance Materials. Brussels, May.
- Simacek, P., Lawrence, J., & Advani, S. G. (2002). Numerical Mould Filling Simulations of Liquid Composite Moulding Processes –

Applications and Current Issues. Proc. 23rd International SAMPE Europe Conference. Paris, April, 137-148.

Skordos, A., Chan, P. H., Vincent, J. F., & Jeronimidis, G. (2002). A Novel Strain Sensor Based on the Campaniform Sensillum of Insects. Philosophical Transactions of the Royal Society of London Part A: Mathematical, Physical and Engineering Sciences 15 , 360 (1791), 239-253.

Smith, C. (2002). Biomimetics: Technology Transfer from Biology to Engineering. Philosophical Transactions: Mathematical, Physical and Engineering Sciences, 360 (1791), 155-157.

Smith, F. C. (1999). The Current Status of Resin Infusion as an Enabling Technology for Toughened Aerospace Structures. Materials Technology , 14, 71-80.

Stadtfeld, H. C., & Mitschang, P. (2005). Holistic Approach to Composite Part Manufacturing Using Preform-LCM Technology. Proc. 26th International SAMPE Europe Conference. Paris, April, 391-397.

Starr, T. F. (2000). Pultrusion for Engineers. Cambridge: Woodhead.

Stenzenberger, H. D. (1993). Recent Developments of Thermosetting Polymers for Advanced Composites. Composite Structures , 24, 219-231.

Summerscales, J., & Searle, T. J. (2005). Low Pressure (Vacuum Infusion) Techniques for Moulding Large Composite Structures. Proc IMechE

Part L - Journal of Materials: Design and Applications , 219 (1), 45-58.

Tenney, D., & Pipes, B. (2001). Advanced Composites Development for Aerospace Applications. Proc. 7th Japan International SAMPE Symposium and Exhibition, Tokyo, November, 17-22.

van Harten, K. (1993). Chap. 4 ; Production by Resin Transfer Moulding. In R. A. Sheno, & J. F. Wellicome, Composite Materials in Maritime Structures (pp. 86–126). Cambridge: Cambridge University Press.

Vogel, S. (2003). Comparative Biomechanics - Life's Physical World. Princeton and Oxford: Princeton University Press.

Warnet, L., Hulskamp, A. W., & Akkerman, R. (2006). Damage Development around Moulded-In Holes in Flat Braided Composites. Proc. 8th International Conference on Textile Composites, Nottingham, UK – 16-18 October 2006.

Warrier, N. A., Rudd, C. D., & Gardner, S. P. (1999). Experimental Studies of Embroidery for the Local Reinforcement of Composite Structures: 1. Stress Concentrations. Composites Science & Technology , 59, 2125-2137.

Weimer, C., Preller, T., Mitschang, P., & Drechsler, K. (2000). Approach to Net-Shape Preforming Using Textile Technologies. Part II: Holes. Composites: Part A , 31, 1269-1277.

Williams, C. D., Summerscales, J. & Grove, S. (1996). Resin Infusion

Under Flexible Tooling (RIFT): A Review. *Composites: Part A*, 27
(7), 517–524.

Yu, J. (2007). Commitment to a Better Future. Proc. 32nd FAA Aviation

Forecast Conference "Aviation's Resurgence: The Shape of Things to
Come". Washington, March.

Bibliography

Arizona Section Newsletter. (2002). Honeywell's Newest Turbofan Engine – The AS-907. ASME International , 54 (2), 1-2.

Asp, L. E. (2007). Local Modes for NCF Composite Materials Mechanical Performance Prediction. Proc. 16th International Conference on Composite Materials (ICCM-16), Kyoto, July.

Barrett, D. J. (1996). The Mechanics of Z-Fiber Reinforcement. Composite Structures, 36, 23-32.

Basford, D. M., Griffen, P. R., Grove, S. & Summerscales, J. (1995). Relationship Between Mechanical Performance and Microstructure in Composites Fabricated with Flow Enhancing Fabrics. Composites, 26 (9), 675-679.

Bascom, W. D. & Gweon, S. Y. (1989). Fractography and Failure Mechanisms of Carbon-Fibre-Reinforced Composite Materials, in Anne C Roulin-Moloney (editor), Fractography and Failure Mechanisms of Polymers and Composites, Elsevier Applied Science, London

Bishop, S. M. (1983). Effect of Moisture on the Notch Sensitivity of Carbon Fibre Composites. Composites, 14 (3), 201-205.

Boukhoulda, B. F., Adda-Bedia, E. & Madani, K. (2006). The Effect of Fiber Orientation Angle in Composite Materials on Moisture

Absorption and Material Degradation after Hygrothermal Ageing,
Composite Structures, 74, 406–418.

Brosius, D. (2002). Extra Large by any Measure. High Performance
Composites, September, 14-23.

Casea, S. L., O'Brien, E. P. & Warda, T., C. (2005). Cure Profiles,
Crosslink Density, Residual Stresses and Adhesion in a Model Epoxy.
Polymer, 46, 10831–10840.

Cox, B. N. & Flanagan, G. (1997). Handbook of Analytical Methods for
Textile Composites. National Aeronautics and Space Administration,
Contractor Report 4750. Virginia.

Crothers, P. J. (1997). The Automated Manufacture of Textile Composite
Structures. Department of Aerospace Engineering. Royal Melbourne
Institute of Technology. Australia.

Crothers, P. J., Drechsler, K., Feltin, D., Herszberg, I. & Kruckenberg, T.
(1997). Tailored Fibre Placement To Minimise Stress Concentrations.
Composites: Part A, 28A, 619–625.

Daniel, I. M., & Ishai, O. (1994). Engineering Mechanics of Composite
Materials. Oxford University Press. Oxford.

Dexter, H. B. (1998). Development of textile reinforced Composites for
Aircraft Structures. Proc. 4th International Symposium for textile
Composites, Kyoto, October.

- Ford, R. A. (2001). Thermo-Ductile Composites: New Materials for 21st Century Manufacturing - Micro-Perforated Thermoplastic Composites. *Materials & Design*, 22 (3), 177-183.
- Franco, F., Cunefare, K. A. & Ruzzene, M. (2007). Structural-Acoustic Optimization of Sandwich Panels. *Journal of Vibration and Acoustics-Transactions of the ASME*, 129 (3), 330-340.
- Ghasemi-Nejhad, M. N. & Chou, T-W. (1990). Compression Behaviour of Woven Carbon Fibre-Reinforced Epoxy Composites with Moulded-In and Drilled Holes. *Composites*, 21 (1), 33-40.
- Ghidossi, P., Mansori, M. E. & Pierron, F. (2004). Edge Machining Effects on the Failure of Polymer Matrix Composite Coupons. *Composites: Part A*, 35, 989–999.
- Groenewoud, W. M. (2001). *Characterisation of Polymers by Thermal Analysis*. Elsevier, Amsterdam.
- Grosveld, F. W., Buehrle, R. D. & Robinson, J. H. (2001). Structural and Acoustic Numerical Modeling of a Curved Composite Honeycomb Panel. *Proc. 7th AIAA/CEAS Aeroacoustics Conference*, Maastricht, May.
- Guild, F. J. & Summerscales, J. (1993). Microstructural Image Analysis Applied to Fibre Composite Materials: A Review. *Composites*, 24(5), 383-394.

- Hahn, H. T. & Williams, J. G. (1986). Compression Failure Mechanisms in Unidirectional Composites. Proc. Composite Materials: Testing and Design (Seventh Conference). ASTM STP 893, Philadelphia, April, 115-139.
- Haines, R. C. (1983). Volume Production with Carbon Fibre Reinforced Thermoplastics. *Plastics and rubber Processing and Applications*, 5 (1), 79-84.
- Hillereau, N., Seyed, A. A. & Gutmark, E. J. (2004). Measurements of the Acoustic Attenuation by Single Layer Acoustic Liners Constructed with Simulated Porous Honeycomb Cores. *Journal of Sound and Vibration* , 286, 21-36.
- Hodgkinson, J. M. (2000). *Mechanical Testing of Advanced Fibre Composites*. Woodhead Publishing Limited. Cambridge.
- Horowitz, S. B. (2001). *Design and Characterization of Compliant Backplate Helmholtz Resonators*. Masters Thesis. University of Florida.
- Kowalski, I. M., Manders, P. W., Owens, G. R. & Sweigart, J. F. (1990). The Effect of Small Angular Fiber Misalignments and Tapping Techniques on the Compressive Performance of Carbon Fiber Composites. Proc. 35th International SAMPE Symposium, Anaheim, April, 1479-1489.

- Kruckenber, T. M. (1998). Resin Transfer Moulding for Aerospace Structures. Dordrecht, Kluwer Academic.
- Landis, E., Fournier, C. & Davids, W. (2003). Modelling Scale Effects in Wood with Lattice Models. Proc. 16th ACSE Engineering Mechanics Conference, Seattle, July.
- Lane, S. A., Henderson, K., Williams, A. & Ardelean, E. (2007). Chamber Core Structures for Fairing Acoustic Mitigation. Journal Of Spacecraft And Rockets, 44 (1), 156-163.
- Lin, Y. C. & Chen, X. (2005). Moisture Sorption-Desorption-Resorption Charactersitics and its Effect on the Mechanical Behavior of the Epoxy System. Polymer, 46, 11994-12003.
- Matthams, T. J. & Clyne, T. W. (1999). Mechanical Properties of Long-Fibre Thermoplastic Composites with Laser Drilled Microperforations: 1. Effect of Perforations in Consolidated Material. Composites Science and Technology, 59 (8), 1169-1180.
- Mrse, A. & Piggott, M. R. (1990). Relation Between Fibre Divagation and Compressive Properties of Fibre Composites. Proc. 35th International SAMPE Symposium, Anaheim, April.
- Murphy, C., Byrne, G. & Gilchrist, M. D. (2002). The Performance of Coated Tungsten Carbide Drills When Machining Carbon Fibre-Reinforced Epoxy Composite Materials. Proceedings of the Institution

of Mechanical Engineers Part B-Journal of Engineering Manufacture,
216 (2): 143-152.

Mulligan, D. R., Gnanih, S. & Sims, G. (2000). Thermal Analysis
Techniques for Composites and Adhesives (Second Edition). National
Physical Laboratory Good Practice Guide (NPL GPG No. 62),
Teddington

Narayanan, S. & Schadler, L. S. (1999). Mechanisms of Kink-Band
Formation in graphite/Epoxy Composites: A Micromechanical
Experimental Study. Composite Science and technology, 59, 2201-
2213.

Nejhad, M. N. G. & Chou, T. W. (1990). Compression Behavior of Woven
Carbon Fiber-Reinforced Epoxy Composites with Molded-In and
Drilled Holes, Composites, 21(1), 33-40.

Partridge, I. K., Cartie, D. D. R. & Bonnington, T. (2003). Chapter 3:
Manufacture and Performance of Z-Pinned Composites. In S., G.O. &
A., S.G. (eds.), Advanced Polymeric Materials: Structure Property
Relationships (pp. 103–137). London: CRC.

Pearce, N. R. L., Summerscales, J. & Guild, F. J. Improving the Resin
Transfer Moulding Process for fabric-Reinforced Composites by
Modification of the Fabric Architecture. Composites: Part A, 31,
1433-1441.

- Rademaker, E. R., Idzenga, S. T., Huisman, H. N., Nijboer, R. J. & Sarin, S. L. (2003). NLR: A New Facility for Hot Stream Acoustic Liner Testing. NLR Report: NLR-TP-2003-202, Holland.
- Razi, H., Ward, S. H. & Bickford, M. D. (1998). Strength Prediction of Notched Thin-Skin Honeycomb Sandwich Structures. *Sandwich Construction* 4, 784-807.
- Red, C. (2007). Automated Manufacturing - The Boom in Advanced Composites. *Proc. Composites Manufacturing 2007*. Salt Lake City, April.
- Rezaeepazhand, J. & Jafari, M. (2005). Stress Analysis of Perforated Composite Plates. *Composite Structures*, 71 (3-4), 463-468.
- Roche, J. M., Leyeikian, L. & Vuillot, F. (2008). Acoustic and Aerodynamic Dissipations Induced by a Sound Wave-Impacted Helmholtz Resonator. *The Journal of the Acoustical Society of America*, 123(5), 3250.
- Rudd, C. D., Long, A. C., Kendall, K. N., & Mangin, C. G. (1997). *Liquid Moulding Technologies*. Cambridge: Woodhead.
- Sanchez-Saez, S., Barbero, E., Zaera, R. & Navarro, C. (2005), Compression After Impact of Thin Composite Laminates. *Composites Science and Technology*, 65, 1911–1919.
- Schell, J. S. U., Dawsey, G. H., Van Lenthe, G. H., Muller, R. & Ermann, P. (2005). Fabric Architecture Investigation by Micro-Computed

Tomography (μ CT). Proc. 26th International SAMPE Europe Conference, Paris, April, 92-97.

Sellen, N., Cuesta, M. & Galland, M. A. (2006). Noise Reduction in a Flow Duct: Implementation of a Hybrid Passive/Active Solution. *Journal of Sound and Vibration*, 297, 492-511.

Shim, S. B., Ahn, K. & Seferis, J. C. (1994). Flow and Void Characterisation of Stitched Structural Composites Using Resin Film Infusion Processes (RFIP). *Polymer Composites*, 15 (6), 453-463.

Silverman, E. M. & Forbes, W. C. (1990). Cost Analysis of Thermoplastic Composites Processing Methods for Spacecraft Structures. *SAMPE Journal*, 26 (6), 9-15.

Summerscales, J. (1990). NDT of Advanced Composites - An Overview of the Possibilities. *British Journal of Non-Destructive Testing*, 32 (11), 568-577.

Summerscales, J. (1994) Non-Destructive Measurement of the Moisture Content in Fibre-Reinforced Plastics. *British Journal of Non-Destructive Testing*, 36 (2), 64-72.

Summerscales, J. (1994). Manufacturing Defects in Fibre-Reinforced Plastics Composites. *Insight*, 36 (12), 936-942.

Summerscales, J., (editor). (1998). *Microstructural Characterisation of Fibre-Reinforced Composites*. Woodhead Publishing, Cambridge.

- Tang, W. C. & Lin, W. Z. (2003). Stiff Light Composite Panels for Duct Noise Reduction. *Applied Acoustics*, 64 (5), 511-524.
- Vaidyanathan, R., Campbell, J., Artz, G., Yarlagadda, S., Gillespie, J. W., Dunaj, D., Guest, B. & Nesmith, K. I. (2003). Water Soluble Tooling Materials for Complex Polymer Composite Components and Honeycombs. *SAMPE Journal*, 39 (1), 22-33.
- Vogler, T. J. & Kyriakides, S. (2000). On the Initiation and Growth of Kink Bands in Fiber Composites : Part I Experiments. *International Journal of Solids and Structures*, 38, 2639-2651.
- Walker, A., & Bowling, C. (2006). Composite Applications in Commercial Aviation. Proc. 2006 International Manufacturing Research Conference, Manchester, May.
- Walker, A., & Bowling, C. (2008). *Future Commercial Aircraft*. Proc. 2008 Advanced Manufacturing for Composite Technologies Conference, Manchester, December.
- Wan, Y. Z., Wang, Y. L., Huang, Y., Zhou, F. G., He, B. M., Chen, G. C. & Han, K. Y. (2005). Moisture Sorption and Mechanical Degradation of VARTMed Three-Dimensional Braided Carbon-Epoxy Composites. *Composites Science & Technology*, 65, 1237-1243.
- Williams, G. (2006). Wing – Centre of Excellence. Proc. 2006 International Manufacturing Research Conference, Manchester, May.

Wright, W. W. (1981). The effect of Diffusion of Water into Epoxy Resins and their Carbon-Fibre Reinforced Composites. *Composites*, July, 201-205..

Zhang, L., Zhang, H. & Wang, X. (2001). A Force Prediction Model for Cutting Unidirectional Fibre-Reinforced Plastics. *Machining Science and Technology*, 5, 293-305.

Zlavog, G. & Eversman, W. (2008). Turbofan Duct Liner Design/Optimization: A Statistical Method. *Journal of Sound and Vibration*, 313, 433-448.